E2F transcription factors:

master controllers of genomic integrity throughout the cell cycle

刘庆午

Qingwu Liu

E2F transcription factors:
master controllers of genomic integrity throughout
the cell cycle

E2F-transcriptiefactoren: hoofdcontrollers van genomische integriteit gedurende de celcyclus

(met een samenvatting in het Nederlands)

Proefschrift

ter verkrijging van de graad van doctor aan de
Universiteit Utrecht
op gezag van de
rector magnificus, prof.dr. H.R.B.M. Kummeling,
ingevolge het besluit van het college voor promoties
in het openbaar te verdedigen op

maandag 19 december 2022 des ochtends te 10.15 uur

door

Qingwu Liu

geboren op 11 september 1990
te Shanxi province, China

Promotor:

Prof. dr. A. de Bruin

Copromotor:

Dr. B. Westendorp

Beoordelingscommissie:

Prof. dr. H. Te Riele
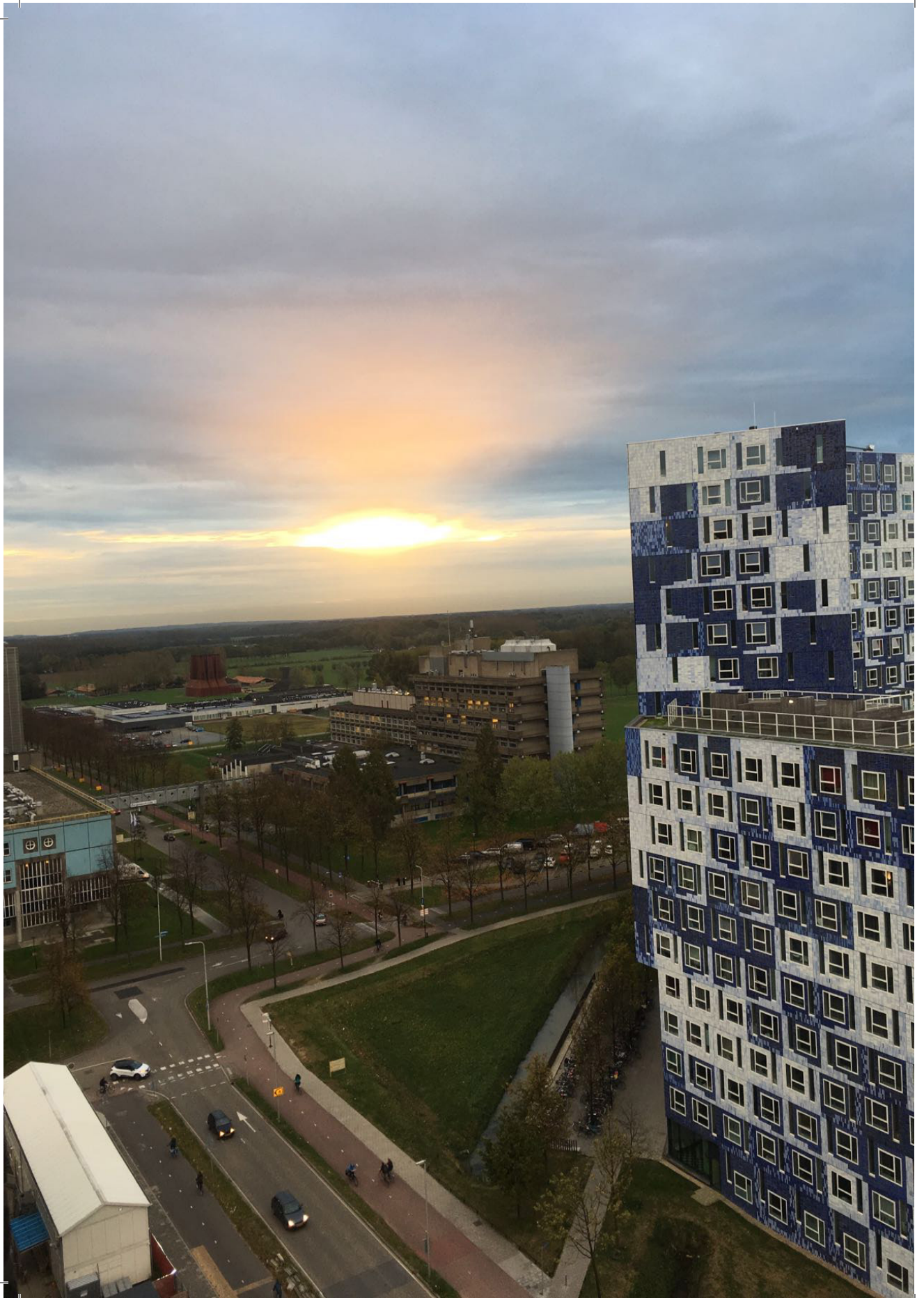
Prof. dr. T.A.E. Stout

Prof. dr. S.M.A. Lens

Prof. dr. J.J. Molenaar

Dr. P. Knipscheer

TABLE OF CONTENTS

Chapter 1

General Introduction

INTRODUCTION

Cell proliferation forms the basis for mammalian development, regeneration and even tumorigenesis. The mother cell divides into two daughter cells through a process named cell cycle, during which the major task is to replicate DNA and distribute the duplicated chromosomes equally into the daughter cells. However, throughout the cell cycle, genome integrity of the mother cell is always challenged by endogenous and exogenous stress, like replication stress and genotoxic agents. If the damaged DNA cannot be repaired timely and accurately, it could result in gene mutations, which is a major source of carcinogenesis. Hence, to maintain a stable genome through rounds of cell division, mammalian cells have evolved a series of sophisticated and precise mechanisms to guard their genome against the deleterious lesions. These mechanisms include cell cycle checkpoints, diverse DNA repair pathways, chromatin reorganization and protein modifications.

Here, in this introductory chapter, an overview is provided of how cells protect genome integrity in each cell cycle phase. I will highlight the important roles of E2F transcription factors and a protein complex called cohesin in controlling the genome integrity. I will then outline key outstanding questions on this subject and delineate how the work in this thesis contributes to answer those open questions.

Genomic integrity control in G1 phase

The major threat to genomic integrity in G1 phase is DNA damage, which can be caused by endogenous metabolic processes like base hydrolysis and oxidative damage[1], and external sources like ultraviolet and chemotherapy agents[2,3]. To cope with potential DNA lesions, eukaryotic cells have evolved an exquisite network to repair the damaged DNA in G1 phase[4,5]. Among the diverse types of DNA lesions, double-strand breaks (DSBs) are probably the most detrimental, which may cause severe genome rearrangements[6].

In response to DSBs, cells first suspend the progression of G1 phase by activating the ataxia-telangiectasia mutated (ATM) kinase[7,8]. This kinase can stabilize P53 protein by phosphorylating p53 and MDM2. MDM2 is an E3 ubiquitin ligase, phosphorylation of which interrupts its binding to p53 and prevents P53 degradation[9]. Stabilized P53 mediates the transcription of *CDKN1A*, which encodes P21 protein[10]. P21 binds to and inhibits the activity of cyclin D-CDK4/6 and cyclin E-CDK2 complexes, which leads to the inactivation of RB/E2F signaling axis, a key pathway mediating the G1/S phase transition (Figure 1)[11-13].

Cells can repair DSBs by either error-free homologous recombination (HR) or the error-prone non-homologous end joining (NHEJ)[14,15]. If DSBs occur in G1 phase, cells preferentially repair it via the NHEJ pathway, due to the lack of a genetically identical or near-identical DNA strand that serves as a repair template. This repair template is usually the sister chromatid, but sister chromatids only become available after replication, during S- and G2-phase[14]. During G1, DSBs are also recognized by the MRE11-RAD50-NBS1 (MRN) complex, followed by the loading of Ku70/80 proteins in mammalian cells. Ku70/80 complex binding prevents extensive nucleolytic processing of the DSB end and promotes the subsequent ligation of the DSB ends via the LIG4-XRCC4 factors[6,16]. However, NHEJ is error-prone, and gene mutations are frequently introduced during this process.

If the DNA lesions are too severe to repair, for example when DNA strands cross-link and bulky DNA adducts are formed, cells exit the cell cycle. The resulting fate is generally either permanent arrest (senescence) or apoptosis. This emergency brake prevents cells with severe DNA damage from proliferation, and thus maintain tissue homeostasis[17].

DNA replication without errors in S phase

Once cells enter S phase, DNA replication is fired at the licensed origin sites. But cells are frequently subject to anomalous conditions, such as nucleotide pool imbalance or shortage, transcription-replication conflicts, aberrant DNA conformation, or DNA damage induced by UV light. These conditions can all hinder DNA synthesis and can lead to DNA replication stress (RS)[18]. Moreover, tumor cells typically experience greater endogenous DNA RS than normal cells. This can be caused by the loss of a tumor suppressor genes or deregulated oncogene expression[19]. DNA RS refers to any condition that interrupts the replication fork progression

and stability, resulting in unfinished DNA replication, intertwined DNA, chromosome break-age in mitosis and potential tumorigenesis[20]. In response to these errors, the intra-S check-point is activated. This checkpoint slows down the progression of S phase, to mitigate DNA damage, and allows time for repair of DNA lesions[21].

Activation of the intra-S checkpoint is mediated by binding of replication protein A (RPA) to single-stranded DNA (ssDNA)[22]. Replicative polymerases tend to stall in face of lesions while the helicase continues to unwind the DNA ahead, which leads to the generation of ssDNA and the subsequent loading of the ssDNA binding protein RPA[23]. RPA binding to ssDNA activates the BRCA2-RAD51 axis and the Fanconi Anemia (FA) pathway to stabilize stalled replication forks[24]. On the other hand, ATR gets recruited to the sites of DNA damage and phosphorylates the checkpoint kinase 1 (CHK1). Active CHK1 phosphorylates CDC25A, target-ing it for ubiquitin-mediated degradation and/or sequestration into cytoplasm[25,26]. CDC25A degradation leads to inhibition of origin firing and elongation of S phase (Figure 1).

During S phase, cells have multiple mechanisms to repair different types of DNA lesions. Nucleotide misincorporation and small insertion or deletion loops are corrected by the mis-match repair (MMR) pathway[27]. DSBs resulting from replication fork collapse are preferably repaired through the HR pathway, due to the availability of sister DNA template in the middle and late S phase[28]. Extensive resection by EXO1 and the MRN complex on the DSB ends al-lows the invasion of single DNA strands into sister double-stranded DNA and repair the break using this undamaged DNA template. In addition, to repair single-strand gaps or nicks, cells have also evolved two mechanisms. One is translesion synthesis (TLS), which enables cells to continue DNA replication by incorporating nucleotides across damage, thereby avoiding rep-lication fork breakdown [29]. The other mechanism is template switching (TS), which uses the undamaged information of the sister duplex to fills in gaps, which seems to share similarities with HR[30]. How cells balance these various mechanisms in S phase is not fully understood.

Key mechanisms in response to DNA damage in G2 phase

G2 phase is a gap period between S phase and mitosis, which allows cells to deal with unre-paired gaps and DSBs that occur during replication. In addition, external DNA damage caused by genotoxins and irradiation (IR) would have to be dissolved prior to mitosis to avoid mitotic catastrophe[31].

Damaged DNA in G2 phase is sensed by the same mechanism depicted in G1 phase, as ATM/ATR become active. In G2 phase they inhibit PLK1 activity by phosphorylation, which in turn prevents WEE1 from degradation by SCF$^{\beta TrCP}$ and stimulates the degradation of CDC25A by the same E3 ubiquitin ligase[32,33]. Stabilized WEE1 kinase and lack of CDC25A phosphatase activity together inhibit CDK1/cyclin B activity. Additionally, CDK1 activity can be also sup-pressed by upregulation of p21 induced by p53[34]. Thus, CDK1/cyclin B activity is repressed in response to DNA damage, thereby preventing cells from entering M phase until the DSB are

repaired (Figure 1).

Because of the availability and proximity of sister chromatids, HR is an optimal mechanism to repair DNA lesions in G2 phase to preserve genome integrity. To favor HR, BRCA1 and phosphorylated CtIP counteract the ssDNA binding of 53BP1 and RIF1, facilitating the extended resection of DSBs and the subsequent binding of RPA and RAD51 to this resected DNA [35-37]. Despite the high fidelity of HR, cells can still choose NHEJ to repair DSBs during G2. Previous work showed that ~85% of DSBs induced by IR in G2 are repaired by NHEJ, whereas HR only repaired ~15% heterochromatin-associated DSBs[38]. NHEJ is easier and faster than HR, and HR may be only reserved for difficult-to-repair DNA breaks[39]. Thus, how cells sense the complexity of DSBs would be interesting to investigate.

1
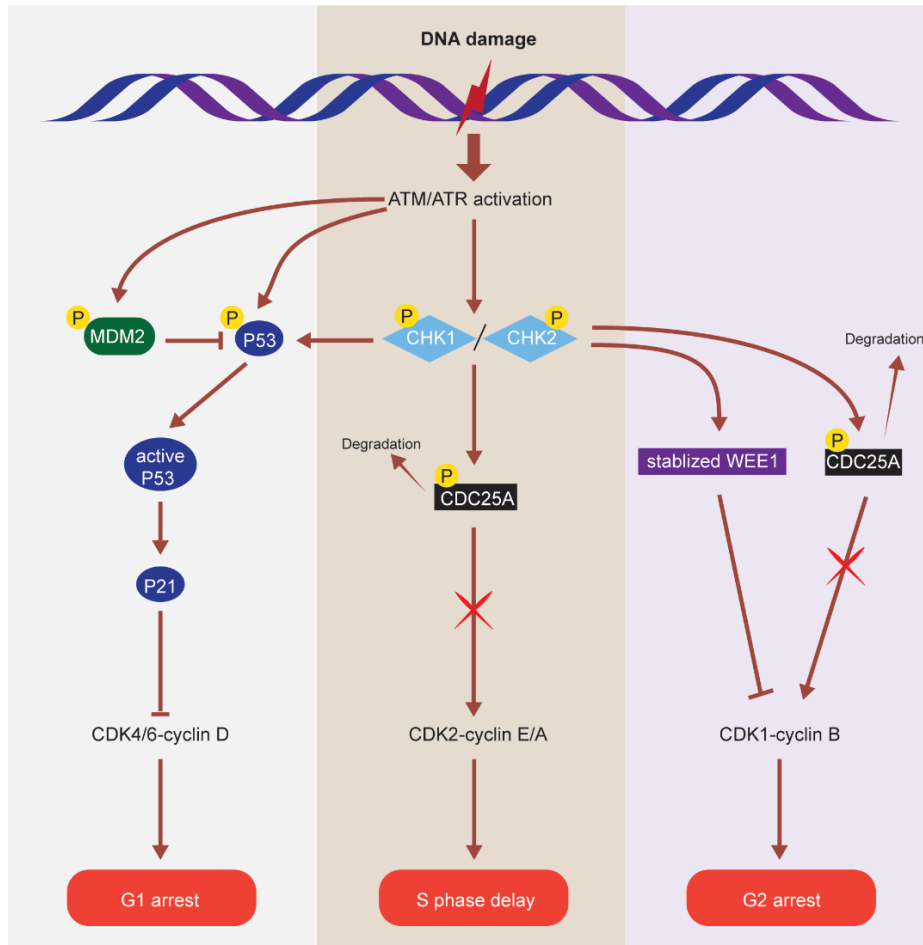
Figure 1. DNA damage response in mammalian cells during interphase. Basically, damaged DNA triggers the activation of ATM and/or ATR, which activates the downstream pathway through phosphorylating CHK2 and CHK1, respectively. In addition, P53 proteins and MDM2 can be phosphorylated by ATM/ATR during G1 phase. Phosphorylation of MDM2 prevents P53 degradation and contributes to p53-mediated induction of P21 expression. P21 inhibits CDK4/6-Cyclin D kinase activity, thereby resulting in G1 arrest. In S phase, active CHK1/CHK2 phosphorylates CDC25A, leading to CDC25A degradation. Without phosphatase CDC25A, CDK2-Cyclin E/A becomes inactive, thus preventing completion of DNA synthesis. In G2 phase, active CHK1/CHK2 phosphorylates PLK1 (not shown) and CDC25A. Then PLK1 target, kinase WEE1, stabilizes and inhibits activation of CDK1-Cyclin B. In parallel phosphorylated CDC25A is targeted for degradation and contributes as well to inactivation of CDK1-Cyclin B causing a G2 arrest.

Precise chromosome segregation in M phase

In order to preserve organism integrity and function, sister chromatids must be evenly divided into two daughter cells during M phase. However, improper separation of sister chromatids can be caused by altered microtubule dynamics, unresolved chromatin bridges, under-replicated or incorrectly repaired chromosomes[40,41]. Errors in generating daughter cells with abnormal numbers of chromosomes may lead to cell death, or alternatively the formation of aneuploid progeny. Aneuploidy has been found in cancer cells and patients with developmental defects, like Down syndrome[42].

To safeguard proper chromosome segregation, the two kinetochores on the sister chromatids must be correctly attached to the spindle apparatus[43]. The kinetochore is a disc-shaped protein structure that assembles on the centromere and link the chromatid to spindle microtubule. Cells employ a mechanism known as the spindle assembly checkpoint (SAC) to coordinate the correct connection between kinetochores and spindle microtubules launched from the two opposite centrosomes[44]. If one (or more) kinetochore are not properly attached[45], the SAC is initiated by the assembly of the Mitotic Checkpoint Complex (MCC). The MCC is a tetrameric complex composed of MAD2, CDC20, BUBR1 and BUB3 in mammalians, which binds the anaphase-promoting complex/cyclosome (APC/C) and inhibits its activity.. Thus, sister chromatids segregation and anaphase are postponed via activation of the SAC and MCC[46]. Hence, the SAC monitors and responds to any errors during kinetochore-microtubule attachment, assuring the following accurate separation of sister chromatids.

Roles of cohesin complex in the maintenance of genome integrity

To protect sister chromatids from premature separation, they are bound together during the formation in S phase until mitosis. This is done by a ring-shaped complex, called cohesin. Cohesin is an evolutionarily conserved protein complex, composed of four main subunits: SMC1, SMC3, RAD21 and SA1/2 in mammalian cells[47]. SMC proteins (SMC1 and SMC3) are rod-like with a hinge domain on one end and an ATPase head domain on the other. The connection between hinge domains leads to the formation of a V-shaped SMC heterodimer. The N- and C-terminal domains of RAD21 bind to the ATPase head domains of SMC3 and SMC1, respectively, forming a ring-shaped structure (Figure 2A). The binding of SA1 or SA2 to RAD21 provides a docking site for multiple cohesin regulators, which control the dynamic association of cohesin with DNA throughout the cell cycle[48]. Cohesin plays key roles in maintaining the genome stability by participating in DNA replication, DNA damage repair and sister chromatid separation, as detailed below.

Cohesin and DNA replication

DNA replication couples with the establishment of sister chromatid cohesion (SCC), during which cohesin rings entrap newly duplicated DNA until the onset of mitosis[49]. To stabilize the cohesin loaded on sister chromatids, SMC3 needs to be acetylated by ESCO1/2 in order to be recognized and bound by Sororin, which can counteract the binding of the cohesin remover, WAPL[50,51] (Figure 2B). Simultaneously, stably loaded cohesin is crucial to sustain replication fork progression[52]. Therefore, cohesin is essential to coordinate DNA replication and genomic integrity.

Cohesion and chromosome segregation

To separate the sister chromatids evenly and timely into daughter cells during mitosis, cohesion is dissolved stepwise in vertebrate cells[53]. As prophase starts, firstly the fraction of cohesin on the sister chromatid arms is removed by the engagement of WAPL, which binds to cohesin after Sororin is phosphorylated by Aurora B and CDK1 and dissociates from cohesin[54,55]. In addition, phosphorylation of SA2 by PLK1 can facilitate this first wave of WAPL-dependent cohesin release[56]. WAPL was reported to mediate this process by disrupting the interaction between SMC3 and the N-terminus of RAD21[57].

To shield the small fraction of cohesin complexes at centromeres required for holding the sister chromatids together until anaphase, Shugoshin 1 (Sgo 1) and its partner the protein phosphatase 2A (PP2A) act against the phosphorylation of cohesin subunits, SA1/2[58]. Moreover, cohesin at centromeres functions to stabilize the attachment of microtubules to kinetochores by opposing the pulling forces of microtubules to generate tension[59]. If the sister chromatids are correctly attached to the opposite mitotic spindles, the remaining cohesin at centromeres is removed following the cleavage of RAD21 by separase, allowing the separation of sister chromatids into daughter cells[60] (Figure 2B). Hence, accurate separation of sister chromatid in mitosis requires precise and step-wise release of cohesin complex.
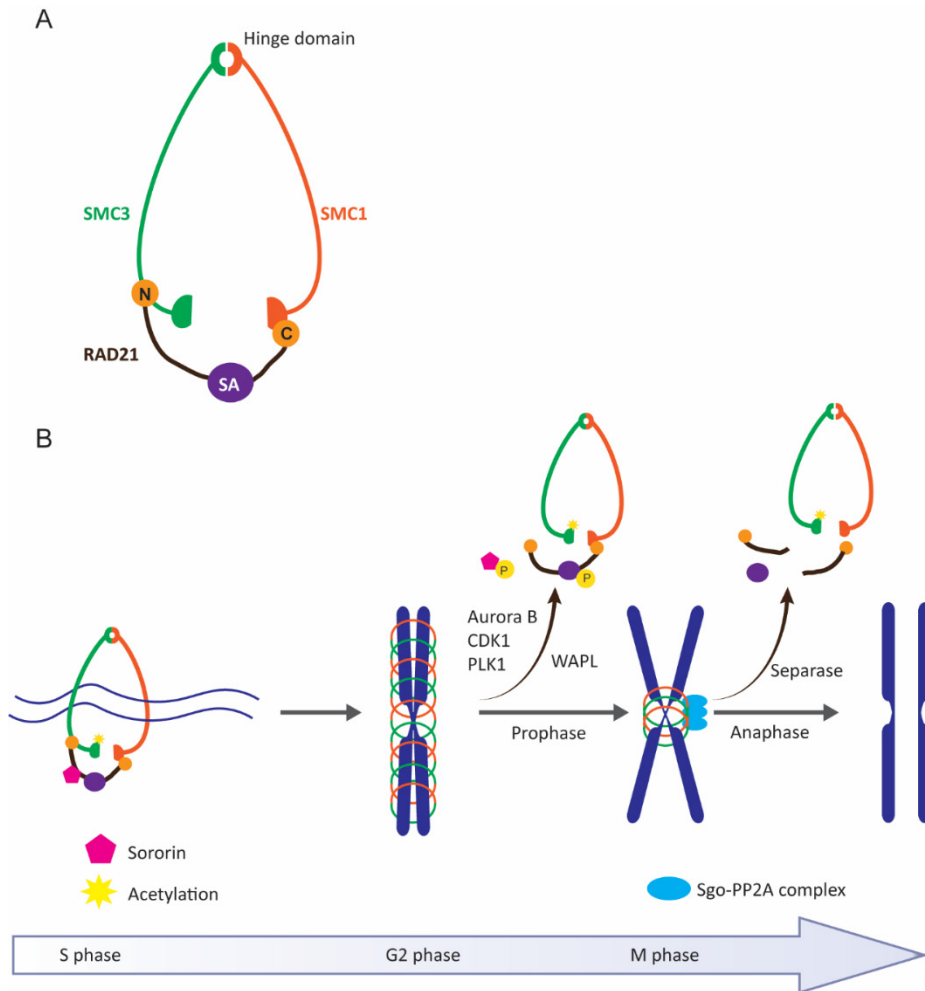
Figure 2. Formation and dissolution of sister chromatid cohesion (SCC). A. Ring-shaped structure of cohesin complex in vertebrates. SMC1 and SMC3 interact to form a V-shaped complex, which is bridged by RAD21, with the N terminus binding to SMC3 and C terminus binding to SMC1. SA1 or SA2 bind to the middle part of RAD21. **B.** SCC is established on replicated DNA molecules and stabilized by SMC3 acetylation and binding of Sororin in S phase. SCC is dissolved in two steps. In prophase, mitotic kinases (Aurora B, CDK1 and PLK1) phosphorylate Sororin and SA1/2, leading to the release of cohesin from the arms of sister chromatids mediated by WAPL. Cohesin at centromere is protected by Sgo-PP2A complex, which counteracts the activity of mitotic kinases. In anaphase, Separase cleaves RAD21, removing the remaining cohesin and allowing separation of sister chromatids.

Roles of E2Fs in the maintenance of genome integrity

As mentioned above RB/E2F axis is a key pathway in mediating G1/S phase transition. There is also mounting evidence showing that E2F proteins engage in DNA replication and DNA damage repair regulation during S- and G2-phase, thereby safeguarding the genome integrity throughout the cell cycle.

The E2Fs are a family composed of eight transcriptional factors in mammals, which drive the expression of genes involved in DNA replication, metabolism, repair and cell cycle regulation[61,62]. They share highly conserved DNA binding domains (DBD), which allow them to bind directly the E2F consensus DNA binding sequence (TTT[C/G][C/G]CGC)[63]. According to the sequence homology and transcriptional function, E2Fs are divided into three categories: activators (E2F1-3A), repressor (E2F3B-E2F6) and atypical repressors (E2F7 and -8) (Figure 3). Since E2F7 and -8 contain two tandem DBDs instead of one in E2F1-6, and bind E2F consensus motif independent of the transcriptional factor dimerization partners (DP), they are therefore designated as atypical E2Fs[64-67].
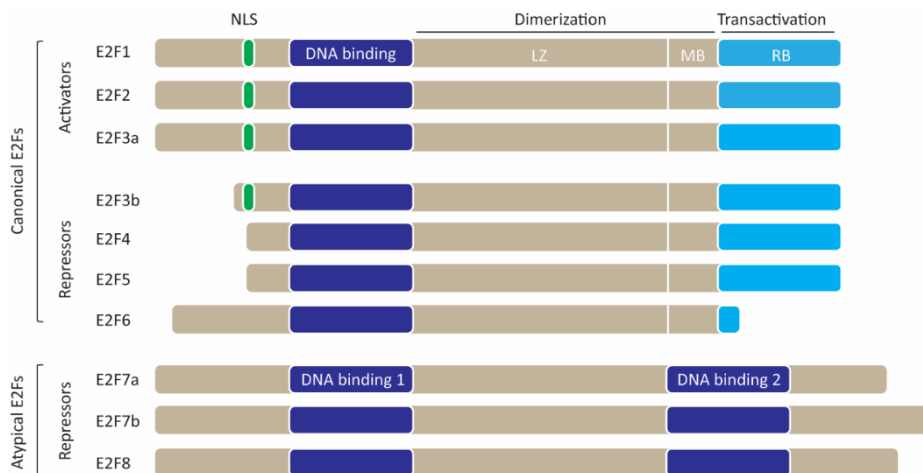
Figure 3. Structure diagram of mammalian E2F family members. All E2F family members contain a distinctive winged-helix DNA binding domain (DBD). E2Fs are divided into activators and repressors based on their transcriptional activity. The dimerization domain in E2F1-6 facilitates their interaction with one of the transcription factor dimerization partners (DP1 or -2) to bind DNA. The transactivation domain grants the binding to pocket proteins (RB1, p107 and p130), which regulate E2Fs transcriptional activity. Unlike canonical E2Fs, E2F7 and -8 have two DBDs and lack the dimerization and transactivation domains. Therefore, E2F7 and -8 are named atypical E2Fs. E2F3 and E2F7 encode two isoforms, a and -b. NLS: Nuclear Localization Signal. LZ: Leuzine Zipper domain. MB: Marked Box domain. Illustration is adapted from *Chen et al. 2009*[68].

E2F-dependent transcription is critical for the timely transition of the G1 to S phase and the accurate DNA duplication[61]. In an unperturbed cell cycle, E2F activators are released from RB binding in G1 phase, to induce the expression of genes such as *MCM2-7*, *ORC1-6*, *CDT1* and *CDC6* required for DNA replication, and *CDK2*, *CCNE1/2* and *CCNA2* for G1/S phase transition[69] (Figure 4, upper panel). Therefore, combined loss of E2F activators led to notable decrease of E2F targets and proliferation, which appears to be depend on P53-mediated transcriptional activity[70]. However, E2F is not simply an on/off switch of S phase. The levels of E2F transcription also affect the speed of DNA replication[71]. As it comes to the mid-S phase, E2F6-8 replace E2F activators and downregulate the levels of E2F transcripts, including E2F activators[72]. The downswing of E2F transcription in late S phase is important to slow down the replication rate and avoid potential DNA damage *in vitro*[71]. On top of E2Fs affecting DNA replication speed, they also control expression of genes involved in DNA repair. For example, sustained E2F-dependent transcription by E2F6 depletion was found sufficient to replication stress-induced DNA damage[73]. Likewise, loss of E2F7 increased the levels of genes involved in DNA repair pathways and subsequently facilitated the repair of genotoxic damage. Hence, it is crucial to control the levels and activity of E2F factors for cells in face of DNA damage.

The strongest evidence that aberrant E2F-dependent transcription results in genomic instability comes from the fact that cancers can arise when E2F family members are genetically altered. For example E2F7 and -8 mediated transcription repression is critical to suppress the formation of hepatocellular carcinoma (HCC) during postnatal liver development in mice[74]. Moreover, experimental amplification of *E2F1* or *E2F3* copies triggered liver cancer in mice[75]. Furthermore, in more than 50% of retinoblastoma and 29% patients with bladder cancer, *E2F3* was found to be amplified or overexpressed[76,77]. Overexpression of *E2F1* or *E2F3* has also been detected in lung, ovarian, breast and colon cancer[78]. Notwithstanding these findings, the mechanisms that could underlie genetic instability in *E2F3*-amplified cancers remains unclear.
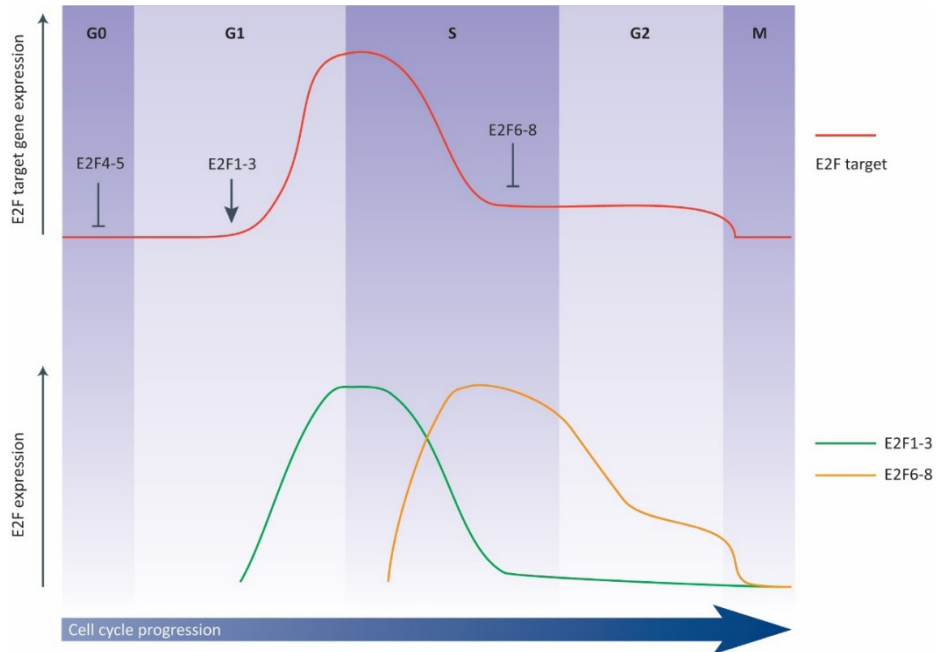
Figure 4. Model of E2F regulation throughout cell cycle. In G0 (quiescent or differentiation) cells, repressors E2F4-5 locate in nuclear to suppress target genes transcription. Upper panel: upon growth stimulus, E2F4-5 translocate into cytoplasm, and activators E2F1-3 get released from RB1 binding and induce E2F target genes expression, facilitating G1-S phase transition. After entering S phase, E2F transcription starts to decrease, attributing to repressors E2F6-8, and stays low during G2-M phase. Lower panel: Since E2F1-3 are per se E2F targets, their protein levels (green curve) peak in cells entering S phase when repressors E2F6-8 accumulate and reach the highest level (orange curve) in the middle of S phase. Whereas, the levels of E2F4-5 remain the same throughout cell cycle. Because they translocate into cytoplasm when cells decide to enter cell cycle. E2F1-3 proteins decrease during S phase due to SCF^{skp2}-mediated degradation and transcriptional repression by E2F6-8. And we previously found that E2F7-8 were targeted by APC/C^{Cdh1} for degradation in M and G1 phases, while the mechanism behind the downswing of E2F6-8 in G2 phase needs to be determined.

Given the crucial oscillation of E2F-dependent transcription over the cell cycle, the stability of E2F factors requires timely regulation. The protein levels of E2F activators (E2F1-3) peak at the G1/S transition, and atypical E2Fs (E2F7 and -8) levels peak in late S phase and stay low in G2-M-G1 phase, while E2F4-5 are constitutively expressed during the whole cell cycle[68]. Whereas E2Fs 1-3 and 6-8 stay in the nucleus throughout the cell cycle, E2F4-5 shuttle between nucleus and cytoplasm. They are located in the nucleus to repress transcription in quiescent cells, but they reside in the cytoplasm in cycling cells, where they cannot repress transcription (Figure 4, lower panel).

To achieve the timely control of E2Fs protein levels, their turnover is carefully timed throughout the cell cycle. E2F1 and E2F3 are degraded by the APC/C[CDC20] complex in early mitosis[79]. We found that during late M phase and G1 phase, atypical E2Fs are degraded by APC/C[CDH1] [80]. But we noticed that the protein levels of atypical E2Fs began to decrease already in G2 phase when APC/C[CDH1] is still inactive. If and how atypical E2Fs are regulated during G2-phase had not been studied prior to the start of this thesis work.

Although E2Fs function mostly as transcription factors in the regulation of DNA replication and cell cycle progression, several studies show non-canonical roles of E2Fs beyond proliferation control[81]. For example, besides regulating E2F activity, RB was found to involve in chromatin regulation and DNA repair as well[82]. E2F1 was shown to assist in these non-classic processes by guiding RB to genome locations for chromatin remodulation and to areas of DNA damage[83]. In addition, E2F7 was reported to accumulate at DNA damage loci and mediates the recruitment of chromatin regulators, carboxy-terminal binding proteins and histone deacetylases (HDAC1 and HDAC2) to permit DNA repair[84]. Additionally, E2F4 physically involves in the formation of centriole during multiciliogenesis[85]. In our previous study, we performed a quantitative SILAC-based proteomic screening to find out novel proteins interacting with atypical E2Fs[86]. Interestingly, E2F7 and -8 bind to components of cohesin complex, which is essential for the formation of sister chromatid cohesion and chromosome segregation in mitosis.

In summary, mammalian cells employ multiple mechanisms during cell division to maintain genome integrity in face of DNA damage, DNA replication stress and chromosome separation disorder. Fine control of E2F-dependent transcription activity and dynamic association of cohesin and DNA throughout cell cycle progression both play a pivotal role in the maintenance of genome stability. However, our understanding of these control processes -and how they are intertwined- is still limited, as they are complicated and involve dynamic actions of many different proteins. In this thesis, we explored the regulation of atypical E2Fs in G2 phase, the physiological function of their interaction with cohesin and the effect of *E2F3* amplification on DNA replication in cancer cells. Lastly, we discuss the studies in this thesis and present an outlook towards the future perspective.

SCOPE AND OUTLINE OF THIS THESIS

After decades of investigation, E2Fs have shown their critical roles as transcription factors in cell cycle control and DNA replication. However, it is not completely clear that how E2F factors themselves are regulated in different cell cycle phases. We and other groups have been dedicated to uncovering the mechanisms underlying the oscillation of E2F factors. In this these, we present the importance of fine control of E2F3 and E2F7/8 protein levels in maintaining the proper cell cycle progression and genome stability. Moreover, a noncanonical function of E2F7/8 is described in the process of cohesin release in prophase, which adds another layer of complexity to the functions of E2F factors.

In *chapter 2*, we found that cyclin F is responsible for the downregulation of E2F7/8 proteins in G2 phase. And the downswing of E2F7/8 is necessary for the expression of E2F targets involved in DNA replication and repair, thereby facilitating the G2/M transition by eliminating the potential DNA lesions. Stabilization of E2F7/8 proteins via cyclin F depletion notably increased the levels of DNA damage and delayed the G2-M progression.

In *chapter 3*, we uncovered that E2F7/8 are able to physically interact with cohesin complex. This interaction is independent of DNA binding and important for the release of cohesin in prophase. Because *E2F7/8* deficiency significantly increased the amount of chromatin loading cohesin and subsequently impaired the resolution of sister chromatid in prometaphase. Thus, E2F7/8 presented a noncanonical function here to preserve the proper cell division.

In *chapter 4*, we discovered that *E2F3* amplified bladder cancer cells and patients display replication stress. This is verified *in vitro* by overexpressing E2F3 in *E2F3* intact bladder cancer cell lines. Further investigation shows that E2F3 overexpression is able to override the suppression of RB1 and accelerate S phase entry. However, how *E2F3* amplification induces replication stress is still unclear.

In *chapter 5*, we discuss the elaborate regulation of E2F factors in the cell cycle and the noncanonical roles of E2F factors reported so far. And we also summarize the findings about the dynamic association of cohesin and chromatin in terms of maintaining genome integrity and propose how possibly E2F7/8 contribute to the timely release of cohesin during prophase.

REFERENCE

1. Tubbs A, Nussenzweig A. Endogenous DNA Damage as a Source of Genomic Instability in Cancer. *Cell.* 2017;168(4):644-656.

2. Lord CJ, Ashworth A. The DNA damage response and cancer therapy. *Nature.* 2012;481(7381):287-294.

3. Hoeijmakers JH. DNA damage, aging, and cancer. *N Engl J Med.* 2009;361(15):1475-1485.

4. Branzei D, Foiani M. Regulation of DNA repair throughout the cell cycle. *Nat Rev Mol Cell Biol.* 2008;9(4):297-308.

5. Hume S, Dianov GL, Ramadan K. A unified model for the G1/S cell cycle transition. *Nucleic Acids Res.* 2020;48(22):12483-12501.

6. Khanna KK, Jackson SP. DNA double-strand breaks: signaling, repair and the cancer connection. *Nat Genet.* 2001;27(3):247-254.

7. Khoronenkova SV, Dianov GL. ATM prevents DSB formation by coordinating SSB repair and cell cycle progression. *Proc Natl Acad Sci U S A.* 2015;112(13):3997-4002.

8. Guo Z, Kozlov S, Lavin MF, Person MD, Paull TT. ATM activation by oxidative stress. *Science.* 2010;330(6003):517-521.

9. Cheng Q, Chen J. Mechanism of p53 stabilization by ATM after DNA damage. *Cell Cycle.* 2010;9(3):472-478.

10. Abbas T, Dutta A. P21 in Cancer: Intricate Networks and Multiple Activities. *Nat Rev Cancer.* 2009;9(6):400-414.

11. Heldt FS, Barr AR, Cooper S, Bakal C, Novak B. A comprehensive model for the proliferation-quiescence decision in response to endogenous DNA damage in human cells. *Proc Natl Acad Sci U S A.* 2018;115(10):2532-2537.

12. Moser J, Miller I, Carter D, Spencer SL. Control of the Restriction Point by Rb and p21. *Proc Natl Acad Sci U S A.* 2018;115(35):E8219-E8227.

13. Yao G, Lee TJ, Mori S, Nevins JR, You L. A bistable Rb-E2F switch underlies the restriction point. *Nat Cell Biol.* 2008;10(4):476-482.

14. Her J, Bunting SF. How cells ensure correct repair of DNA double-strand breaks. *J Biol Chem.* 2018;293(27):10502-10511.

15. Mehta A, Haber JE. Sources of DNA double-strand breaks and models of recombinational DNA repair. *Cold Spring Harb Perspect Biol.* 2014;6(9):a016428.

16. Jackson SP. Sensing and repairing DNA double-strand breaks. *Carcinogenesis.* 2002;23(5):687-696.

17. Roos WP, Kaina B. DNA damage-induced cell death by apoptosis. *Trends Mol Med.* 2006;12(9):440-450.

18. Zeman MK, Cimprich KA. Causes and consequences of replication stress. *Nat Cell Biol.* 2014;16(1):2-9.

19. Primo LMF, Teixeira LK. DNA replication stress: oncogenes in the spotlight. *Genet Mol Biol.* 2019;43(1 suppl 1):e20190138.

20. Magdalou I, Lopez BS, Pasero P, Lambert SA. The causes of replication stress and their consequences on genome stability and cell fate. *Semin Cell Dev Biol.* 2014;30:154-164.

21. Bartek J, Lukas C, Lukas J. Checking on DNA damage in S phase. *Nat Rev Mol Cell Biol.* 2004;5(10):792-804.

22. Jackson SP. Sensing and repairing DNA double-strand breaks. *Carcinogenesis.* 2002;23(5):687-696.

23. Byun TS, Pacek M, Yee MC, Walter JC, Cimprich KA. Functional uncoupling of MCM helicase and DNA polymerase activities activates the ATR-dependent checkpoint. *Genes Dev.* 2005;19(9):1040-1052.

24. Jensen RB, Carreira A, Kowalczykowski SC. Purified human BRCA2 stimulates RAD51-mediated recombination. *Nature.* 2010;467(7316):678-683.

25. Sorensen CS, Syljuasen RG, Falck J, et al. Chk1 regulates the S phase checkpoint by coupling the physiological turnover and ionizing radiation-induced accelerated proteolysis of Cdc25A. *Cancer Cell.* 2003;3(3):247-258.

26. Lopez-Girona A, Furnari B, Mondesert O, Russell P. Nuclear localization of Cdc25 is regulated by DNA damage and a 14-3-3 protein. *Nature.* 1999;397(6715):172-175.

27. Jiricny J. The multifaceted mismatch-repair system. *Nat Rev Mol Cell Biol.* 2006;7(5):335-

346.

28. Aparicio T, Baer R, Gautier J. DNA double-strand break repair pathway choice and cancer. *DNA Repair (Amst).* 2014;19:169-175.

29. Prakash S, Johnson RE, Prakash L. Eukaryotic translesion synthesis DNA polymerases: specificity of structure and function. *Annu Rev Biochem.* 2005;74:317-353.

30. Branzei D, Vanoli F, Foiani M. SUMOylation regulates Rad18-mediated template switch. *Nature.* 2008;456(7224):915-920.

31. O'Connell MJ, Walworth NC, Carr AM. The G2-phase DNA-damage checkpoint. *Trends Cell Biol.* 2000;10(7):296-303.

32. Watanabe N, Arai H, Iwasaki J, et al. Cyclin-dependent kinase (CDK) phosphorylation destabilizes somatic Wee1 via multiple pathways. *Proc Natl Acad Sci U S A.* 2005;102(33):11663-11668.

33. Watanabe N, Arai H, Nishihara Y, et al. M-phase kinases induce phospho-dependent ubiquitination of somatic Wee1 by SCFbeta-TrCP. *Proc Natl Acad Sci U S A.* 2004;101(13):4419-4424.

34. Bunz F, Dutriaux A, Lengauer C, et al. Requirement for p53 and p21 to sustain G2 arrest after DNA damage. *Science.* 1998;282(5393):1497-1501.

35. Schlegel BP, Jodelka FM, Nunez R. BRCA1 promotes induction of ssDNA by ionizing radiation. *Cancer Res.* 2006;66(10):5181-5189.

36. Aparicio T, Baer R, Gautier J. DNA double-strand break repair pathway choice and cancer. *DNA Repair (Amst).* 2014;19:169-175.

37. Yu X, Chen J. DNA damage-induced cell cycle checkpoint control requires CtIP, a phosphorylation-dependent binding partner of BRCA1 C-terminal domains. *Mol Cell Biol.* 2004;24(21):9478-9486.

38. Beucher A, Birraux J, Tchouandong L, et al. ATM and Artemis promote homologous recombination of radiation-induced DNA double-strand breaks in G2. *EMBO J.* 2009;28(21):3413-3427.

39. Shibata A, Conrad S, Birraux J, et al. Factors determining DNA double-strand break repair pathway choice in G2 phase. *EMBO J.* 2011;30(6):1079-1092.

1

40. Zhang CZ, Spektor A, Cornils H, et al. Chromothripsis from DNA damage in micronuclei. *Nature.* 2015;522(7555):179-184.

41. Maciejowski J, Li Y, Bosco N, Campbell PJ, de Lange T. Chromothripsis and Kataegis Induced by Telomere Crisis. *Cell.* 2015;163(7):1641-1654.

42. Santaguida S, Amon A. Short- and long-term effects of chromosome mis-segregation and aneuploidy. *Nat Rev Mol Cell Biol.* 2015;16(8):473-485.

43. Musacchio A, Desai A. A Molecular View of Kinetochore Assembly and Function. *Biology (Basel).* 2017;6(1):10.3390/biology6010005.

44. Lara-Gonzalez P, Westhorpe FG, Taylor SS. The spindle assembly checkpoint. *Curr Biol.* 2012;22(22):966.

45. Rieder CL, Cole RW, Khodjakov A, Sluder G. The checkpoint delaying anaphase in response to chromosome monoorientation is mediated by an inhibitory signal produced by unattached kinetochores. *J Cell Biol.* 1995;130(4):941-948.

46. Jia L, Kim S, Yu H. Tracking spindle checkpoint signals from kinetochores to APC/C. *Trends Biochem Sci.* 2013;38(6):302-311.

47. Yatskevich S, Rhodes J, Nasmyth K. Organization of Chromosomal DNA by SMC Complexes. *Annu Rev Genet.* 2019;53:445-482.

48. Uhlmann F. SMC complexes: from DNA to chromosomes. *Nat Rev Mol Cell Biol.* 2016;17(7):399-412.

49. Onn I, Heidinger-Pauli JM, Guacci V, Unal E, Koshland DE. Sister chromatid cohesion: a simple concept with a complex reality. *Annu Rev Cell Dev Biol.* 2008;24:105-129.

50. Lafont AL, Song J, Rankin S. Sororin cooperates with the acetyltransferase Eco2 to ensure DNA replication-dependent sister chromatid cohesion. *Proc Natl Acad Sci U S A.* 2010;107(47):20364-20369.

51. Nishiyama T, Ladurner R, Schmitz J, et al. Sororin mediates sister chromatid cohesion by antagonizing Wapl. *Cell.* 2010;143(5):737-749.

52. Terret ME, Sherwood R, Rahman S, Qin J, Jallepalli PV. Cohesin acetylation speeds the replication fork. *Nature.* 2009;462(7270):231-234.

53. Morales C, Losada A. Establishing and dissolving cohesion during the vertebrate cell

cycle. *Curr Opin Cell Biol.* 2018;52:51-57.

54. Shintomi K, Hirano T. Releasing cohesin from chromosome arms in early mitosis: opposing actions of Wapl-Pds5 and Sgo1. *Genes Dev.* 2009;23(18):2224-2236.

55. Nishiyama T, Sykora MM, Huis in 't Veld, P J, Mechtler K, Peters JM. Aurora B and Cdk1 mediate Wapl activation and release of acetylated cohesin from chromosomes by phosphorylating Sororin. *Proc Natl Acad Sci U S A.* 2013;110(33):13404-13409.

56. Hauf S, Roitinger E, Koch B, Dittrich CM, Mechtler K, Peters JM. Dissociation of cohesin from chromosome arms and loss of arm cohesion during early mitosis depends on phosphorylation of SA2. *PLoS Biol.* 2005;3(3):e69.

57. Ouyang Z, Yu H. Releasing the cohesin ring: A rigid scaffold model for opening the DNA exit gate by Pds5 and Wapl. *Bioessays.* 2017;39(4):10.1002/bies.201600207. Epub 2017 Feb 21.

58. Liu H, Rankin S, Yu H. Phosphorylation-enabled binding of SGO1-PP2A to cohesin protects sororin and centromeric cohesion during mitosis. *Nat Cell Biol.* 2013;15(1):40-49.

59. Marston AL. Shugoshins: tension-sensitive pericentromeric adaptors safeguarding chromosome segregation. *Mol Cell Biol.* 2015;35(4):634-648.

60. Sun Y, Kucej M, Fan HY, Yu H, Sun QY, Zou H. Separase is recruited to mitotic chromosomes to dissolve sister chromatid cohesion in a DNA-dependent manner. *Cell.* 2009;137(1):123-132.

61. Bertoli C, Skotheim JM, de Bruin RA. Control of cell cycle transcription during G1 and S phases. *Nat Rev Mol Cell Biol.* 2013;14(8):518-528.

62. Ren B, Cam H, Takahashi Y, et al. E2F integrates cell cycle progression with DNA repair, replication, and G(2)/M checkpoints. *Genes Dev.* 2002;16(2):245-256.

63. Helin K, Harlow E. Heterodimerization of the transcription factors E2F-1 and DP-1 is required for binding to the adenovirus E4 (ORF6/7) protein. *J Virol.* 1994;68(8):5027-5035.

64. Iaquinta PJ, Lees JA. Life and death decisions by the E2F transcription factors. *Curr Opin Cell Biol.* 2007;19(6):649-657.

65. Di Stefano L, Jensen MR, Helin K. E2F7, a novel E2F featuring DP-independent repression of a subset of E2F-regulated genes. *EMBO J.* 2003;22(23):6289-6298.

1

66. de Bruin A, Maiti B, Jakoi L, Timmers C, Buerki R, Leone G. Identification and characterization of E2F7, a novel mammalian E2F family member capable of blocking cellular proliferation. *J Biol Chem.* 2003;278(43):42041-42049.

67. Lammens T, Li J, Leone G, De Veylder L. Atypical E2Fs: new players in the E2F transcription factor family. *Trends Cell Biol.* 2009;19(3):111-118.

68. Chen HZ, Tsai SY, Leone G. Emerging roles of E2Fs in cancer: an exit from cell cycle control. *Nat Rev Cancer.* 2009;9(11):785-797.

69. Harbour JW, Dean DC. The Rb/E2F pathway: expanding roles and emerging paradigms. *Genes Dev.* 2000;14(19):2393-2409.

70. Wu L, Timmers C, Maiti B, et al. The E2F1-3 transcription factors are essential for cellular proliferation. *Nature.* 2001;414(6862):457-462.

71. Pennycook BR, Vesela E, Peripolli S, et al. E2F-dependent transcription determines replication capacity and S phase length. *Nat Commun.* 2020;11(1):3503-z.

72. Frolov MV, Huen DS, Stevaux O, et al. Functional antagonism between E2F family members. *Genes Dev.* 2001;15(16):2146-2160.

73. Bertoli C, Herlihy AE, Pennycook BR, Kriston-Vizi J, de Bruin, Robertus A. M. Sustained E2F-Dependent Transcription Is a Key Mechanism to Prevent Replication-Stress-Induced DNA Damage. *Cell Rep.* 2016;15(7):1412-1422.

74. Kent LN, Rakijas JB, Pandit SK, et al. E2f8 mediates tumor suppression in postnatal liver development. *J Clin Invest.* 2016;126(8):2955-2969.

75. Kent LN, Bae S, Tsai SY, et al. Dosage-dependent copy number gains in E2f1 and E2f3 drive hepatocellular carcinoma. *J Clin Invest.* 2017;127(3):830-842.

76. Grasemann C, Gratias S, Stephan H, et al. Gains and overexpression identify DEK and E2F3 as targets of chromosome 6p gains in retinoblastoma. *Oncogene.* 2005;24(42):6441-6449.

77. Orlic M, Spencer CE, Wang L, Gallie BL. Expression analysis of 6p22 genomic gain in retinoblastoma. *Genes Chromosomes Cancer.* 2006;45(1):72-82.

78. Cooper CS, Nicholson AG, Foster C, et al. Nuclear overexpression of the E2F3 transcription factor in human lung cancer. *Lung Cancer.* 2006;54(2):155-162.

79. Peart MJ, Poyurovsky MV, Kass EM, et al. APC/C(Cdc20) targets E2F1 for degradation in prometaphase. *Cell Cycle.* 2010;9(19):3956-3964.

80. Boekhout M, Yuan R, Wondergem AP, et al. Feedback regulation between atypical E2Fs and APC/CCdh1 coordinates cell cycle progression. *EMBO Rep.* 2016;17(3):414-427.

81. Kent LN, Leone G. The broken cycle: E2F dysfunction in cancer. *Nat Rev Cancer.* 2019;19(6):326-338.

82. Velez-Cruz R, Manickavinayaham S, Biswas AK, et al. RB localizes to DNA double-strand breaks and promotes DNA end resection and homologous recombination through the recruitment of BRG1. *Genes Dev.* 2016;30(22):2500-2512.

83. Chen J, Zhu F, Weaks RL, et al. E2F1 promotes the recruitment of DNA repair factors to sites of DNA double-strand breaks. *Cell Cycle.* 2011;10(8):1287-1294.

84. Zalmas LP, Coutts AS, Helleday T, La Thangue NB. E2F-7 couples DNA damage-dependent transcription with the DNA repair process. *Cell Cycle.* 2013;12(18):3037-3051.

85. Mori M, Hazan R, Danielian PS, et al. Cytoplasmic E2f4 forms organizing centres for initiation of centriole amplification during multiciliogenesis. *Nat Commun.* 2017;8:15857.

86. Yuan R, Vos HR, van Es RM, et al. Chk1 and 14-3-3 proteins inhibit atypical E2Fs to prevent a permanent cell cycle arrest. *EMBO J.* 2018;37(5):10.15252/embj.201797877. Epub 2018 Jan 23.

1

Appendix

Abbreviation	Meaning
P53	Tumor protein P53
DSBs	Double Strand Breaks
CDKN1A	Cyclin Dependent Kinase Inhibitor 1A
CDK2	Cyclin Dependent Kinase 2
CDK4	Cyclin Dependent Kinase 4
CDK6	Cyclin Dependent Kinase 6
RB	Retinoblastoma 1
E2F	adenoviral Early region 2 binding Factor
HR	Homologous Recombination
NHEJ	Non-Homologous End Joining
UV	Ultraviolet
RS	Replication Stress
RPA	Replication Protein A
CHK1	Checkpoint Kinase 1
CDC25A	Cell Division Cycle 25A
MMR	Mismatch Repair
EXO1	Exonuclease 1
TLS	Translesion Synthesis
TS	Template Switching
ATM	Ataxia-telangiectasia mutated kinase
ATR	Ataxia-telangiectasia and Rad3 related kinase
PLK1	Polo Like Kinase 1
SCF	SKP1-CUL1-F-box protein ubiquitin ligase
SAC	Spindle Assembly Checkpoint
MCC	Mitotic Checkpoint Complex
SMC	Structure Maintenance of Chromosomes
SA	Stromal Antigen
SCC	Sister Chromatid Cohesion
ESCO1/2	Establishment of Sister Chromatid Cohesion N-Acetyltransferase 1/2
PP2A	Protein Phosphatase 2A
DBD	DNA-binding Domain
MCM	Minichromosome Maintenance Complex Component

1
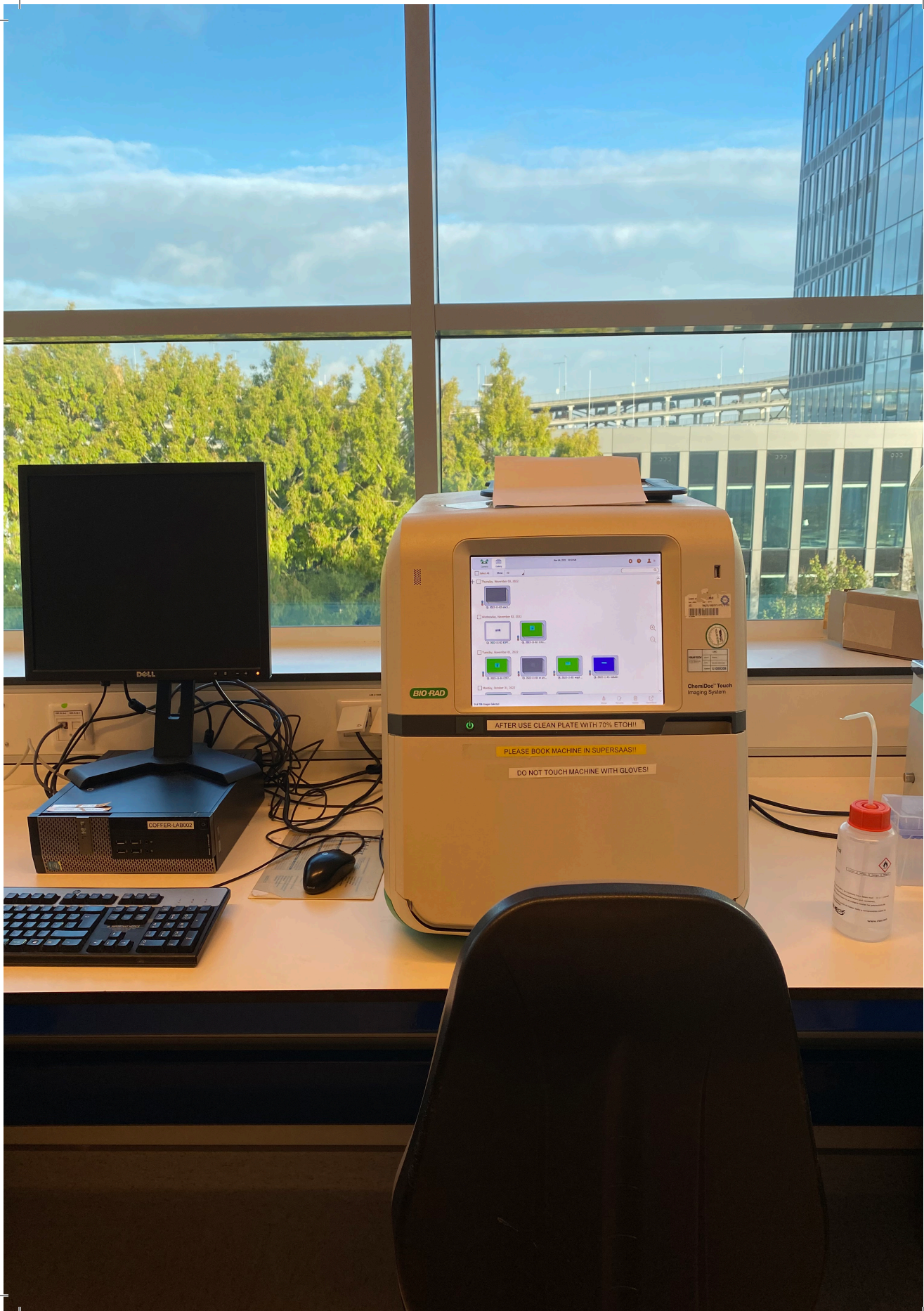
Chapter 2

Cyclin F-dependent degradation of E2F7 is critical for DNA repair and G2-phase progression

Ruixue Yuan[1#], Qingwu Liu[1#], Hendrika A Segeren[1], Laurensia Yuniati[2], Daniele Guardavaccaro[2,3], Robert Jan Lebbink[4], Bart Westendorp[1], Alain de Bruin[1,4].

1. Department of Pathobiology, Faculty of Veterinary Medicine, Utrecht University, Utrecht, The Netherlands;
2. Hubrecht Institute-KNAW and University Medical Center Utrecht, Utrecht, The Netherlands; Department of Biotechnology, University of Verona, Italy;
3. Medical Microbiology, University Medical Center Utrecht, Utrecht, The Netherlands;
4. Division Molecular Genetics, Department Pediatrics, University Medical Center Groningen, Groningen, The Netherlands;

[#] These authors contributed equally to this work.

ABSTRACT

E2F7 and E2F8 act as tumor suppressors via transcriptional repression of genes involved in S-phase entry and progression. Previously, we demonstrated that these atypical E2Fs were degraded by APC/C^{Cdh1} during G1 phase. However, the mechanism driving the downregulation of atypical E2Fs during G2-phase is unknown. Here, we show that E2F7 is targeted for degradation by the E3 ubiquitin ligase SCF$^{cyclin\ F}$ during G2-phase. Cyclin F binds via its cyclin domain to a conserved C-terminal CY motif on E2F7. An E2F7 mutant unable to interact with SCF$^{cyclin\ F}$ remains stable during G2. Furthermore, SCF$^{cyclin\ F}$ can also interact and induce degradation of E2F8. However, this does not require the cyclin domain of SCF$^{cyclin\ F}$ nor the CY motifs in the C-terminus of E2F8, implying a different regulatory mechanism than for E2F7. Importantly, depletion of cyclin F causes an atypical E2F-dependent delay of the G2/M transition, accompanied by reduced expression of E2F target genes involved in DNA repair. Live cell imaging of DNA damage revealed that cyclin F-dependent regulation of atypical E2Fs is critical for efficient DNA repair and cell cycle progression.

INTRODUCTION

The atypical E2Fs, E2F7 and E2F8, are transcriptional repressors controlling a network of genes that drive cell cycle progression. Our previous studies have revealed that classical E2F7/8 target genes, such as CDT1, CDC6 and RAD51, are involved in DNA replication, repair and metabolism[1,2]. Ectopic expression of atypical E2Fs leads to downregulation of these target genes accompanied by a permanent S-phase arrest and severe DNA damage[2,3]. In contrast, depletion of E2F7 and E2F8 leads to upregulation of E2F targets, loss of DNA damage checkpoint control and spontaneous development of hepatocellular carcinomas[1,4]. As such, activity of E2F7 and E2F8 must be tightly regulated during the cell cycle and in response to DNA damage. Nonetheless, the regulation of the atypical E2Fs is not fully elucidated. Recently, we have shown that APC/CCdh1 targets E2F7 and E2F8 for degradation during the G1 phase of the cell cycle, and that inhibition of the APC/CCdh1-mediated degradation of E2F7 and E2F8 impairs S-phase entry, eventually resulting in cell death[5]. Additionally, in response to replication stress the repressor activity of atypical E2Fs is inhibited by Checkpoint Kinase 1 (Chk1) to prevent a permanent cell cycle arrest[3]. These studies demonstrated that the proper regulation of atypical E2Fs during cell cycle progression and DNA damage is critical to avoid a detrimental effect on cell survival.

In previous studies, while investigating the oscillating expression pattern of atypical E2Fs, we observed that the protein levels of E2F7 and E2F8 peak in S-phase and are down-regulated during the G2-phase of the cell cycle. However, the regulatory mechanism behind the downregulation in G2 is unknown[5]. Since the transcript levels of E2F7 and E2F8 are only slightly lower in G2- compared to S-phase, it is likely that atypical E2Fs are subjected to proteasomal degradation during this phase of the cell cycle. Previous studies have linked the E2F family members with G2 to M transition[6-8]. In addition to genes that are involved in DNA replication and repair, a substantial number of mitotic genes such as CDK1, CCNB1 and PLK1 were also identified as E2F-regulated genes. We consistently found that E2F7 and E2F8 transcriptionally regulate a subset of genes that are related to chromatin and cytoskeleton organization[2]. Together, these studies give rise to the research questions of how atypical E2Fs are regulated and what their function during G2-phase is.

We thereby focused on the potential involvement of the Skp, Cullin, F-box protein containing complex (SCF), an E3 ubiquitin ligase complex that controls the transition between G1/S and G2/M phases by targeting a number of key cell cycle regulators for proteasomal degradation[9]. The substrate specificity of the SCF complex is determined by the F-box protein subunits. To date, over 70 human F-box proteins have been identified, and the founding member of the F-box family is cyclin F. Mouse embryonic fibroblasts (MEF) lacking cyclin F exhibited cell cycle defects, indicating that cyclin F plays a role in cell cycle regulation[10]. In addition, emerging evidence supports the importance of cyclin F in promoting the G2/M phase transition and preventing genomic instability[11,12].

In the current study, we discovered that SCF[cyclin F] targets E2F7 and E2F8 for proteasomal degradation during G2-phase in human cells. Inhibition of cyclin F-dependent E2F7/8 degradation caused a defect in G2 progression and increased DNA damage accompanied by downregulation of E2F target genes involved in DNA replication and DNA repair. These findings suggest that degradation of atypical E2Fs via cyclin F might be necessary for efficient repair of DNA lesions during G2. Taken together, this study provides new mechanistic insights into how human cells control the progression through G2-phase of the cell cycle.

RESULTS

E2F7 and E2F8 are subjected to Cullin-RING ligase-dependent degradation during G2- and early M-phase.

Our previous study showed that E2F7 and E2F8 are substrates of APC/C[Cdh1] during G1 phase and that their protein levels peak during S phase when APC/C[Cdh1] is inactive[5]. However, protein levels of atypical E2Fs already begin to decline during G2 phase, when APC/C[Cdh1] is still inactive. This suggests an additional mechanism targeting E2F7 and E2F8 proteins for degradation in G2. To monitor the protein levels of E2F7 and E2F8 throughout the cell cycle, HeLa cells were synchronized at the onset of S-phase by double thymidine treatment and subsequently released into fresh medium. Both atypical E2Fs were already expressed at the onset of the double thymidine release and their protein levels peaked 6 hours after the release during late S-phase (Fig 1A, S1A). Notably, the levels of E2F7 and to a lesser extent E2F8 decreased 9-12 hours after release when most cells were in G2-phase. Release from a hydroxyurea (HU) block also showed that E2F7/8 markedly decreased after 8 hours when most cells were in G2 (Fig S 1B). In line with this, E2F7/8 protein levels were low in cells treated with nocodazole, a microtubule inhibitor that arrests cells in prophase (Fig 1B). Together these findings suggest that E2F7/8 peak in S-phase and are degraded during G2 and early mitosis.

We investigated which mechanism could be responsible for degradation of E2F7/8 during G2 and prophase, and we reasoned that the SCF (Skp-Cullin-F-box protein) ubiquitin ligase complex would be a highly likely candidate[13]. The SCF is the largest member of E3 ligase family and among its many functions is the control of G2/M phase transition by proteasomal degradation of key cell cycle regulators, including the APC/C[Cdh1] inhibitor Emi1[14-16]. We therefore tested whether the Cullin-RING ligase promotes the degradation of E2F7 and E2F8 by treating HeLa cells for 16 hours with MLN4924, a potent and selective Cullin-RING ligases inhibitor[17]. To avoid bias from effects of this inhibitor on cell cycle progression, Hela cells were arrested in prophase with nocodazole. Under these conditions, the degradation of the atypical E2Fs was rescued by MLN4924, suggesting that E2F7/8 are targets of the SCF complex (Fig 1C). To test whether Cullin-RING ligases inhibition increases the half-life of E2F7 and E2F8, cells were treated with cycloheximide (CHX), to inhibit protein synthesis, in the presence or absence of MLN4924. Indeed, both E2F7 and E2F8 were stabilized by MLN4924

treatment (Fig 1D). These data demonstrate that atypical E2Fs are subjected to degradation by the Cullin-RING ligases during G2- and early M-phase of the cell cycle.
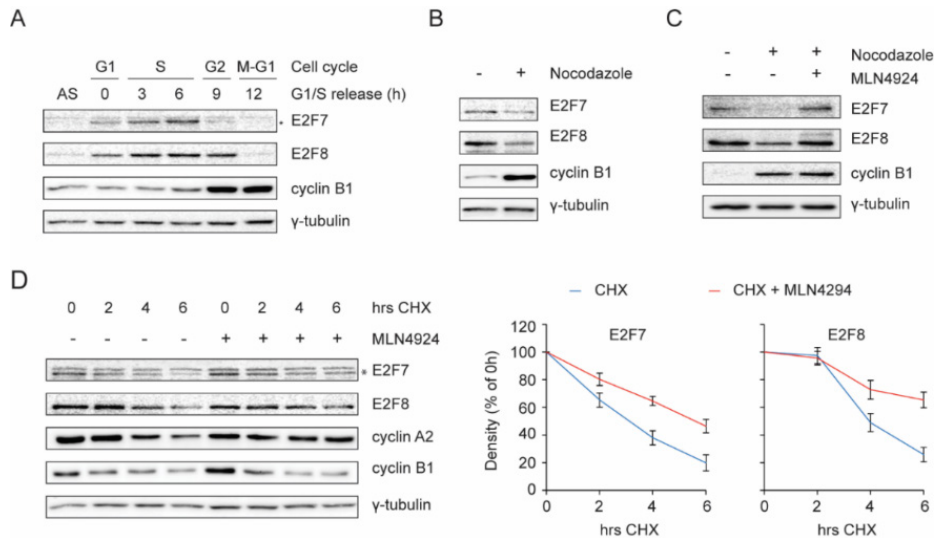

Figure 1. E2F7 and E2F8 are subjected to Cullin-RING ligase-dependent degradation during G2- and early M-phase. A. Protein levels of E2F7 and E2F8 during cell cycle progression. HeLa cells were synchronized by a double thymidine block and released into fresh medium. Cells were harvested at the indicated time points and an asynchronous (AS) condition was used as control. Protein levels were measured by immunoblotting and cell cycle progression was determined by flow-cytometry (shown in Fig S1A). The asterisk indicates the E2F7-specific band. **B.** Decreased stability of E2F7 and E2F8 in nocodazole-arrested cells. HeLa cells were either treated with DMSO or nocodazole (50 ng/ml) for 16 hours. Cells were harvested and lysed for immunoblotting. Protein expression of cyclin B1 was used as a marker for G2 or M, and γ-tubulin was used as loading control. **C.** Selective Cullin-RING inhibitor MLN4924 rescued the degradation of E2F7/8 under nocodazole-arrested condition. HeLa cells were treated with DMSO, nocodazole or nocodazole plus MLN4924 (0.1 μM) for 16 hours. Cells were harvested and lysed for immunoblotting. cyclin B1 expression was used as a marker for G2 or M cell cycle progression, and γ-tubulin was used as loading control. **D.** Increased half-life of E2F7/8 by MLN4924 treatment. HeLa cells were either treated with cycloheximide (CHX, 50 ug/ml) with or without MLN4924 (0.1 μM). Protein levels of E2F7 and E2F8 were determined by immunoblotting (left panel). Asterisk indicates the E2F7-specific band. cyclin B1 and cyclin A2 expressions were used as a marker for G2 or M cell cycle pro-gression, γ-tubulin was used as loading control. Quantifications (right panels) were performed based on two independent experiments.

Cyclin F binds to E2F7 and E2F8 via defined C-terminal motifs.

The SCF complex selectively binds to its substrates via specific F-box protein subunits[9]. Since the degradation of E2F7/8 occurred during G2 and prophase, we therefore hypothesize that

the F-box protein cyclin F, a SCF ubiquitin ligase complex that is also active in G2 phase, could be a putative candidate for E2F7/8 degradation. This atypical cyclin does not interact with cyclin-dependent kinases but instead functions as a conserved substrate recognition subunit of the SCF ubiquitin ligase complex. It mediates degradation of multiple proteins including SLBP, RRM2 and CDC6 during G2 phase, to control cell cycle progression and to maintain genome stability[18-20]. Previous work demonstrated that cyclin F can bind its substrates via a cyclin-binding sequence (known as CY motif) which contains a hydrophobic patch RxL or RxI motifs[21]. We mapped three conserved putative CY motifs within murine E2F7 and four within murine E2F8 (Fig 2A). Immunoprecipitation was performed to examine the interaction between cyclin F and E2F7/8. We overexpressed EGFP-tagged-E2F7 and -E2F8, or only EGFP and found that E2F7/8-EGFP, but not EGFP alone interacts with endogenous cyclin F (Fig S1C). Reciprocal immunoprecipitation showed that Flag-tagged cyclin F can also pull down exogenous E2F7/8-EGFP (Fig S1D).

Next, we aimed to identify the cyclin F-binding motif in E2F7/8 and mutated RxL or RxI motifs to two alanines (AxA). A series of binding experiments using both wild-type and AxA mutants were carried out to evaluate their interactions with cyclin F (Fig 2B). We found that E2F7 and E2F8 with mutations at their C-terminal CY motifs (E2F7$^{RxL/AxA\ 894/896}$ and E2F8$^{RxL/AxA\ 860/862}$, hereafter abbreviated to E2F7^{R894A} and E2F8^{R860A}) failed to interact with endogenous cyclin F. These data provide strong evidence that cyclin F binds to both E2F7 and E2F8 via a canonical CY motif. E2F7 and -8 have highly similar amino acid sequences and these C-terminus motifs are located at parallel positions on E2F7 and E2F8. Furthermore, these C-terminal motifs are conserved across multiple species (Fig S1E) suggesting that the interaction between cyclin F and atypical E2Fs also occurs in other species. We then performed co-immunoprecipitations with truncated versions of cyclin F to test their interactions with EGFP-tagged E2F7/8. We found that a △ 270 mutant version of cyclin F, which lacks the cyclin domain, lost its binding to E2F7 while wild-type version and other truncated mutants still bound to E2F7 (Fig 2C). Of note mutating the hydrophobic patch domain (ML/AA) of cyclin F did not interfere with its binding to E2F7. This suggests that the interaction between cyclin F and E2F7 required the cyclin domain, but not specifically via hydrophobic patch domain of cyclin F. EGFP-E2F8 interacted with all truncated or mutants versions of cyclin F, indicating that cyclin F binds via its F-box to E2F8 (Fig 2C).
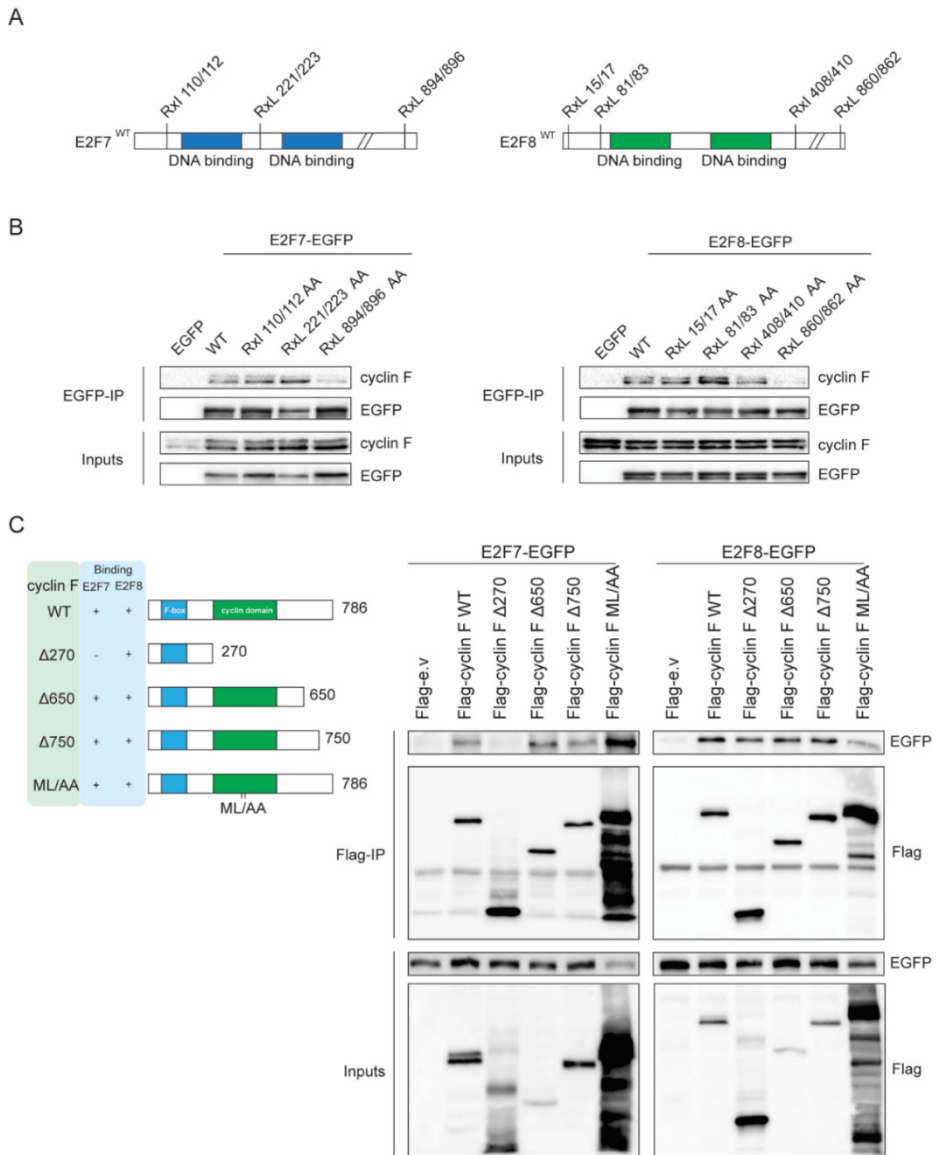
Figure 2. Cyclin F binds to E2F7 and E2F8 through a defined motif at the C-terminus.

Figure 2. Cyclin F binds to E2F7 and E2F8 through a defined motif at the C-terminus. A. Schematic view showing the location of putative cyclin F recognition motifs (RxL or RxI) on murine E2F7 and E2F8 proteins. **B.** C-terminus motifs at parallel positions on E2F7 and E2F8 are essential for binding to cyclin F. The residues on each motif were mutated to alanines (R to A, I/L to A) with site-direct mutagenesis PCR. HEK293 cells were transfected with either EGFP-tagged empty vector (EGFP), wild-types E2F7/8 (WT) or alanine mutants. Nocodazole (50 ng/ml) was added 32 hours after transfection, and MG132 (1 μg/ml) was added 5 hours before harvesting at 48 hours post transfection. Cells were harvested and lysed for immunoprecipitation using anti-EGFP resin followed by immunoblotting with antibodies against cyclin F and EGFP. **C.** Schematic view showing the truncated mutants and ML/AA mutant of cyclin F (Left). HEK cells were transfected with indicated constructs and co-immunoprecipitation was performed using Flag resin (Right).

E2F7 and E2F8 are targeted for ubiquitination and degradation by cyclin F during G2/M phases.

Since cyclin F interacts with atypical E2Fs, we hypothesized that over-expression of cyclin F would result in de-stabilization of wild-type E2F7/8 but not of the E2F7[R894A] and E2F8[R860A] mutants that show reduced interaction with cyclin F. By performing co-transfection and immunoblotting we did indeed observe that protein levels of wild-type E2F7 but not the E2F7[R894A] mutant were down-regulated by over-expression of cyclin F in G2/M phases, suggesting that cyclin F mediates degradation of E2F7 via the motif at the C-terminus (Fig 3A). Overexpression of cyclin F decreased also the expression of endogenous E2F7/8 (Fig S2A). The extent of downregulation was similar to the effect of cyclin F overexpression on CDC6, a known cyclin F target[20]. Interestingly, although the E2F8[R860A] mutant was more stabilized compared to wild-type E2F8 in G2/M phases, both versions were down-regulated by cyclin F (Fig 3A). The E2F8[R408A] which showed also reduced interaction with cyclin F (Fig 2B) was also degraded by cyclin F (Fig S1F), suggesting that the degradation of E2F8 by cyclin F is not exclusively mediated through these conserved RxL interaction motifs.

If cyclin F targets E2F7 and E2F8 for degradation, then downregulation of cyclin F would result in stabilization of atypical E2Fs. To test this, cyclin F was knocked down by a pool of siRNAs and the protein expression of endogenous E2F7/8 was measured by immunoblotting. *Cyclin F* knockdown resulted in increased expression of E2F7/8 compared to cells transfected with a scrambled siRNA (Fig 3B). In line with this finding, we also showed that two different siRNAs against cyclin F lead to stabilization of endogenous E2F7/8 (Fig S2B). In addition, we measured the half-life of E2F7/8 with CHX treatments and found that E2F7/8 were stabilized in the presence of *cyclin F* siRNA compared to the scrambled siRNA (Fig S2C). These data demonstrate that cyclin F targets E2F7/8 for degradation. To determine during which phase in the cell cycle this process occurs, we monitored the expression of atypical E2Fs during cell cycle progression after release from a double thymidine block in the presence and
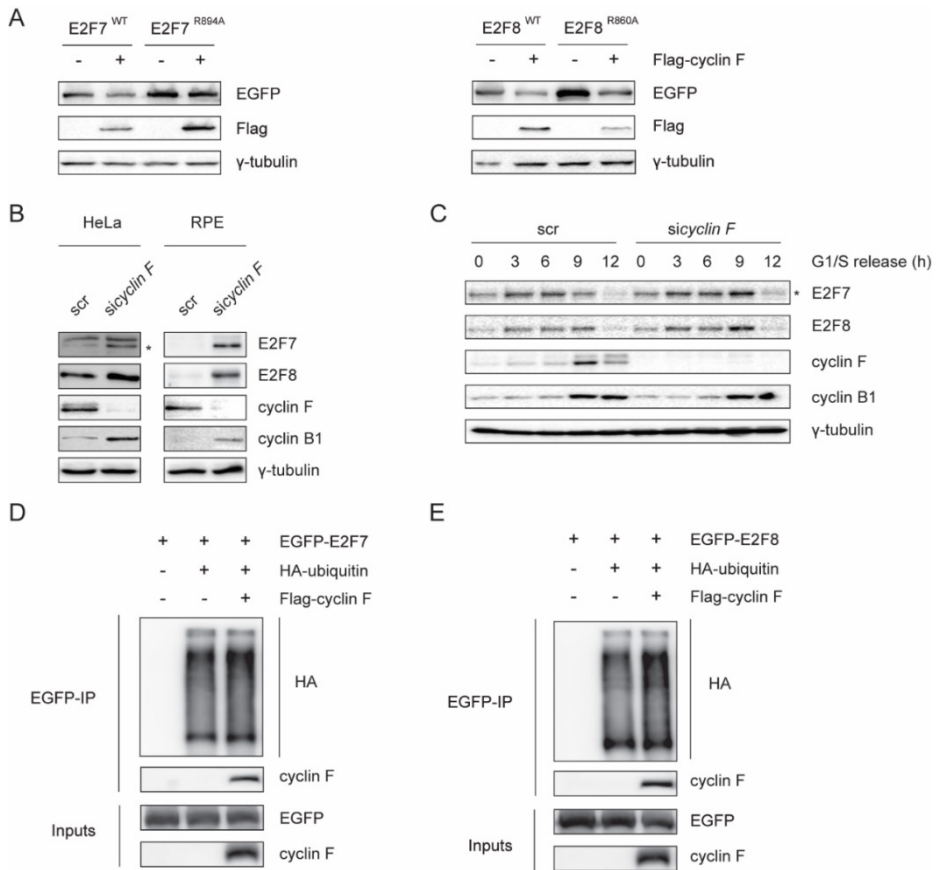
Figure 3. E2F7 and E2F8 are targeted for ubiquitination and degradation by cyclin F during G2/M. A. Wild-type or mutant versions of EGFP-tagged E2F7/8 were co-transfected with either empty vector or Flag-tagged cyclin F in HEK293 cells. Nocodazole was added to cells 8h before harvest. 48 hours after transfection, cells were collected and lysed for immunoblotting. **B.** Knockdown of cyclin F stabilized E2F7 and E2F8. HeLa and RPE cells were transfected with either scramble siRNA or pool cyclin F siRNA. Cells were harvested at 48 hours post transfection. Protein levels of E2F7/8 were analyzed by immunoblotting. Asterisk indicates the specific band of E2F7 detection. **C.** Cyclin F targets atypical E2Fs during G2/M. HeLa cells were transfected with either scrambled siRNA (scr) or cyclin F siRNA (*sicyclin F*) for 24 hours. Then cells were synchronized by double thymidine block and released into fresh medium after the second block. Cells were harvested at the indicated timepoints after the release. Protein expression was measured by immunoblotting and cell cycle progression was determined by flow-cytometry (shown in Fig S1A). Asterisk indicates the specific detection of endogenous E2F7. **D and E.** Cyclin F contributes to the ubiquitylation of E2F7 and E2F8 *in vivo*. HEK293 cells were transfected with HA-E2F7/8, with or without Flag-cyclin F, and with HA-tagged ubiquitin. 5 hours before harvest, cells were treated with MG132. 48 hours after transfection, HEK cells were harvested and lysed for immunoprecipitation pull-down assay with anti-HA resin followed by immunoblotting.

absence of cyclin F siRNA. We observed that protein levels of cyclin F gradually increased from early S phase and peaked 9 hours after release, when most cells were in G2-phase (Fig 3C and Fig S2D). E2F7 levels started to decrease at that same time point. E2F8 proteins decreased later (12 hours). At 12 hours, when the majority of cells were still in G2, E2F7 and E2F8 protein and transcript levels had almost completely disappeared (Fig 3C and Fig S2D,E). Importantly, cyclin F knockdown enhanced the protein levels of E2F7 and E2F8 at 9 hours after thymidine release, when cells were in G2-phase. The mRNA levels of E2F7 were not affected by cyclin F knockdown (Fig S2E), supporting that the stabilization of E2F7 resulted from reduced proteasome degradation. E2F8 transcript levels were slightly higher at 0h and 9h and lower at 3h and 6h in cyclin F knockdown conditions compared to scr-treated cells. This finding suggests that increased transcript levels of E2F8 at 9h might have contributed to the increased protein expression of E2F8.

To verify whether cyclin F controls the stability of E2F7/8 through ubiquitin-mediated degradation, we performed in vivo ubiquitination assays. Atypical E2Fs and HA-tagged wild-type ubiquitin were co-expressed in the presence and absence of cyclin F. Then E2F7 and E2F8 were subjected to immunoprecipitation followed by immunoblotting for HA-ubiquitin (Fig 3D and E). We found that E2F7 and E2F8 were poly-ubiquitylated. Over-expression of cyclin F enhanced the ubiquitination of E2F7/8. In addition, we demonstrated that E2F7R894A displayed a reduction in ubiquitination compared to E2F7WT (Fig S2F). Taken together, our data suggest that E2F7/8 are targeted for degradation by SCFcyclin F-mediated ubiquitination.

Failure to degrade E2F7 and E2F8 results in defected G2/M transition.
Next, we aimed to investigate the biological significance of the cyclin F-dependent degradation of atypical E2Fs. In the flow cytometry data from Fig S2D, knockdown of *cyclin F* induced a delay in the progression of cells through G2- or M-phase, reflected by a smaller G1 cell population at 9 and 12 hours after thymidine release. Given that protein levels of E2F7/8 were stabilized during G2 phase upon cyclin F depletion (Fig 3C), we hypothesized that the G2/M transition delay by cyclin F loss resulted from stabilized expression of E2F7 and E2F8. To test our hypothesis, we analyzed whether loss of E2F7/8 would rescue the cell cycle delay caused by loss of cyclin F. To this end, *E2F7* and *E2F8* (*7/8^KO^*) were deleted in non-transformed human cells - Retina Pigment Epithelial cells (RPE-hTERT) expressing the Fluorescent Ubiquitin Cell Cycle Indicator (FUCCI system) using CRISPR-CAS9 technology[22]. RPE-hTERT cells carrying a Cas9-construct lacking a small guiding RNA (sgRNA) were used as control (Ctrl). Complete and permanent deletion of both *E2F7* and *E2F8* was confirmed by immunoblotting (Fig S3A). To monitor the cell cycle progression through the G2- and M phases, these two cell lines were synchronized at the onset of S-phase by HU treatment for 16 hours. After release from HU, the progression of each individual cell was recorded by live cell imaging (Fig 4A). Around 50% of Ctrl cells reached mitosis within 24 hours after HU release, while only 20%

of cells with *cyclin F* siRNA progressed through mitosis (Fig 4B). Importantly, the delay in cell cycle progression induced by the knockdown of cyclin F was completely rescued in cells with deletion of E2F7/8.

Since HU treatment results in DNA damage and loss of E2F7/8 leads to an impaired DNA damage response[4,23,24], the impact of cyclin F-mediated degradation of E2F7/8 was investigated under unperturbed conditions. Similar to the setting in panel Fig 4A, both Ctrl and *7/8^KO* cells were transfected with either scrambled siRNA or siRNA against *cyclin F* and subjected to fluorescent live cell imaging. Four cell cycle stages, i.e. G1 phase, G1-S transition, late S to G2, and M, were analyzed based on the fluorescence signal (see Material and Methods). For each condition, 50 cells were followed and their cell cycle progression starting from G1 phase was recorded (Fig 4C). We found that 70% of the Ctrl cells (35/50) completed mitosis during the observed time window, while *cyclin F* knockdown resulted in a delayed cell cycle progression with only 44% (22/50) of all cells finishing mitosis in the same time period (Fig 4D). In line with the HU-synchronized cells, deletion of *E2F7/8* could rescue the delayed cell cycle progression induced by *cyclin F* knockdown under unperturbed conditions, with 60% of scrambled siRNA *7/8^KO* cells completing mitosis within 24 hours compared to 58% (29/50) of *cyclin F* siRNA *7/8^KO* cells. Moreover, the time from G1-S transition to mitosis for those cells that completed this process was measured (Fig 4E). We found that Ctrl cells with *cyclin F* siRNA moved from S-phase entry to completion of mitosis in an average time of approximately 18 hours, compared to less than 16 hours in Ctrl cells incubated with scrambled siRNA. This delayed cell cycle progression phenotype was absent in the 7/8^KO cell lines treated with cyclin F siRNA; they also needed less than 16 hours to complete mitosis from the moment of S-phase entry. We also quantified the fates of the whole cell population (50/each, at the last frame of the live imaging). Strikingly, 42% of the Ctrl cells with *cyclin F* knockdown were in late S or G2, compared to only 18% in scrambled condition (Fig 4F, individual cells were shown in Fig S3B). More importantly, such delay was not observed in the 7/8^KO cells, suggesting that the delay in S and/or G2 progression by *cyclin F* knockdown is a consequence of stabilized E2F7/8.

Overexpression of E2F7^R894A mutant delays G2-M progression
If cyclin F dependent degradation of atypical E2Fs is important for G2/M progression, then a non-degradable version of an atypical E2F should slow down cell cycle progression. To test this, we first compared the appearance of E2F7^WT and E2F7^R894A proteins when adding doxycycline immediately after HU release (Fig 5A). Immunoblotting analysis revealed that 6 to 12 hours after addition of doxycycline the protein levels of mutant version E2F7^R894A were increased compared to E2F7^WT, whereas mRNA levels of E2F7^R894A were lower than E2F7^WT (Fig 5B). This finding excluded the possibility that the enhanced expression of E2F7^R894A was
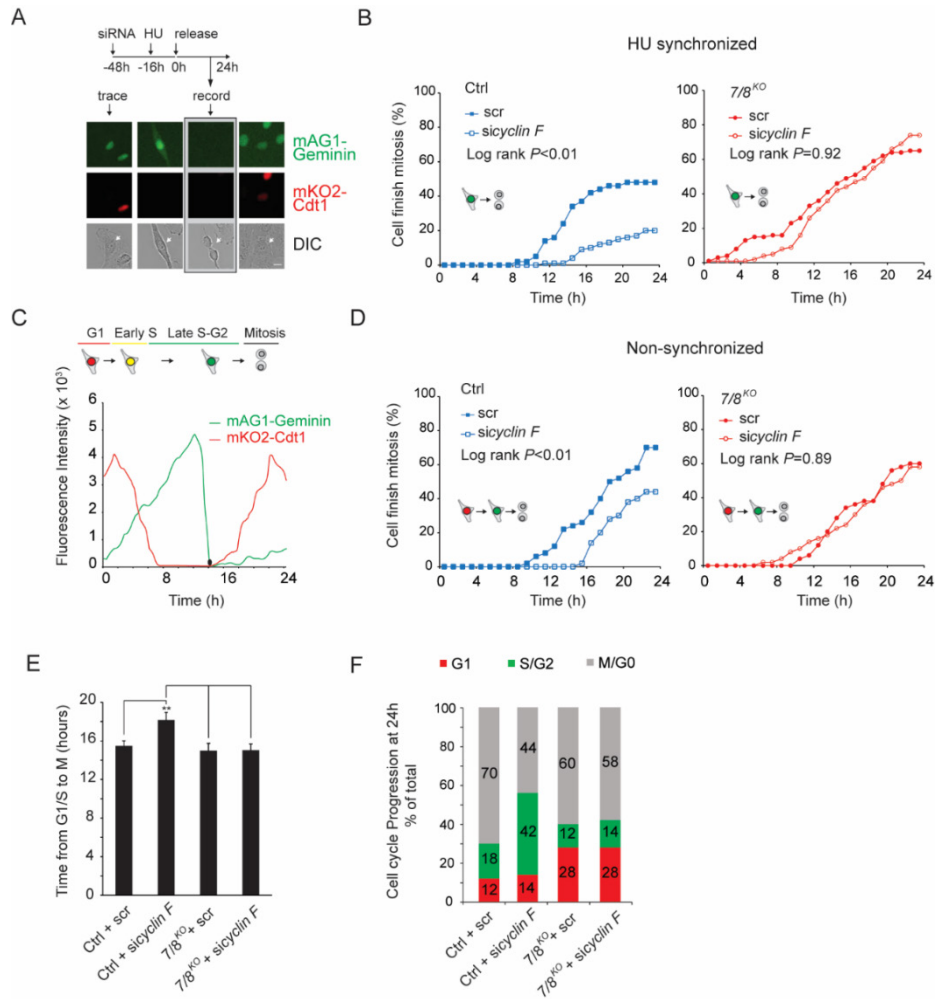
Figure 4. Failure to degrade E2F7 and E2F8 results in delayed G2/M progression.

related to higher transcript levels. Then we compared the G2/M progression between the HeLa cell lines in which either E2F7^{WT} or E2F7^{R894A} were induced by doxycycline after HU release (Fig 5C). In this live cell imaging assay, over-expression of E2F7^{WT} caused a minor cell cycle delay towards mitosis (Log rank P=0.054), while E2F7^{R894A} significantly reduced the number of cells finishing mitosis after 24h (Log rank P<0.01). Interestingly, we found the γ-H2AX level was significantly higher in cells expressing E2F7^{R894A} than E2F7^{WT}, suggesting that expressing E2F7^{R894A} induced DNA damage and thereby delayed cell cycle progression (Fig S3C). Together, these data demonstrated that expression of mutant version E2F7^{R894A} resulted in delayed G2-M progression.

Fig 4. Failure to degrade E2F7 and E2F8 results in delayed G2/M progression. A. Schematic view of the experimental setting for the HU-synchronized live cell imaging. 48 hours before imaging, RPE-FUCCI cells were transfected with siRNA against scramble or cyclin F. 16 hours before imaging, cells were synchronized at the G1/S border by HU (2 mM) treatment. Representative images from different channels are shown, and white arrows in Differential Interference Contrast DIC channel indicate the traced cell. **B.** Quantification of the number of Ctrl (left panel) and *7/8^KO* (right panel) RPE-FUCCI cells with *scr* or *sicyclin F* that completed mitosis after HU release. For each condition, 100 cells were monitored by live cell imaging. Each cell was followed until it successfully finished mitosis and divided into two daughter cells for a maximum of 24 hours. Log-rank tests were performed to analyze the statistical significance. **C.** Schematic view of the experimental setting for live imaging of asynchronous cells. 48 hours before imaging, RPE-FUCCI cells were transfected with siRNA against scramble or cyclin F. At the start of the imaging, G1 cells (red: mKO2-Cdt1 > mAG1-Geminin, 50 cells per condition) were enrolled and subsequently monitored though their entire cell cycle until mitosis. **D.** Knockdown of cyclin F causes a delay in mitotic entry that is dependent on E2F7 and E2F8. Number of Ctrl (left panel) or 7/8^KO (right panel) RPE-FUCCI cells with *scr* or *cyclin F* RNAi that finished mitosis during live cell imaging is shown. For each condition, 50 cells at G1 were monitored by live cell imaging. Each cell was followed until it successfully progressed through S and G2 phase, finished mitosis and divided into two daughter cells, for a maximum of 24 hours. Log-rank tests were performed to analyze the statistical significance. **E.** Loss of cyclin F delays the progression from G1/S transition to mitosis. Histogram shows the time from G1/S (mAG1-Geminin intensity increases to higher than 10% of the maximum value in three consecutive imaging frames) to completed mitosis. Only cells that finished mitosis were enrolled in this quantification. Student *t*-test was used to test the statistical significance, asterisks indicates the P value <0.01. **F.** Depletion of cyclin F stalls the cell cycle at late S/ G2. After 24 hours of live cell imaging, the cell cycle progression from panel E was quantified. Histogram shows the percentage of cells at each stage (at 24h) over the whole population (50 cells per condition).
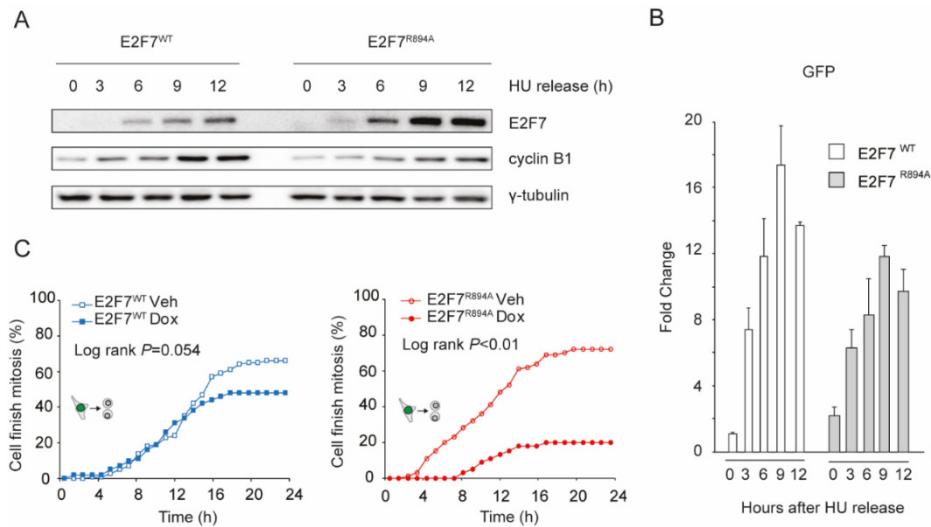
Figure 5. Overexpression of E2F7^{R894A} mutant delays G2/M progression. A. Disruption of cyclin F binding site increased stability of E2F7. E2F7^{WT} and E2F7^{R894A} constructs were integrated in to HeLa/TO system. Cells were arrested with HU for 16 hours before releasing into doxycycline containing medium, and cells were collected every 3 hours for immunoblotting. **B.** qPCR showing that mRNA level of E2F7^{WT} and E2F7^{R894A} were at comparable levels. **C.** Over-expression of E2F7^{R894A} delays cell cycle progression through G2-M phase. HeLa/TO cells expressing either wild-type or mutant version of E2F7 were arrested with 16h of HU, and then cells were released into fresh medium with or without doxycycline. Live cell imaging was performed to trace the G2-M progression of HeLa/TO cells.

Cyclin F controls transcription of DNA repair genes via degradation of E2F7/8.

To determine in an unbiased manner which transcripts are regulated by atypical E2Fs in a cyclin F dependent manner, we performed RNA sequencing on nocodazole-synchronized cells treated with scrambled (scr), *cyclin F*, *E2F7/8* or *cyclin F/E2F7/8 (triple)* siRNAs. We observed a substantial overlap between genes that were downregulated by *cyclin F* siRNA compared to scr, and genes that were upregulated in *cyclin F/E2F7/8* siRNAs compared to *cyclin F* siR-NAs. (Fig 6A, S4A). Gene ontology analysis showed that these genes, which were downregulated genes after cyclin F knockdown and rescued by additional E2F7/8 knockdown, were strongly enriched for DNA repair and replication pathways (Fig 6B, Fig S4B). Among these DNA repair genes, we observed many known E2F7/8 target genes, such as RAD51, MSH2/6, EXO1, and CHEK1[2]. Quantitative PCR and immunoblotting on a subset of these DNA repair genes confirmed that they were indeed downregulated by cyclin F depletion in an E2F7/8-dependent manner (Fig 6C, D). Consistently, the expressions of E2F7/8 target genes involved in DNA replication showed a similar expression pattern (Fig 6C, lower panel). We also confirmed
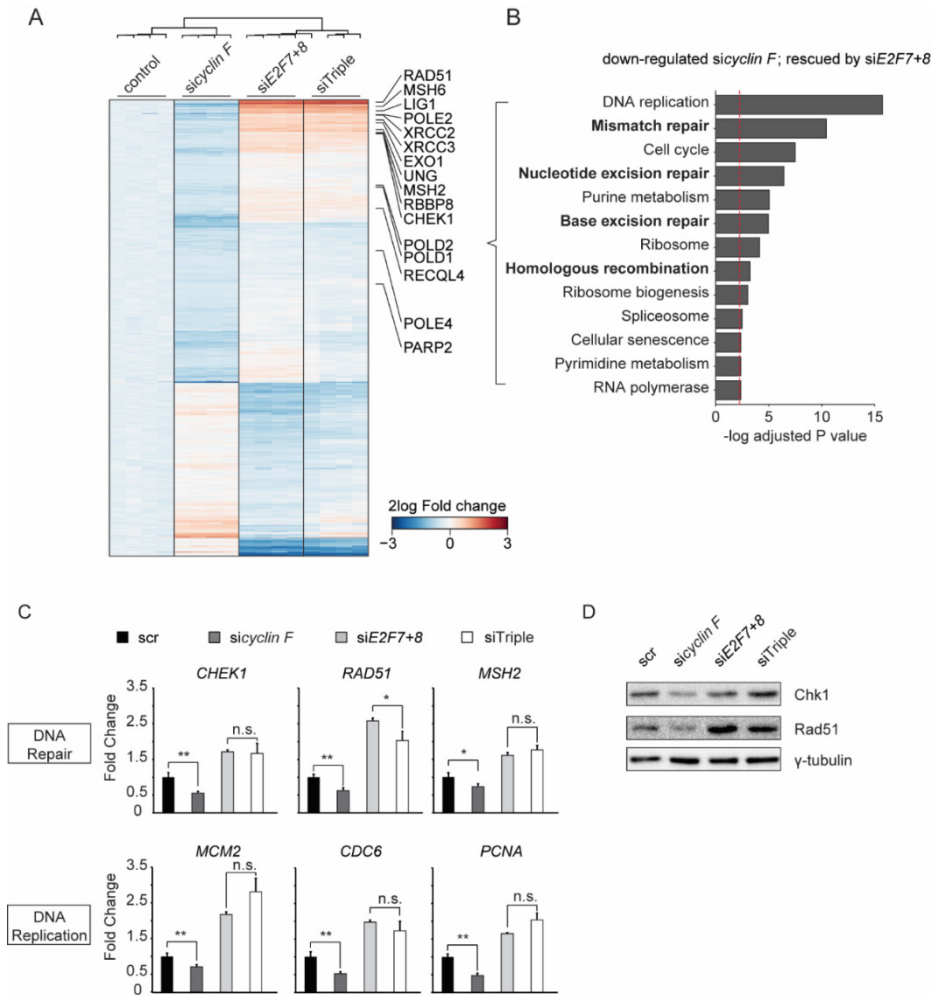
Figure 6. Cyclin F regulation of DNA replication and DNA repair genes is dependent on E2F7/8. A. Heatmap showing differentially expressed genes after cyclin F knockdown, and rescued by additional E2F7/8 depletion. Highlighted genes are all involved in DNA repair. Cells were arrested with nocodazole for 16 hours prior to harvesting to minimize bias from potential differences in cell cycle progression between the different conditions. **B.** KEGG pathway analysis of genes downregulated by cyclin F knockdown, and rescued by additional E2F/8 depletion. Bars represent -log P values, such that larger values mean stronger statistical significance. The cut-off P value 0.05 is shown as a red dotted line. **C.** qPCR showing the RNA expression of atypical E2F- target genes that are involved in DNA replication or DNA repair. HeLa cells were transfected for 48 hours with siRNAs as indicated. Cells were incubated with nocodazole for 16 hours before harvesting. Data represent averages ± SEM (n=3); *P<0.05 or **P<0.01 (Student's t-test). n.s.: not significant. **D.** Immunoblotting showing the protein levels of Chk1 and Rad51 in the indicated siRNA conditions. HeLa cells were treated with nocodazole for 16 hours prior to harvesting.

this finding in RPE cells (Fig S4C). Interestingly, we found that genes known to control mitotic entry, such as *PLK1* (polo-like kinase 1) and *CCNB1* (cyclin B1) were upregulated in response to *cyclin F* knockdown (Fig S4D), but were not affected by knockdown of atypical E2Fs. This is in line with a previous study where it has been shown that cyclin F suppresses a B-Myb driven transcriptional program regulating mitotic gene expression[25]. Phosphorylated MPM2 as an indicator of M phase was slightly increased in si*cyclin F* and siTriple conditions compared to scr and si*E2F7+8* conditions, suggesting that depletion of cyclin F also affects mitotic entry through regulation of B-Myb target gene expression (Fig S4E).

Degradation of atypical E2Fs sustains DNA repair functions in G2

Multiple DNA damage repair pathways, including mismatch repair (MMR), nucleotide excision repair (NER), base excision repair (BER) and homologous recombination (HR) are regulated by atypical E2Fs in a cyclin F dependent manner (Fig 6B). We wondered if these transcriptional effects of cyclin F depletion would have functional consequences. Therefore, we tested if HR repair was impaired in cyclin F-depleted cells. We found that knockdown of cyclin F significantly reduced HR repair efficiency, and this repair deficiency was fully recovered by additional knockdown E2F7 and E2F8 (Fig 7A and Fig S5A, see Material and Methods).

If failure to degrade atypical E2Fs resulted in enhanced repression of DNA damage repair genes, then DNA lesions would accumulate. To test this idea, the level of phosphorylated γ-H2AX was measured using immunofluorescence staining in nocodazole-arrested cells (Fig 7B). Indeed, loss of *cyclin F* resulted in a significant increase of γ-H2AX levels, when compared with the scrambled condition. In addition, combined knockdown of *E2F7/8* and *cyclin F* rescued the DNA lesions, suggesting that DNA repair capacity during G2 was restored by sustaining E2F-dependent DNA repair gene expression.

To monitor the dynamics of DNA damage repair by live cell imaging, a truncated version of 53BP1-mApple construct was integrated into RPE cells[26]. In response to DNA damage, mApple-tagged 53BP1 localizes to damage sites, which can be seen as bright foci. Therefore measurement of the numbers of 53BP1 foci in the nucleus can be used to monitor the onset and repair of DNA damage. RPE cells stably expressing this construct were transfected with siRNA targeting *cyclin F* or *E2F7/8*, and then treated with HU for 16 hours to arrest the cell cycle at the onset of S phase before live cell imaging. We first quantified the number of 53BP1 foci in the nucleus at the start of HU release. Interestingly, in the non-treated conditions, knockdown of *cyclin F* significantly increased the number of 53BP1 foci compared to scrambled siRNA (Fig S5B). Furthermore, combined knockdown of *cyclin F* and *E2F7/8* attenuated this increase, suggesting that DNA damage repair function was restored. This result indicated again that the cell cycle delay caused by loss of *cyclin F* was due to a decrease in DNA repair capacity by enhanced repressor activity of E2F7/8. We noticed that the average number of
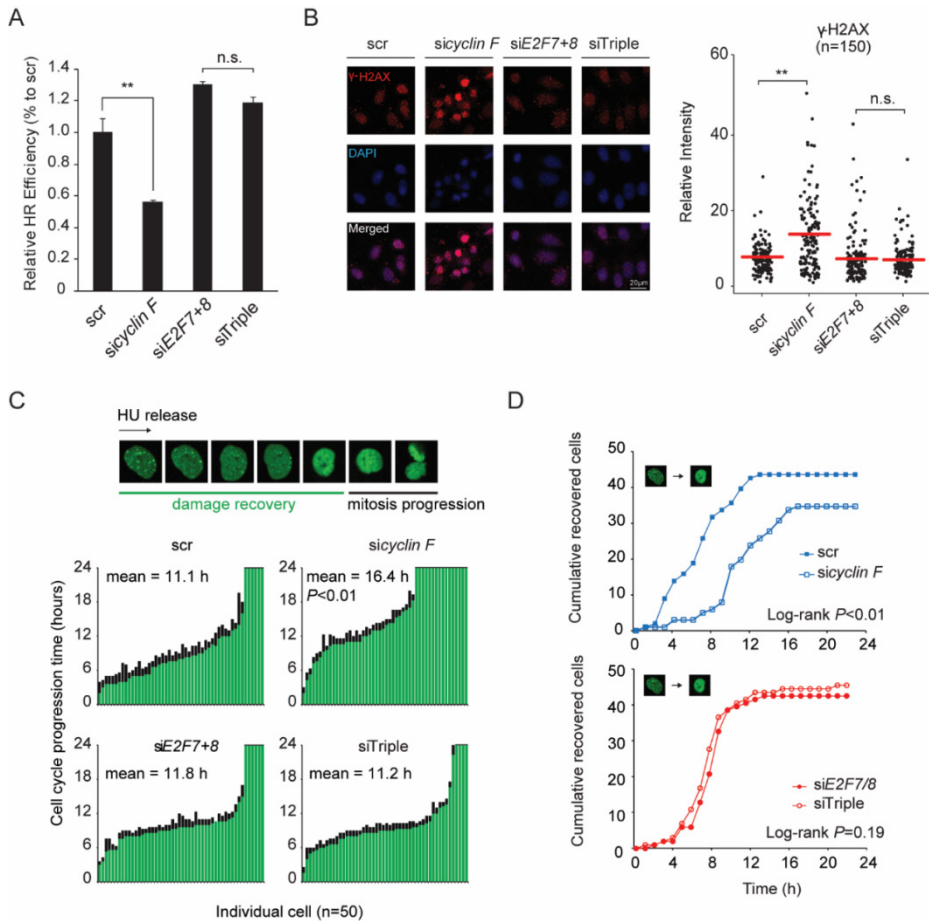
Figure 7. Degradation of atypical E2Fs maintains DNA damage repair.

53BP1 foci per nucleus was significantly higher in scr and si*cyclin F* conditions compared to si*E2F7+8* and siTriple conditions when cells were synchronized with HU (Fig S5B). This result suggested that depletion of E2F7 and E2F8 can elevate the DNA damage repair capacity not only to compensate the loss of cyclin F but also to an even higher level. This is consistent with our RNA-seq data showing that si*E2F7+8* and siTriple had enhanced expression of DNA repair genes compared to the control and si*cyclin F* conditions. We then quantified the DNA damage recovery time (from HU release until all 53BP1 foci disappeared) and cell division events of individual cells (Fig 7C and D). We found that loss of cyclin F significantly lengthened the damage recovery time to 16.4 hours, compared to 11.1 hours of scrambled condition. Furthermore, a substantial number of si*cyclin F* cells failed to recover from DNA damage within 24 hours, compared to scrambled control (Fig 7C). Most importantly, the DNA damage recovery time decreased to a length similar to the scrambled group by additional knockdown

of *E2F7/8*, indicating that the delay of damage recovery was dependent on the atypical E2Fs functions. To further investigate when the DNA damage repair occur after HU release, we measured the average 53BP1 foci number over time (Fig S5C). We found that depletion of cyclin F caused an prolonged recovery from 53BP1 at 6-8 hours after HU release. More importantly, this is the time window when the cells progressed to G2 phase (Fig S5D), supporting our reasoning that cyclin F dependent degradation of E2F7/8 impact on G2 progression through regulation of DNA damage repair.

Figure 7. Degradation of atypical E2Fs maintains DNA damage repair. A. Loss of *cyclin F* induced E2F7/8-dependent Homologous Recombination deficiency. HeLa cells that were stably transformed with pDR-GFP were transfected with siRNA as indicated. After 24h, cells were transfected with GFP-HR plasmid. 48h after the initial transfection, cells were harvested for Flow-cytometry. GFP positive cells were gated (Fig EV5A). Relative HR efficiency were adjusted to the scramble siRNA condition. Data represent averages $\pm$ SEM (n=3); *P<0.05 or **P<0.01 (Student's *t*-test). n.s.: not significant. **B.** Loss of *cyclin F* induced E2F7/8-dependent γ-H2AX accumulation. HeLa cells were transfected with indicated siRNA for 24 hours, and then treated with nocodazole for 16 hours before fixation for immunofluorescence staining of γ-H2AX. DAPI was used to stain the cell nucleus. Relative intensity of γ-H2AX was quantified by Image J software, and 150 cells were quantified for each condition. Red bars represent averages; **P<0.01 (Student's *t*-test). n.s.: not significant. Scale bar 20 μm. **C.** Loss of *cyclin F* increased DNA damage recovery time before cell division. RPE cells integrated with the 53BP1 construct were transfected with indicated siRNA for 24 hours, and then treated with HU for 16 hours. At the beginning of the imaging, only the single cells with at least one 53BP1 foci were traced, till the time frame that no 53BP1 foci was observed. The mitotic progression of the cells was defined as the duration from damage recovery to cell division. Histogram shows the damage recovery time (green) and the mitotic progression (black) of 50 cells for each condition. Chi-square analysis was performed to test the statistical significance (P<0.01). **D.** Knockdown of *cyclin F* caused a delay in DNA lesion recovery that is dependent on E2F7/8. The cumulative curves represent the add-up number of cells that overcome the DNA damage lesions, for a time frame of 24 hours. For each condition, 50 cells were quantified. Log-rank tests were performed to analyze the statistical significance.

DISCUSSION

In the current study, we demonstrated a biological model that cyclin F-dependent degradation of atypical E2Fs is critical for DNA repair and G2-phase progression (Fig 8). We first showed that E2F7 and E2F8 are targeted for degradation by cyclin F during G2/M phases. In an unperturbed cell cycle , cyclin F promotes the degradation of atypical E2Fs to allow a timely G2/M transition. Previous studies demonstrated that cyclin F functions a key regulator of the cell cycle[10,11,27]. *CCNF*, the gene encoding cyclin F, is highly conserved across different species. Moreover, its function is essential in the embryonic development of mice[10]. MEFs (mouse embryonic fibroblasts) derived from *Ccnf⁻/⁻* mice show reduced population doubling times and a delay in cell cycle re-entry from quiescence, indicating that cyclin F is required for cell proliferation. Interestingly, this slowdown in cell cycle re-entry may be partially explained by the inhibition of APC/C^Cdh1 by cyclin F during G0/G1 phase. Cdh1 is a substrate of cyclin F, and deletion of cyclin F resulted in stabilization of Cdh1 and inhibition of S-phase entry[11]. However, it is important to note that cyclin F expression is low at G0/G1 and gradually increases after S phase, and most of cyclin F-mediated degradation occurs during G2 phase (also shown in Fig 3C). These findings raised the question whether cyclin F regulates G2 phase progression and, if it does, by which mechanism. In this study, we showed that cyclin F knockdown leads to an E2F7/8-dependent G2/M transition delay. Most importantly, by using single live cell imaging, we demonstrated that this G2/M transition delay was likely due to a prolonged DNA repair period (Fig 7C). Cyclin F induces the degradation of E2F7/8 to maintain the expression of DNA repair genes thereby ensuring flawless cell cycle progression through G2 until mitotic entry.

Another central function of cyclin F is its role in guarding cells against genotoxic stress and genomic instability during the cell cycle. It has been shown that cyclin F promotes the degradation of the centrosomal protein CP110 and the DNA replication protein CDC6 thereby ensuring mitotic fidelity and preventing DNA re-replication[12,20]. Moreover, cyclin F targets the ribonucleotide reductase RRM2 and stem loop binding protein SLBP for proteasomal degradation, which provides a balanced dNTP pool for DNA repair, and prevents SLBP-dependent accumulation of *H2AFX* mRNA translation to reduce susceptibility to genotoxic stress[18,19]. In line with these findings, our data demonstrate that cyclin F sustains the expression of DNA repair genes such as *RAD51*, *CHEK1* and *BRCA1*, through degradation of the atypical E2Fs in G2 phase. Interestingly, in response to irradiation, cyclin F has been shown to be down-regulated in an ATR-dependent manner, which resulted in stabilization of SLBP and RRM2 to promote DNA repair[18,19]. Interestingly, both *SLBP* and *RRM2* are *bona fide* targets of E2F7/8[1,2]. Therefore, we hypothesized that cyclin F controls SLBP and RRM2 expression at two different levels: directly via their ubiquitin-dependent degradation, and indirectly via degradation of the transcriptional repressors E2F7/8. These complex regulation mechanisms mediated by cyclin F could be significant to the cancer field, since aberrant expression of RRM2 has been

found in multiple type of cancers and failure to maintain the balance of dNTP can cause genome instability[28-30].

In addition to *RRM2* and *SLBP,* cyclin F targets CDC6 for degradation, which is also transcriptionally regulated by atypical E2Fs[1,2]. Thus, E2F-dependent transcription and SCF[cyclin F] appear to have partially overlapping functions. Therefore, the repressor functions of atypical E2Fs could potentially compensate for the loss of cyclin F. In addition, failure to degrade these overlapping targets (such as CDC6) in G2 phase could result in the re-initiation of DNA replication leading to genome instability[20]. Therefore, we hypothesized that atypical E2Fs might act as a fail-safe mechanism to repress the expression of key cell cycle genes in case of inactivation of SCF[cyclin F]. Such a compensation mechanism could help to minimize the occurrence of genome instability.

Our data indicate that the biological significance to keep an intermediate level of E2F7/8 during the G2 phase is most likely to support DNA damage repair before a cell can enter mitosis. This is in line with our previous work, which showed that the DNA replication stress kinase Chk1 phosphorylates E2F7/8 to inhibit its transcriptional repressor function on DNA repair genes and thereby promotes DNA lesion recovery upon replication stress[31]. Moreover, two recent studies indicated that loss of E2F7 conferred resistance to DNA damaging drugs by elevating expression of DNA repair genes such as *Rad51*, *51BP1* and *FANCD2*[32,33]. These results raise the question whether stabilization of E2F7/8 would in turn sensitize cancer cells towards chemotherapy.

To conclude, our study discovered a novel regulatory mechanism for atypical E2Fs whereby cyclin F-mediates degradation during the G2- phase of the cell cycle. Degradation of E2F7 and E2F8 is of importance for proper G2 progression as depletion of cyclin F leads to a defect in cell cycle progression that depends on atypical E2Fs. Moreover we provide novel insights into the regulation of DNA damage repair gene expression during G2/M phases, in which cyclin F-mediated degradation of atypical E2Fs promotes DNA damage repair by sustaining DNA repair gene transcription.

MATERIAL AND METHODS

Cell culture, cell line generation and transfection

HeLa, hTERT-RPE1 and HEK 293T cell lines were purchased from ATCC and cultured in DMEM medium (41966052, Thermo Fisher Scientific) containing 10% fetal bovine serum (10500064, Life Technologies). The HeLa cell line with stably transformed with pDR-GFP was a gift from prof. dr. M.A.T.M. (Marcel) van Vugt, University of Groningen, The Netherlands. Site-directed mutagenesis was performed by a two-step PCR amplification (PCR protocol and primers are provided in Table 1). Successful mutations were confirmed by Sanger sequencing (Macrogen, Inc). Other drugs used in this study are: Nocodazole (50 ng/ml, M1404, Sigma Aldrich); Hydroxyurea (2 mM, H8627, Sigma Aldrich); Thymidine (2mM, T9250, Sigma Aldrich); Cycloheximide (50 μg/ml, 01810, Sigma Aldrich), MLN4924 (0.1 μM, MLN-4924, Active Biochem), MG132 (1 μg/ml, Peptide International, IZL-3175-v_5mg).

To transfect HEK cells, 130 μg/ml PEI (Polyethylenimine, 23966, Polysciences) was mixed with the desired plasmids (15 μg) containing DMEM (ratio of 1:1). Mixtures were added directly to the cells and incubated for 6 hours before being replaced with fresh media. ON-Target plus Smartpool siRNAs (2 nM) were products from GE Dharmacon; siRNA transfection was carried out according to the manufacturer's protocol using RNAiMax (13778075, Thermo Fisher Scientific). The following siRNAs were used: Dharmacon L-003215-00-0005 (si*cyclin F/*), Thermo Fisher HSS175354 (si*E2F7*), Thermo Fisher HSS128758 /HSS128760 (si*E2F8*), Dharmacon D-001210-02-05 (Scrambled).

The lentiviral construct containing a truncated version of 53BP1 tagged with mApple was obtained from Addgene (Apple-53BP1trunc was a gift from Ralph Weissleder (Addgene plasmid # 69531 ; http://n2t.net/addgene:69531; RRID:Addgene_69531)). Lentivirus was produced by transfecting HEK 293T cells with 10ug lentiviral packaging plasmids (1:1:1) and 10 ug of the 53BP1 construct with PEI for 2h. Then 10ml fresh medium was added and virus was harvested after 48h. 3ml of virus containing medium and polybrene (8 ug/mL) was added to PRE cells for an incubation of 24hours. RPE cells containing the construct were selected with puromycin (1.0 μg/ml) for 5 days.

Immunoprecipitation and Immunoblotting

Cells were washed twice with cold PBS and collected by scraping and spinning. Cells were lysed in RIPA buffer composed of 50 mM Tris-HCl, 1 mM EDTA, 150 mM NaCl, 0.25% deoxycholic acid, 1% Nonidet-P40, 1 mM NaF and NaV$_3$O$_4$, and protease inhibitor cocktail (11873580001, Sigma Aldrich) for 30 minutes on ice. Then lysates were centrifuged at 12,000 g for 10 min to collect supernatants. Finally Laemmli buffer was added, and the samples were subjected to SDS-PAGE and immunoblotting. For immunoprecipitations, cells were lysed in RIPA buffer and immunoprecipitations were carried out by incubating 20 μl of anti-FLAG M2 Affinity Gel

(A2220, Sigma-Aldrich) or GFP-Trap (gta-20, Chromotek). After the pull-down, the agarose beads were washed three times with RIPA and PBS before proceeding to a standard SDS-PAGE and immunoblotting. All antibodies used in this paper are listed in Table 1.

Flow cytometry

Cells were harvested by trypsinization and subsequent fixation with 70% ethanol and over-night storage at 4 °C. Before staining, cells were washed twice with ice cold Tris-buffered saline (TBS) and re-suspended with 500 µl staining buffer that contained 20 µg/ml propidium iodide (P4170, Sigma Aldrich), 250 µg/ml RNase A (RNASEA-RO ROCHE) and 0.1% bovine serum albumin (A8531, Sigma Aldrich). Samples were loaded on a BD FACS Canto II Flow cy-tometer. Cell cycle analysis was conducted using the Cell Cycle analysis function from FlowJo v10.0 software.

RNA-sequencing

Total mRNA was collected using Qiagen's RNeasy kits. Sequencing libraries were then pre-pared using the Truseq Poly-A kit, according to the manufacturer's instructions. All 16 sam-ples were pooled into one lane of an Illumina Nextseq500 sequencer. Quality of the raw sequencing data was first checked using the program FastQC. Then, sequencing reads were trimmed for adapter sequences, and mapped to the human genome (assembly hg38) us-ing STAR version 2.4.2a. All mapped reads were counted using HTSeq version 0.6.1 in union mode. The raw count data were then used to perform differential expression analysis using DESeq2. Heat-maps were created using the software package pheatmap, and represent fold changes calculated from normalized count data. The RNA-sequencing data have been de-posited in NCBI's Gene Expression Omnibus and are accessible through GEO Series accession number GSE133416 (https://www.ncbi.nlm.nih.gov/geo/query/acc.cgi?acc=GSE133416). Down-regulated genes in *cyclin F* knockdown, and rescued by additional E2F7/8 knockdown are shown in Table 2. DEgenes_RNAseq_CCNF.

Live imaging

For live cell imaging, 4,000 RPE-FUCCI cells were seeded into a glass-bottom µ-Slide 8-well plate. siRNA transfections were carried out the next day, and imaging started at 48 hours after cell seeding. A Nikon Stochastic Optical Reconstruction Microscope (A1R-STORM) was used for live imaging. For each condition, 5x5 fields (63x magnification / field) were obtained. Auto-focus was set to capture photos from GFP (488 nm), RFP/mApple (555 nm) and differ-ential interference contrast (DIC) channels every 20 minutes for 24 hours.

The software NIS-Element version 4.51.01 was utilized for the quantification. For the HU arrest/release experiment, 100 cells were traced manually under the DIC channel as previ-ously described[31]. For the asynchronized experiment, the quality of the movies was first im-

proved with the auto-scale rolling balls option, with the radius set to 30. Each cell was marked and traced with the ROI (Regions Of Interest) function. In total 50 individual cells were selected for each condition, and one additional blank ROI was made to rule out the background signal. The fluorescence intensity from 480nm and 560nm channels (based on each selected ROI) was obtained with the "Time measurement" option in ROI panel. Cell cycle stages were determined by the fluorescence signal intensities of CDT1-mKusabira Orange (mKO) and Geminin-mAzami Green (mAG): G1 stage: Red, mKO signal > mAG signal; G1-S transition: Yellow, mAG signal increases to 10% of maximum in three consequent frames; Late S to G2: Green, mAG signal > mKO signal; M to early G1: Colorless, disappearance of mAG signal, and evidence of mitotic division from Differential Interference Contrast DIC image.

For quantification of 53BP1 foci in Fig S5B, cell image was obtained from each time point and 50 cells per condition were randomly selected for foci counting.

Quantitative PCR

Isolation of RNA, cDNA synthesis and quantitative PCR were performed based on manufacturers' instructions for QIAGEN (RNeasy Kits), Thermo Fisher Scientific (cDNA synthesis Kits) and Bio-Rad (SYBR Green Master Mix), respectively. Gene transcript levels were determined using $\Delta\Delta C_t$ method for multiple-reference gene correction. β-actin and GAPDH were used as references. qPCR primer sequences are provided in Table 1.

CRISPR-CAS9 knockout

RPE-*hTERT*-FUCCI cells (a kind gift from prof. Rene Medema; Netherlands Cancer Institute) were transduced with a lentiviral expression vector encoding both Flag-tagged Cas9, and a single guide (sg) RNA sequence against E2F7 (sgRNA #1: GTGCTGCCAGCCCAGATATA, sgRNA #2: GAGCTAGAAACTTCTGGCAC) or E2F8 (sgRNA #1: GTTCCTCTGCCACTTCGTCA, sgRNA #2: GATCTCTGTTGCGGATCTCA) cloned into a pSicoR backbone as previously described[34]. Lentiviral particles were produced by co-transfecting the pSicoR construct with 3rd generation packaging plasmids into 239T cells. The sgE2F7 and sgE2F8 vectors contained puromycin and blasticidin resistance cassettes, respectively, thus allowing for sequential selection of E2F7- and E2F8-mutant clones by manual picking. Indel mutations were confirmed with Sanger sequencing, and complete deletion of E2F7 and E2F8 was verified by immunoblotting for E2F7/8. Cells expressing the vector containing only Cas9, but no sgRNA, served as control cell lines.

Statistical analysis

Immunoblots, immunoprecipitation, flow cytometry, FACS sorting and qPCR results were repeated three times unless otherwise described in the figure legends. Statistical analyses on qPCR were analyzed by Student *t*-test. Statistical test on Fig 5C was analyzed by Chi-square

test, and cumulative curves from 4B/C, 5D were analyzed by Log-rank tests.

ACKNOWLEDGEMENTS

AUTHOR CONTRIBUTIONS

R.Y and Q.L performed the experiments. H.A.S helped quantification of the live cell imaging and generated *E2F7/8*-mutant cell lines. L.Y performed the ubiquitylation assays, D.G. kindly provided the plasmid constructs encoding F-box proteins and provided valuable input in the identification of cyclin F as E2F7/8 binding partner. R.J.L. designed and created the lentiviral CRISPR constructs. R.Y, D.G., B.W and A.d.B conceived the study and experimental approaches, data analysis and wrote the manuscript.

CONFLICT OF INTEREST

The authors declare no conflict of interest in the present study.

SUPPLEMENTARY MATERIAL

Table 1: Mutagenesis primers

Mutagenesis	Forward primer (5'-3')	Reverse primer (3'-5')
E2F7 RxI 110/112 AxA	G A A C G C A T C C T C C T T A T-T C T C A G C G G G T G C G A A-CAGCTCCTTTTTCTTCTCC	GGAGAAGAAAAAGGAGCT-GTTCGCACCCGCTGAGAATAAG-GAGGATGCGTTC
E2F7 RxL 221/223 AxA	CTCTCCCAGTCTCTGTGCGGTC-GCCAGGGTTTTGGGGAGG	CCTCCCCAAAACCCTGGCGAC-CGCACAGAGACTGGGAGAG
E2F7 RxL 894/896 AxA	C C C G C T G C T A G A G A T T T C T-G C T C T C G C C T G G G C T-GAGCTAGTGTTT	AAACACTAGCTCAGCCCAGGC-GAGAGCAGAAATCTCTAGCAG-CGGG
E2F8 RxL 15/17 AxA	CAGGGGGCTTTTCATCGCTC-CCGCTTTATGTGGCTCAGAAAA-GAGGTTTTCCT	AGGAAAACCTCTTTTCTGAG-CCACATAAAGCGGGAGCGAT-GAAAAGCCCCCTG
E2F8 RxL 81/83 AxA	GCACTTCGGTTGTCAGACGCGC-CCGCTTTCTGATCTCGACTTCGG	CCGAAGTCGAGATCAGAAAG-C G G G C G C G T C T G A C A A C-CGAAGTGC
E2F8 RxI 408/410 AxA	GCTGCTGGGAGCGGAACTGG-CCTTCGCCCGATCATTTTCTAT-GCTC	GAGCATAGAAAATGATCGGGC-GAAGGCCAGTTCCGCTCCCAG-CAGC
E2F8 RxI 860/862 AxA	T A T C C T C A G T T G A G A C T T C-CGCTTTGGCCTGTGGGACAAA-GAGGGTTC	GAACCCTCTTTGTCCCACAGG-CCAAAGCGGAAGTCTCAACT-GAGGATA

Table 2: qPCR primers

Genes	Forward primer (5'-3')	Reverse primer (3'-5')
ACTB	GATCGGCGGCTCCATCCTG	GACTCGTCATACTCCTGCTTGC
GAPDH	CTCTGCTCCTCCTGTTCG	GCCCAATACGACCAAATCC
E2F7	CTCCTGTGCCAGAAGTTTC	CATAGATGCGTCTCCTTTCC
E2F8	AATATCGTGTTGGCAGAGATCC	AGGTTGGCTGTCGGTGTC
CCNE1	GACACCATGAAGGAGGACGG	ATTGTCCCAAGGCTGGCTC
CDC6	AAACCCGATCCCAGGCACAG	AGGCAGGGCTTTTACACGAGGAG
MCM2	GGCAATGATCCTCTCACCTCC	CATCCTCTTCTTCCTCCAGGG
CDT1	CGTCCAGGACATGATGCGTAGG	TTGAAGGTGGGGACACTGCG
CCNF	AGGTGGTGTGTCAGAGTCTCCC	TCCCATAAGGAAAGACCTGTGC
RAD51	TGCTTATTGTAGACAGTGCCACC	CACCAAACTCATCAGCGAGTC
CDC25A	GAGATCGCCTGGGTAATGAA	TGCGGAACTTCTTCAGGTCT

Table 3: Antibodies for immunoblotting

Name	Company	Catalog	Dilution
GFP	Abcam	AB6673	1:1000
Flag	Sigma-Aldrich	F3165	1:2000
E2F7	Santa Cruz	sc-66870	1:1000
E2F8	Abcam	109596	1:1000
γ-tubulin	Sigma-Aldrich	T6557	1:5000
CDC6	Santa Cruz	sc-9964	1:1000
Cyclin B1	Santa Cruz	sc-245	1:1000
Cyclin F	Santa Cruz	sc-952	1:1000
Myc	Santa Cruz	sc-40	1:1000

Figure S1. Cyclin F binds to E2F7 and E2F8. A. Cell cycle analysis of the double thymidine block and release experiment shown in Fig 1A. HeLa cells were synchronized by double thymidine block and then released in fresh medium. Asynchronized (AS) and synchronized cells were harvested at the indicated time points for propidium iodide staining and flow-cytometry analysis. **B.** E2F7 and E2F8 are degraded during G2/M phases. HeLa cells were treated with hydroxyurea (HU, 2 mM) for 16 hours to arrest cells at G1/S border. Then HU was removed and cells were released into fresh medium. Protein samples were harvested at the onset of release and 8 hours after release. E2F7/8 levels were measured by immunoblotting. Protein expression of cyclin B1 was used as a marker for G2 or M cell cycle progression, and γ-tubulin was used as loading control. Asterisk indicates the specific band of E2F7 detection. **C.** Immunoprecipitation shows that cyclin F physically interacts with E2F7/8 *in vitro*. HEK293 cells were transiently transfected with either EGFP-tagged empty vector (EGFP), EGFP-tagged E2F7 or EGFP-tagged E2F8. MG132 was added to the cells 5 hours before harvesting at 48 hours post transfection. Cells were harvested and lysed for immuno-precipitation using GFP resin. Asterisk indicates the E2F8-specific band. **D.** Reciprocal IP demonstrated the bindings between cyclin F and E2F7/8. HEK cells were transfected with Flag-tagged empty vector or cyclin F, together with GFP-tagged E2F7 or E2F8. MG132 was added to cells 5h before harvesting, and Co-IP was performed using Flag resin. **E.** Homology of atypical E2Fs at their C-terminus shows that the cyclin F-binding motifs are conserved among different species. **F.** Wild-type or R408A mutant of EGFP-tagged E2F8 were co-transfected with either empty vector or Flag-tagged cyclin F in HEK293 cells. Nocodazole was added to cells 8h before harvest. 48 hours after transfection, cells were collected and lysed for immunoblotting.
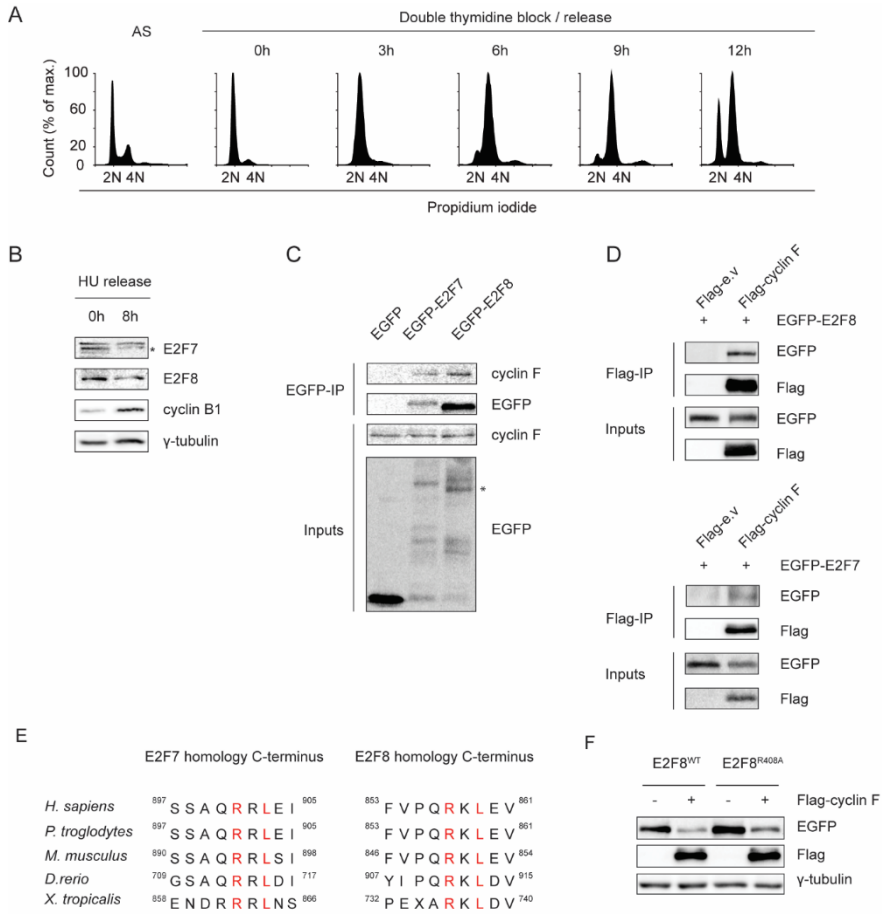
Figure S1. Cyclin F binds to E2F7 and E2F8.

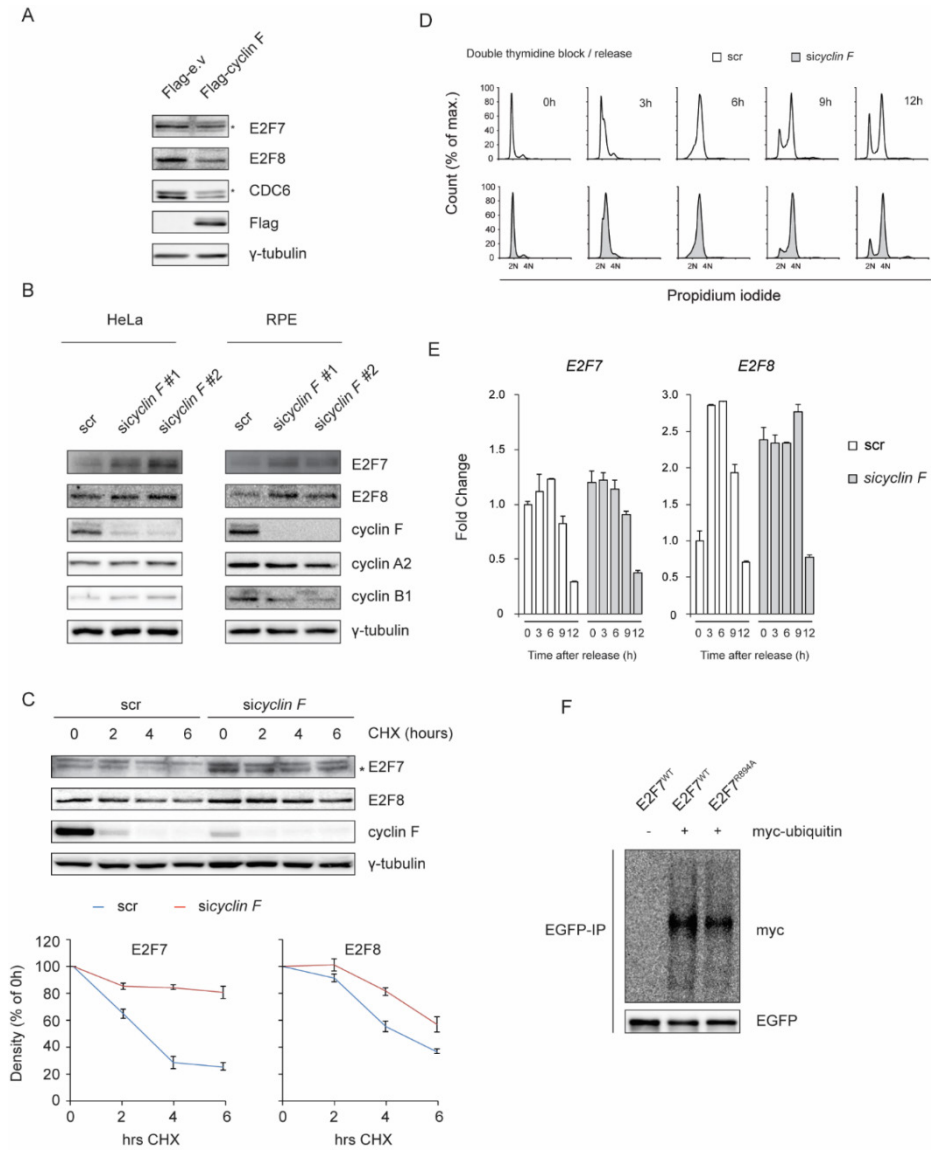**Figure S2. Cyclin F-dependent degradation of E2F7 and E2F8.**

Figure S2. Cyclin F-dependent degradation of E2F7 and E2F8. A. Over-expression of cyclin F down-regulates endogenous E2F7 and E2F8. HEK cells were transiently transfected with Flag-tagged empty vector or cyclin F. Cells were harvested and lysed 48 hours after transfection. Endogenous E2F7 and E2F8 were measured by immunoblotting. Detection of CDC6, a known cyclin F target, served as a positive control. Asterisk indicates the E2F7 and CDC6 specific bands detection. **B.** Knockdown of cyclin F stabilized E2F7 and E2F8. HeLa and RPE cells were transfected with either scramble siRNA or individual cyclin F siRNA. Cells were harvested at 48 hours post transfection. Protein levels of E2F7/8 were analyzed by immunoblotting. **C.** The knockdown of cyclin F increases the half-life of E2F7/8. HeLa cells were transfected with scrambled siRNA (scr) or cyclin F siRNA (*si-cyclin F*). 24 hours after transfection, HeLa cells were treated with cycloheximide (CHX). Cells were harvested at the indicated time point after CHX treatment. Asterisk indicates the specific detection of endogenous E2F7. Quantifications (lower panels) were performed based on two independent experiments. **D.** Cell cycle analysis of the double thymidine block and release of the experiment shown in Fig 3D. HeLa cells were transfected with siRNA against scrambled (scr) or cyclin F for 24 hours. Then cells were synchronized with double thymidine block and released into fresh medium. Samples were harvested at the indicated time points for propidium iodide staining and flow-cytometry analysis. **E.** mRNA levels of E2F7 and E2F8 were not affected by knockdown of cyclin F. qPCR was preformed to analyze the double thymidine block and release of the experiment shown in Fig 3D. **F.** E2F7[R894A] mutant has reduction of ubiquitylation. HEK cells were transiently transfected with either empty empty vector or myc-tagged ubiquitin, together with either EGFP-tagged E2F7[WT] or E2F7[R894A] . MG132 was added to cells 5h before harvesting, and EGFP-IP was performed.
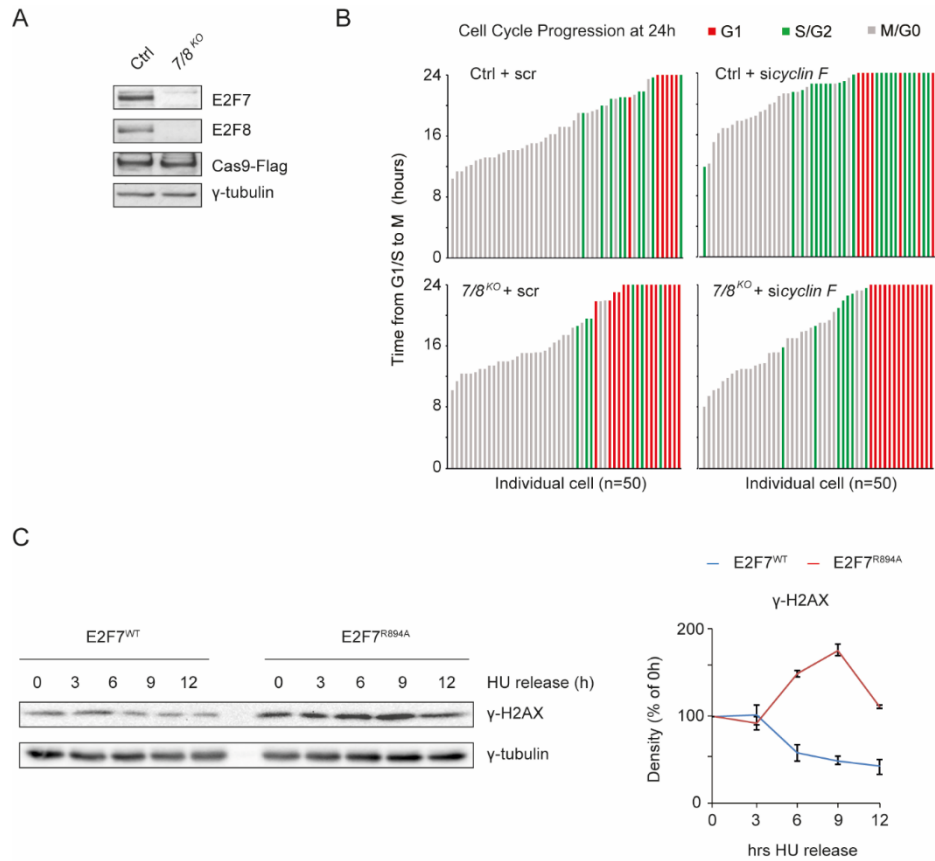
Figure S3. Failure to degrade E2F7/8 caused cell cycle delay and DNA damage accumulation. A. Confirmation of efficient deletion of *E2F7* and *E2F8* in RPE-FUCCI cells utilizing CRISPR-CAS9 technology. Cells were transduced with Flag-tagged Cas9, and either a construct lacking sgRNA (Ctrl), or a construct containing sgRNA directed against *E2F7* and *E2F8* (*7/8*^{KO}). Protein levels were analyzed by immunoblotting. **B.** Depletion of cyclin F stalls the cell cycle at late S/G2. Each bar in the histogram shows the time that each individual of cell has spent from G1/S to Mitosis (correspond to Fig 4F). Red (G1), Green (S/G2) and Gray (M/G0) indicate the cell cycle stage of each cell after 24h live cell imaging. **C.** Over-expression of E2F7^{R894A} mutant caused DNA damage. HeLa/TO cells were arrested 16h with HU and then released into fresh medium containing doxycycline. Protein samples were harvested every 3 hours and immunoblot for γ-H2AX (Left). Quantifications were performed based on two independent experiments (Right).
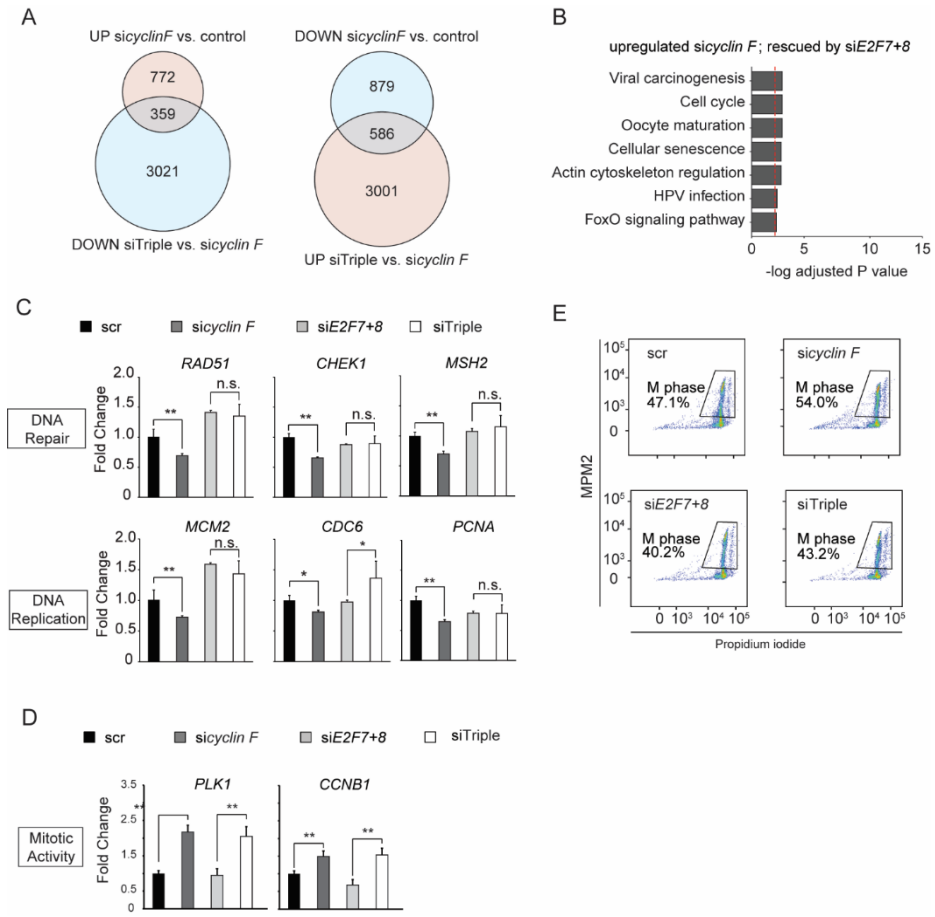
Figure S4. Cyclin F controls transcription of DNA repair via E2F7/8. A. Venn diagrams of differentially expressed transcripts in RNA-sequencing analysis of nocodazole-arrested HeLa cells depleted for cyclin F and/or E2F7/8 as indicated. **B.** KEGG pathway analysis of genes upregulated by cyclin F knockdown, and rescued by additional E2F/8 depletion. Bars represent -log P values, such that larger values mean stronger statistical significance. The cut-off *P* value 0.05 is shown as a red dotted line. **C.** qPCR assay showing the expression of atypical E2F target genes that are involved in DNA damage and repair. RPE cells were transfected for 48 hours with siRNA as indicated. 16 hours before harvesting, cells were treated with nocodazole. Data represent averages ± SEM (n=3); *P<0.05 or **P<0.01 (Student's *t*-test). n.s.: not significant. **D.** qPCR showing the RNA expression of *PLK1* and *CCNB1*. HeLa cells were transfected for 48 hours with siRNAs as indicated. Cells were incubated with nocodazole 16 hours before harvesting. Data represent averages ± SEM (n=3); *P<0.05 or **P<0.01 (Student's *t*-test). n.s.: not significant. **E.** Phosphorylated MPM2 staining in flow-cytometry demonstrated that mitotic activity was regulated in a cyclin F dependent manner.
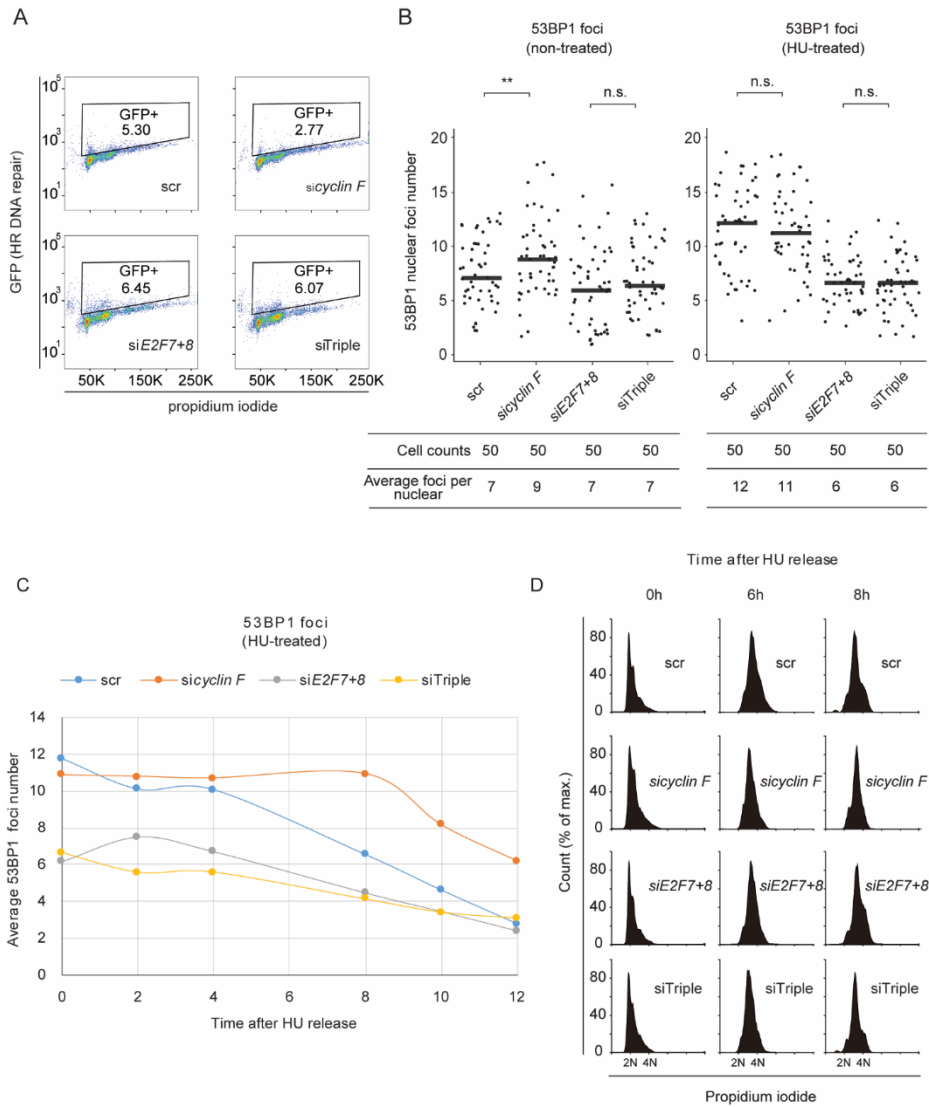
Figure S5. Cyclin F-dependent degradation of E2F7/8 promotes DNA repair in G2.

Figure S5. Cyclin F-dependent degradation of E2F7/8 promotes DNA repair in G2. A. Loss of *cyclin F* induced E2F7/8-dependent Homologous Recombination deficiency. HeLa cells were transfected with siRNA as indicated. After 24h, HeLa cells with stably transformed pDR-GFP were transfected with siRNA and harvested after 48h for flow-cytometry. **B.** Quantification of the 53BP1 foci at the beginning of live imaging (Left: non-treated, Right: HU treated 16 hours). Dot-plots show the 53BP1 foci number from each cell. The number of cells and the average foci per nucleus were showed in the table below. Red bars represent averages; **$P<0.01$ (Student's *t*-test) and n.s. (not significant). **C.** Dynamics of the number of 53BP1 foci per cell after HU release. At each time point after HU release, 50 random cells were picked and 53BP1 foci in each cell were counted. **D.** Flow cytometry showing the cell cycle progression of each condition at different time points after HU release.

REFERENCES

1. Kent LN, Rakijas JB, Pandit SK, et al. E2f8 mediates tumor suppression in postnatal liver development. *J Clin Invest.* 2016;126(8):2955-2969.

2. Westendorp B, Mokry M, Groot Koerkamp, Marian J. A., Holstege FCP, Cuppen E, de Bruin A. E2F7 represses a network of oscillating cell cycle genes to control S-phase progression. *Nucleic Acids Res.* 2012;40(8):3511-3523.

3. Yuan R, Vos HR, van Es RM, et al. Chk1 and 14-3-3 proteins inhibit atypical E2Fs to prevent a permanent cell cycle arrest. *EMBO J.* 2018;37(5):10.15252/embj.201797877. Epub 2018 Jan 23.

4. Thurlings I, Martínez-López LM, Westendorp B, et al. Synergistic functions of E2F7 and E2F8 are critical to suppress stress-induced skin cancer. *Oncogene.* 2017;36(6):829-839.

5. Boekhout M, Yuan R, Wondergem AP, et al. Feedback regulation between atypical E2Fs and APC/CCdh1 coordinates cell cycle progression. *EMBO Rep.* 2016;17(3):414-427.

6. Ishida S, Huang E, Zuzan H, et al. Role for E2F in control of both DNA replication and mitotic functions as revealed from DNA microarray analysis. *Mol Cell Biol.* 2001;21(14):4684-4699.

7. Polager S, Kalma Y, Berkovich E, Ginsberg D. E2Fs up-regulate expression of genes involved in DNA replication, DNA repair and mitosis. *Oncogene.* 2002;21(3):437-446.

8. Zhu W, Giangrande PH, Nevins JR. E2Fs link the control of G1/S and G2/M transcription. *EMBO J.* 2004;23(23):4615-4626.

9. Nakayama KI, Nakayama K. Regulation of the cell cycle by SCF-type ubiquitin ligases. *Semin Cell Dev Biol.* 2005;16(3):323-333.

10. Tetzlaff MT, Bai C, Finegold M, et al. Cyclin F disruption compromises placental development and affects normal cell cycle execution. *Mol Cell Biol.* 2004;24(6):2487-2498.

11. Choudhury R, Bonacci T, Arceci A, et al. APC/C and SCF(cyclin F) Constitute a Reciprocal Feedback Circuit Controlling S-Phase Entry. *Cell Rep.* 2016;16(12):3359-3372.

12. D'Angiolella V, Donato V, Vijayakumar S, et al. SCF(Cyclin F) controls centrosome homeostasis and mitotic fidelity through CP110 degradation. *Nature.* 2010;466(7302):138-142.

13. Nakayama KI, Nakayama K. Ubiquitin ligases: cell-cycle control and cancer. *Nat Rev Cancer.* 2006;6(5):369-381.

14. Guardavaccaro D, Kudo Y, Boulaire J, et al. Control of meiotic and mitotic progression by the F box protein beta-Trcp1 in vivo. *Dev Cell.* 2003;4(6):799-812.

15. Herrero-Ruiz J, Mora-Santos M, Giráldez S, et al. βTrCP controls the lysosome-mediated degradation of CDK1, whose accumulation correlates with tumor malignancy. *Oncotarget.* 2014;5(17):7563-7574.

16. Margottin-Goguet F, Hsu JY, Loktev A, Hsieh HM, Reimann JDR, Jackson PK. Prophase destruction of Emi1 by the SCF(betaTrCP/Slimb) ubiquitin ligase activates the anaphase pro-moting complex to allow progression beyond prometaphase. *Dev Cell.* 2003;4(6):813-826.

17. Soucy TA, Smith PG, Milhollen MA, et al. An inhibitor of NEDD8-activating enzyme as a new approach to treat cancer. *Nature.* 2009;458(7239):732-736.

18. D'Angiolella V, Donato V, Forrester FM, et al. Cyclin F-mediated degradation of ribonucle-otide reductase M2 controls genome integrity and DNA repair. *Cell.* 2012;149(5):1023-1034.

19. Dankert JF, Rona G, Clijsters L, et al. Cyclin F-Mediated Degradation of SLBP Limits H2A.X Accumulation and Apoptosis upon Genotoxic Stress in G2. *Mol Cell.* 2016;64(3):507-519.

20. Walter D, Hoffmann S, Komseli E, Rappsilber J, Gorgoulis V, Sørensen CS. SCF(Cyclin F)-de-pendent degradation of CDC6 suppresses DNA re-replication. *Nat Commun.* 2016;7:10530.

21. D'Angiolella V, Esencay M, Pagano M. A cyclin without cyclin-dependent kinases: cy-clin F controls genome stability through ubiquitin-mediated proteolysis. *Trends Cell Biol.* 2013;23(3):135-140.

22. Sakaue-Sawano A, Kurokawa H, Morimura T, et al. Visualizing spatiotemporal dynamics of multicellular cell-cycle progression. *Cell.* 2008;132(3):487-498.

23. Aksoy O, Chicas A, Zeng T, et al. The atypical E2F family member E2F7 couples the p53 and RB pathways during cellular senescence. *Genes Dev.* 2012;26(14):1546-1557.

24. Zalmas LP, Zhao X, Graham AL, et al. DNA-damage response control of E2F7 and E2F8. *EMBO Rep.* 2008;9(3):252-259.

25. Klein DK, Hoffmann S, Ahlskog JK, et al. Cyclin F suppresses B-Myb activity to promote cell cycle checkpoint control. *Nat Commun.* 2015;6:5800.

26. Yang KS, Kohler RH, Landon M, Giedt R, Weissleder R. Single cell resolution in vivo imaging of DNA damage following PARP inhibition. *Sci Rep.* 2015;5:10129.

27. Choudhury R, Bonacci T, Wang X, et al. The E3 Ubiquitin Ligase SCF(Cyclin F) Transmits AKT

2

Signaling to the Cell-Cycle Machinery. *Cell Rep.* 2017;20(13):3212-3222.

28. Ahluwalia D, Schaaper RM. Hypermutability and error catastrophe due to defects in ribonucleotide reductase. *Proc Natl Acad Sci U S A.* 2013;110(46):18596-18601.

29. Kumar D, Abdulovic AL, Viberg J, Nilsson AK, Kunkel TA, Chabes A. Mechanisms of mutagenesis in vivo due to imbalanced dNTP pools. *Nucleic Acids Res.* 2011;39(4):1360-1371.

30. Xu X, Page JL, Surtees JA, et al. Broad overexpression of ribonucleotide reductase genes in mice specifically induces lung neoplasms. *Cancer Res.* 2008;68(8):2652-2660.

31. Yuan R, Vos HR, van Es RM, et al. Chk1 and 14-3-3 proteins inhibit atypical E2Fs to prevent a permanent cell cycle arrest. *EMBO J.* 2018;37(5):10.15252/embj.201797877. Epub 2018 Jan 23.

32. Clements KE, Thakar T, Nicolae CM, Liang X, Wang H, Moldovan G. Loss of E2F7 confers resistance to poly-ADP-ribose polymerase (PARP) inhibitors in BRCA2-deficient cells. *Nucleic Acids Res.* 2018;46(17):8898-8907.

33. Mitxelena J, Apraiz A, Vallejo-Rodríguez J, et al. An E2F7-dependent transcriptional program modulates DNA damage repair and genomic stability. *Nucleic Acids Res.* 2018;46(9):4546-4559.

34. van Diemen FR, Kruse EM, Hooykaas MJG, et al. CRISPR/Cas9-Mediated Genome Editing of Herpesviruses Limits Productive and Latent Infections. *PLoS Pathog.* 2016;12(6):e1005701.
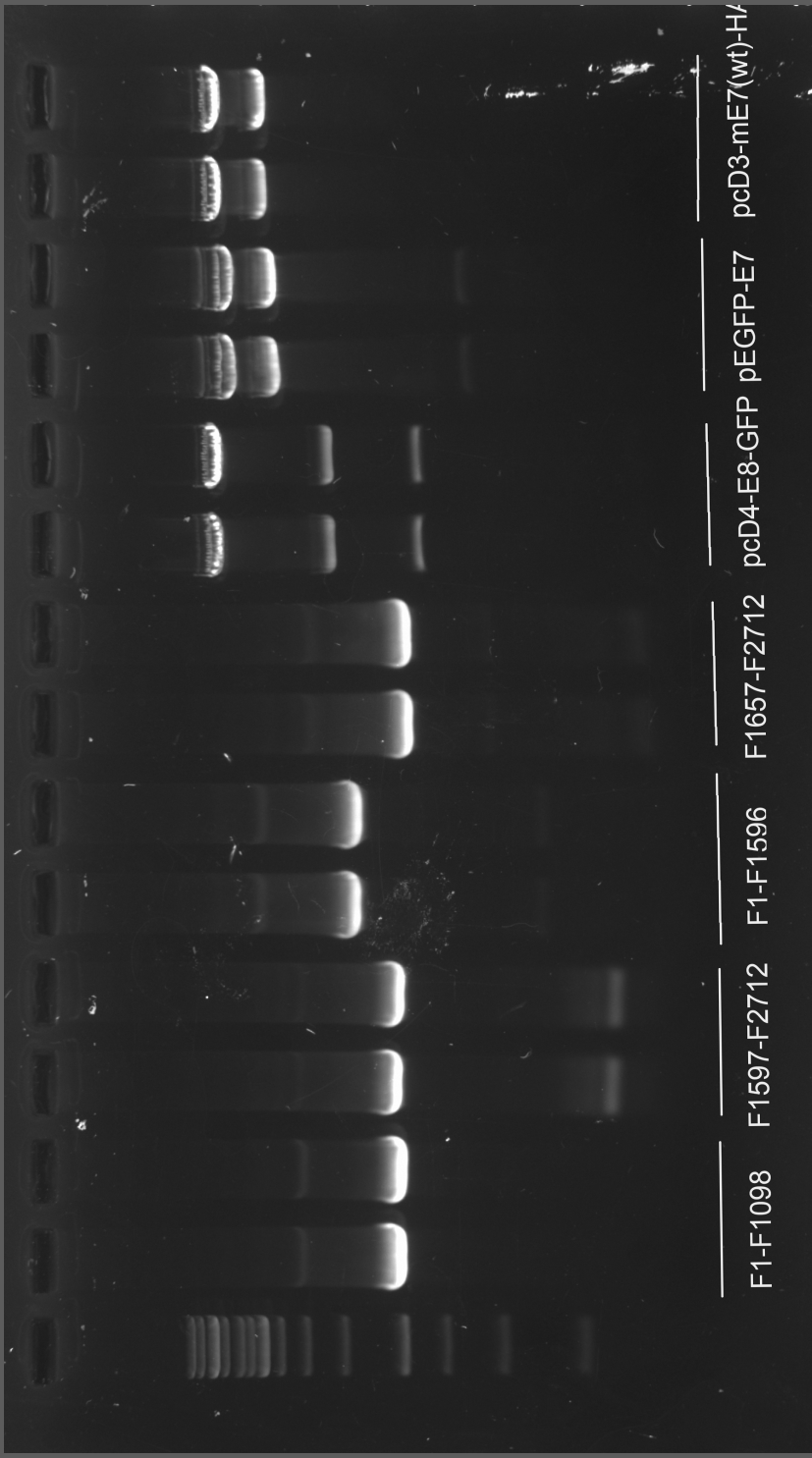
Chapter 3

Atypical E2Fs interact with SMC1 to promote cohesin release during mitosis

Qingwu Liu[1], Ingrid Thurlings[1], Elsbeth van Liere[1], Amity Manning[2], Judith H.I. Haarhuis[3], Benjamin D. Rowland[3], Bart Westendorp[1], Alain de Bruin[1,4]

1 Department of Biomolecular Health Sciences, Faculty of Veterinary Medicine, Utrecht University, Utrecht, the Netherlands

2 Department of Biology and Biotechnology, Worcester Polytechnic Institute, Worcester, MA, USA

3 Division of Cell Biology, Netherlands Cancer Institute, Amsterdam, the Netherlands

4 Department of Pediatrics, University of Groningen, University Medical Center Groningen, Groningen, the Netherlands

ABSTRACT

E2F transcription factors regulate cell cycle progression through timely expression of cell cycle genes. However, it is unclear whether E2Fs have also transcription-independent functions that control cell cycle progression. Here we show that atypical E2Fs, E2F7 and E2F8, directly interact with the cohesin subunit SMC1, compete with RAD21 for binding to SMC1, and enable cohesin release from sister chromatids during prophase. Cells depleted for E2F7/8 fail to efficiently remove cohesin from chromosome arms, and show delayed mitotic progression. In conclusion, we uncover a novel and transcription-independent function of atypical E2F proteins in regulating cohesin release and the timely progression through mitosis.

INTRODUCTION

E2Fs are a family of transcription factors that control the expression of many genes that drive cell cycle progression and proliferation[1]. Mammalian cells express eight different family members, which can be classified into transcriptional activators (E2F1-3) and repressors (E2F4-8). Among them, E2F7 and E2F8 are atypical as they have two tandem DNA binding domains instead of one, as is the case in the canonical E2Fs. E2F7 and E2F8 also are atypical in that they bind to the promoter of the target genes independent of transcription factor dimerization partners and pocket proteins[2]. Atypical E2Fs work as transcriptional repressors during S- and G2-phase, downregulating hundreds of genes involved in DNA replication, metabolism and repair[3]. However, atypical E2Fs may engage in different multiprotein complexes with various functions. As a striking example, we found that E2F7 and -8 could also physically interact with HIF1. This interaction stimulates VEGFA expression, a key factor driving angiogenesis[4]. To better understand the molecular actions of E2F7 and -8 we further investigated their interaction partners and the physiological functions of these protein-protein interactions. Interestingly, we find that E2F7 and -8 interact with the cohesin complex.

In cycling cells, it is of critical importance that the DNA is copied faithfully and that the genomic information is distributed evenly to the daughter cells. To achieve this goal, the sister DNAs need to be held together from S phase until anaphase through a process known as sister chromatid cohesion[5]. Cohesion is mediated by a ring-shaped multi-subunit protein complex, called cohesin, which at its core consists of SMC1, SMC3, RAD21, and SA1 or SA2. The SMC subunits are rod-like proteins with a hinge domain on one end and a head domain on the other. The interface connecting the SMC3 head domain and the RAD21 N-terminus is proposed to be the exit gate for DNA release[6].

The establishment of cohesion is coupled with DNA replication during S-phase, when cohesin rings connect the newly duplicated DNAs. These linkages are maintained along the length of chromosomes until the end of G2 phase. As cells progress into mitosis, the bulk of cohesin rings along the chromosome arms is removed[7,8]. Disruption of cohesin dissociation from chromosome arms can impair the decatenation of sister chromatids and the correct attachment of microtubules to kinetochores, leading to chromosome segregation errors[9,10]. The latter step depends on WAPL, which opens the interface between SMC3 and RAD21, allowing the exit of DNA[11-13]. In addition, phosphorylation of SA2 and Sororin is also essential for the efficient removal of cohesin during prophase[14,15]. Sororin is a cohesin protector, which competes with WAPL for the binding to the cohesin ring[16]. Notwithstanding these findings, the cellular processes that control cohesin release from DNA during prophase remain incompletely understood.

Here, we demonstrate that E2F7/8 contributes to removal of cohesin during prophase in human and mouse cells. Deficiency of E2F7/8 increases the amount of undissolved sister chromatids in prometaphase and delays mitotic progression. Surprisingly, we find that this

effect is independent from the DNA-binding or transcription-repressing capacity of E2F7/8. Instead, we provide evidence that E2F7/8 binding to SMC1 competes with RAD21. We propose that E2F7/8 facilitates cohesin release by opening up cohesin rings.

RESULTS

Atypical E2Fs interact with cohesin independent of DNA-binding

To identify novel proteins interacting with atypical E2Fs we had carried out a quantitative SILAC-based proteomic screening[17]. In this experiment, doxycycline inducible EGFP-E2F7-, EGFP-E2F8- and EGFP Hela cell lines were cultured in 'light" or "heavy" medium and treated with doxycycline for 16h. Then, nuclear fractions derived from these cells were incubated with GFP-trap beads and subjected to tandem mass spectrometry. Next, we compared the relative abundances of proteins pulled down by EGFP- E2F7 or E2F8 over EGFP only and settled on those with above two-fold enrichment from both forward and reverse labeling experiments. We found that both E2F7 and E2F8 had about 200 putative binding partners, and 90 ones in common (Fig. 1A). We noticed that the mutual hits contained both SMC1 and SMC3, two core subunits of the cohesin complex (Fig 1B). Additionally, another cohesin subunit, RAD21, was found in the list of putative E2F8 binding partners. To validate these interactions, EGFP-E2F7 or E2F8 were transfected in HEK 293T cells, followed by GFP immunoprecipitation. The results showed that SMC1, SMC3 and RAD21 were all pulled down efficiently by E2F7 as well as E2F8 (Fig. 1C).

Since both cohesin and atypical E2Fs can associate with DNA, we wondered if DNA binding could indirectly mediate their interactions in these pull-down experiments. To this end, we performed another GFP immunoprecipitation with either EGFP- E2F7/8 wildtype or EGFP-E2F7/8 DNA binding domain (DBD) mutants carrying point mutations required to bind to the canonical E2F binding motifs[3]. We found that E2F7/8 DBD-mutants could still bind to SMC1 (Fig. 1D). Moreover, when lysates from cells transfected with E2F7-EGFP or EGFP-E2F8 wildtype were treated with 200 ug/ml ethidium bromide to break down the interaction between DNA and proteins prior to immunoprecipitation[18], SMC1 was still pulled down (Fig. 1D). These results demonstrate that atypical E2Fs can directly associate with cohesin.
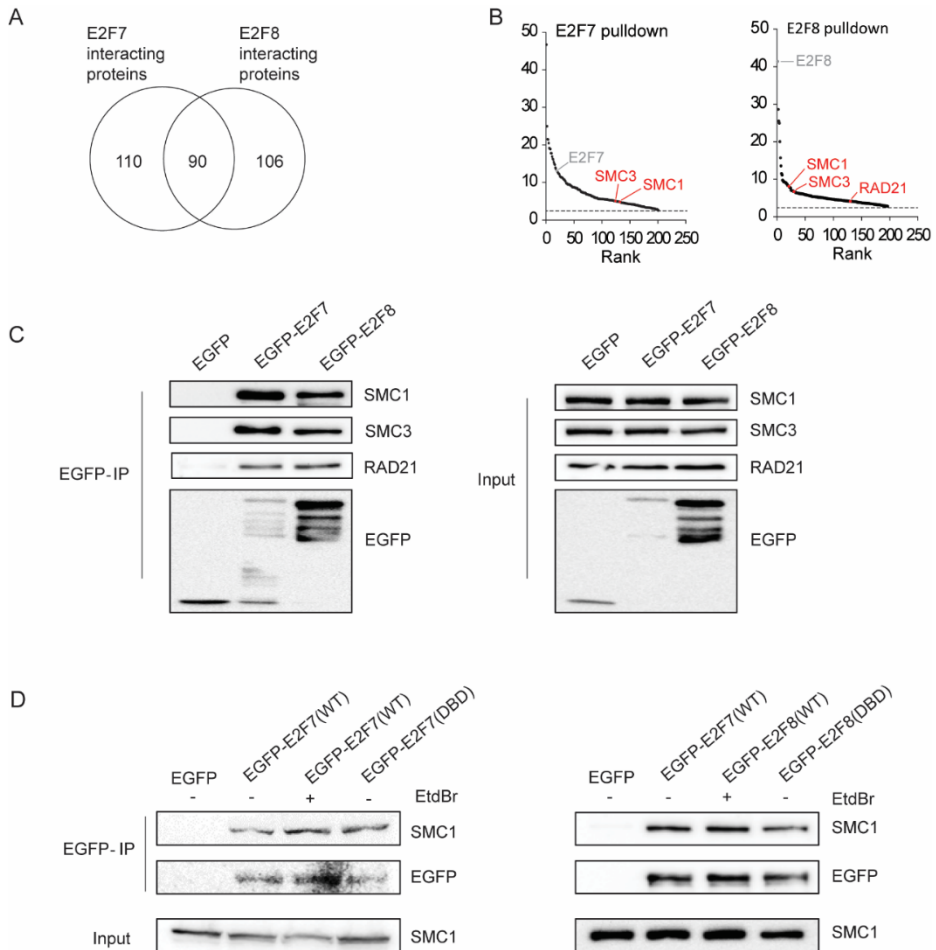
Figure 1. Atypical E2Fs bind to cohesin. A. Venn diagram showing comparative analysis of overlap between putative E2F7 and E2F8 binding partners identified with SILAC. **B.** Top hits of E2F7-EGFP and E2F8-EGFP binding partners that were enriched 2-fold or more compared to EGFP pull-downs. **C.** Verification of the interaction between atypical E2Fs and cohesin components. HEK cells were transfected with EGFP, EGFP-tagged E2F7 or E2F8 for 48 hours. MG132 (1 µg/ml) was added 5 hours prior to harvesting. Cells were lysed with RIPA buffer and incubated with anti-EGFP resin for immunoprecipitation. Immunoblotting was then performed. **D.** Atypical E2Fs binds to SMC1 independent of DNA binding. HEK cells were transfected with indicated plasmids and collected as described in C). Cell lysates were incubated with 200 µg/ml ethidium bromide (EtdBr) for 1 hour prior to immunoprecipitation.

Atypical E2Fs directly bind to SMC1

To understand in more detail cohesin's interactions with atypical E2Fs, we investigated whether cohesin subunits might directly bind to atypical E2Fs. To this end, we performed an *in vitro* protein interaction assay where GST-tagged E2F7 or E2F8 derived from E. coli cells was immobilized with GST beads. These *in vitro* translated recombinant E2F proteins were incubated separately with four different His-tagged cohesin subunit proteins (SMC1, SMC3, RAD21 or SA1) and then subjected to immunoblotting. We found that atypical E2Fs specifically pulled down SMC1 (Fig. 2A), demonstrating that atypical E2Fs interact with the cohesin complex via binding to SMC1.

Next, we sought to map the specific interaction domain that enables atypical E2Fs to interact with SMC1. A series of E2F7 truncation and deletion constructs were made and transfected in HEK293T cells to pull down endogenous SMC1. We found that the interaction between E2F7 and SMC1 requires amino acids 264 until 552, including the second DBD of E2F7 (Fig. 2B). Attempts to further narrow down the SMC1-interacting domain of E2F7 were unsuccessful, indicating that this entire E2F7[264-552] domain is required for the interaction with SMC1. For example, a Δ367-552 mutant version of E2F7 only partially lost the capacity to interact with SMC1 (Fig. S1A). However, secondary structure prediction utilizing two platform tools[19,20] (http://bioinf.cs.ucl.ac.uk/psipred/), shows that the domain stretching between amino acids 264 to 552 of E2F7 contains several clusters of helix domains (Fig. S1B and S2). It was reported that both DBDs in E2F8 belonged to the winged-helix family[21]. E2F8 is highly homologous to E2F7 and we observed similar clusters of helix domains when subjecting E2F8 to the same analysis (Fig. S1C). Based on the homology of E2F7 and E2F8, we speculate that the second DBD in E2F7 would also form a winged-helix, which probably promotes the interaction between E2F7 and SMC1. Collectively, these results provide strong evidence that atypical E2Fs bind the cohesin subunit SMC1 via helix-rich domains.
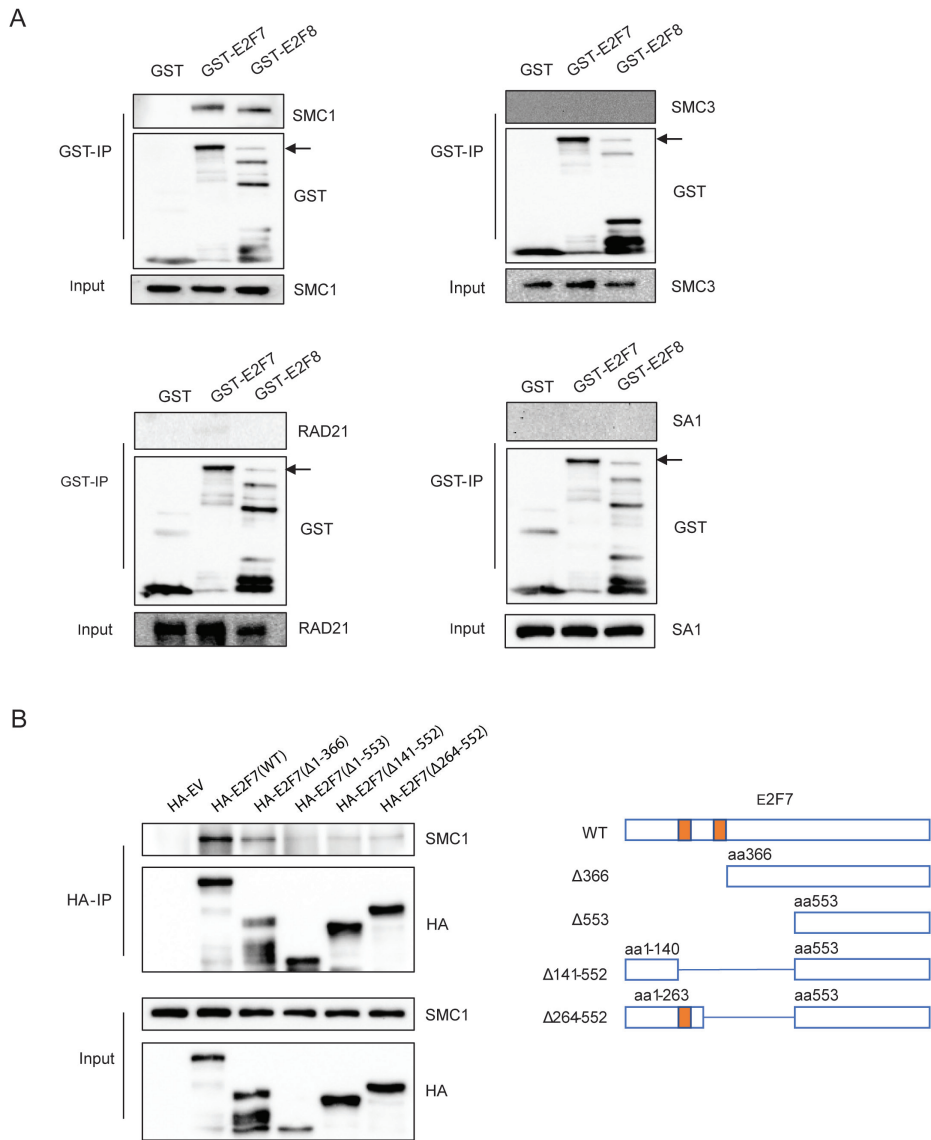
Figure 2. Atypical E2Fs bind to SMC1 specifically. A. Interactions between atypical E2Fs and individual cohesin subunits *in vitro*. GST and GST-tagged E2F7 and E2F8 were pulled down with GST resin from E.coli cell lysates, and incubated with ~10 μg 6His-tagged cohesin proteins overnight. Immunoblotting was then performed. **B.** Co-immunoprecipitations with SMC1 and truncated versions of E2F7 to map the interaction domain of E2F7. The indicated HA-tagged E2F7 fragments were transfected into HEK cells and HA immunoprecipitation was then performed, followed by immunoblotting (left). Schematic view showing the truncated mutants of E2F7 (right). Orange boxes indicate the DNA-binding domains of E2F7.

Atypical E2Fs are required for the dissociation of cohesin from chromosome arms

Next, we studied the relevance of E2F7/8 on cohesin function. We tested the effect of E2F7 and E2F8 loss on sister chromatid cohesion. We knocked down *E2F7* and *E2F8* with siRNAs in Hela cells and analyzed sister chromatid cohesion by performing chromosome spreads. Eighty-five percent of the spreads from control cells incubated with scrambled siRNA showed the "normal" X-shape chromosomes with clearly resolved sister chromatid arms and tightly connected at the centromere, but this percentage was strongly reduced in spreads from cells with knockdown of *E2F7, E2F8* or both. Instead, roughly 50% of the *E2F7/8*-knockdown cells showed "closed" chromosomes, in which the individual sister chromatids were hardly distinguishable (Fig. 3A). Human retinal pigment epithelium cell lines (hTERT-RPE1) with homozygous deletion of both *E2F7* and *E2F8*, hereafter referred to as *E2F7/8*KO cells also showed an increase in the percentage of closed chromosomes compared to their *E2F7/8*-intact counterparts (Fig. S3A). To quantify the distance between sister chromatids, we applied a FISH-based analysis on prometaphase spreads using two different DNA markers located on chromosome 16 [22]. Knockdown of *E2F7* and/or *E2F8* in Hela cells resulted in reduced distances between sister chromatids compared to the ones from control cells (Fig. 3B). To verify whether the requirement of E2F7 and E2F8 for cohesin dissociation is conserved across species, we also analyzed the chromosome spreads from three mouse cell lines. Specifically, these are *E2f7loxP/loxP; E2f8loxP/loxP* double knockout mouse embryonic fibroblasts (MEFs), immortalized with retroviral construct containing *Myc* and *Ras61L* [23], in which *Cre* was either expressed permanently or induced via a tamoxifen inducible construct. In addition, chromosome spreads from primary conditional *E2f7loxP/loxP; E2f8loxP/loxP* double knockout keratinocytes were analyzed [24]. All these cell lines showed robust increases in closed chromosomes after deletion of *E2f7* and *E2f8* (Fig. 3C).

This failure to separate sister chromatids during prometaphase was not caused by an overall increase in expression of cohesin proteins in *E2F7/8*-knockdown cells, because the overall expression levels of cohesin proteins levels did not differ after *E2F7* and *E2F8* knockdown (Fig. 3D). To confirm that the increase of spreads with closed sister chromatids results from a defect in cohesin release in *E2F7/8*-depleted cells, we extracted chromatin fractions from RPE *wildtype* cells and RPE-*E2F7/8*KO cells. We observed that there was indeed an increase in SMC1 and RAD21 accumulation on chromatin of *E2F7/8*KO cells that were arrested in prometaphase with nocodazole compared to control cells (Fig. 3E). Remarkably, chromatin-bound cohesin was not elevated in S and G2 phase cells with combined *E2F7/8* deletion or knockdown, showing that this phenotype specifically occurs during mitosis (Fig. S3B, C). Finally, we induced ectopic E2F7 expression in Hela cells, leading to a ~15% increase in spreads presenting premature sister chromatids separation (Fig. S3D). In addition, FISH-analysis on chromosome spreads in Hela cells with inducible overexpression of E2F7 or E2F8 showed increased distances between sister chromatids compared to the non-induced cells (Fig. S3E). These findings demonstrate that atypical E2Fs are essential for efficient cohesin removal

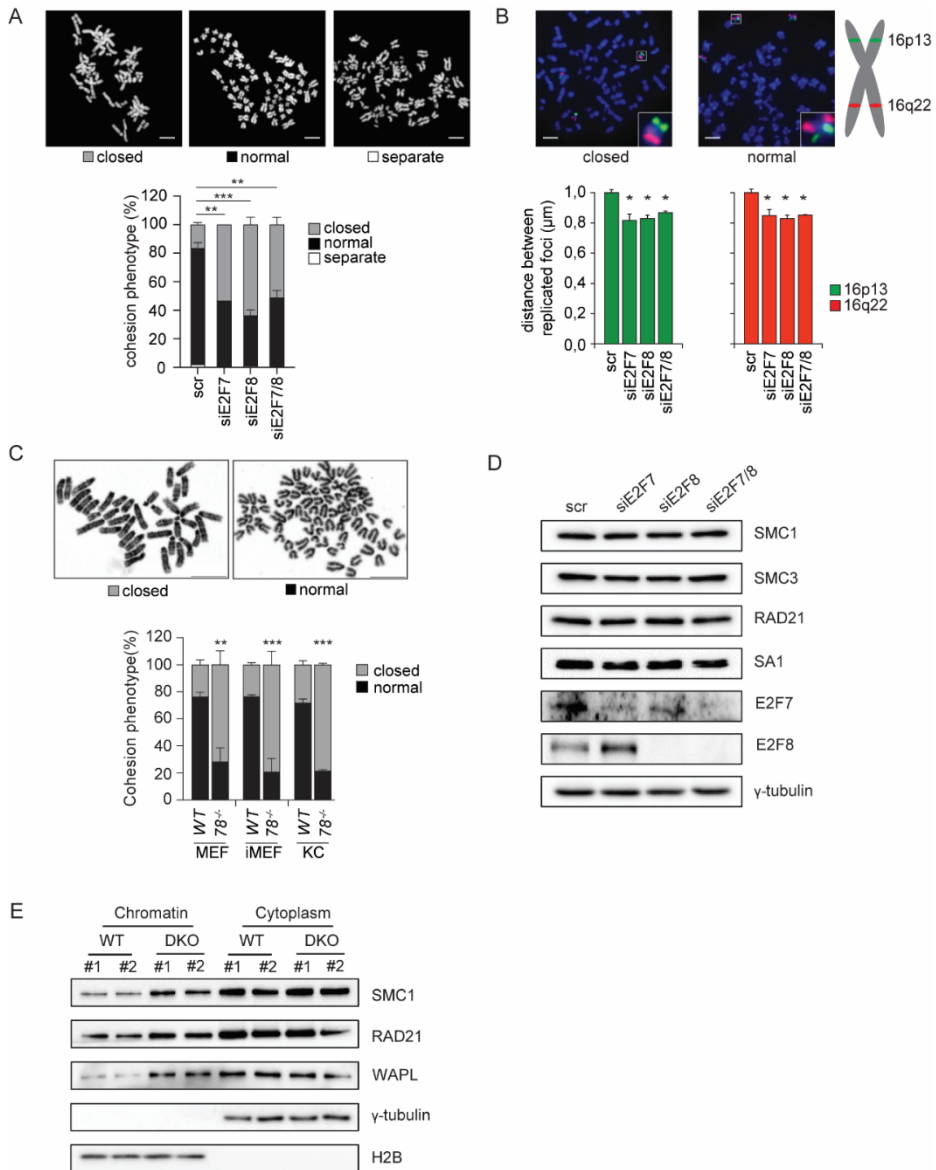from sister chromatids during the early stages of mitosis.

Figure 3. Atypical E2Fs are required for prophase pathway cohesin release.

Figure 3. Atypical E2Fs are required for prophase pathway cohesin release. A. Quantification of three types of chromosome spreads (pictures above) in Hela cells after knockdown of *E2F7*, *E2F8* or both. Nocodazole (200 ng/ml) was added 3 hours prior to collecting mitotic cells. Over 100 spreads were counted per condition in each experiment. **B.** FISH staining of chromosome 16 with specific probes for 16p13 (green) and 16q22 (red) in Hela cells transfected with indicated siRNAs. Pictures above show two types of chromosome 6 with closed arms and arms at normal distance, respectively. **C.** Quantification of three types of chromosome spreads (pictures above) in primary murine cells after knockout of *E2f7*, *E2f8* or both. Primary cells were treated with Nocodazole (200 ng/ml) for 3 hours to accumulate mitotic cells. Over 100 spreads were counted per condition in each experiment. **D.** Immunoblots of cohesin subunits in Hela cells depleted for *E2F7, E2F8* or both. **E.** Immunoblots showing the cohesin subunits levels in chromatin and cytoplasm in RPE1 cells *wildtype* clones (#1 and #2) and *E2F7/8* double knockout clones (#1 and #2). Cells were treated with Nocodazole (200 ng/ml) for 16 hours to collect mitotic cells.

Atypical E2Fs destabilize the integrity of cohesin complexes and regulate mitotic progression

Previous studies have shown that WAPL interacts directly with the cohesin complex and is required for cohesin release from sister chromatids arms prior to metaphase[25,26]. Since loss of either atypical E2Fs or WAPL resulted in a similar defect in cohesin removal, as displayed by an increased number of closed chromosomes (Fig. 3A, Fig. 4D), we investigated if atypical E2Fs could act as a docking site or co-factor for WAPL to facilitate the release of cohesin in prometaphase. We evaluated the interaction between E2F7/8 and WAPL in HEK 293T cells by transfecting EGFP-tagged DBD-mutant E2F7 and E2F8 and found that endogenous WAPL was indeed pulled down and that this interaction is not dependent on the atypical E2F DNA binding (Fig. 4A). To determine a potential direct interaction between atypical E2Fs and WAPL, we performed an in vitro pulldown assay where 6xHis-tagged WAPL was incubated with GST or GST-tagged E2F7 or E2F8 followed by His immunoblotting. However, we did not observe a direct interaction between WAPL and atypical E2Fs *in vitro*, indicating that atypical E2Fs likely interact with WAPL via their common binding partners, the cohesin subunits (Fig. S4A). Additionally, we showed that WAPL binding to cohesin is not altered in the absence of atypical E2Fs by performing co-immunoprecipitations assays between SMC3 and WAPL in *wildtype* and *E2F7/8* deficient RPE cells (Fig. S4B). In the same cell line the overall and cytoplasmic expression of WAPL did not differ in presence or absence of atypical E2Fs. However, we observed increased WAPL levels on chromatin during prophase in *E2F7/8*-deficient RPE cells compared to *wildtype* cells, probably due to enhanced cohesin abundance (Fig. 3E).

Given that deletion of atypical E2Fs delays cohesin release, we hypothesized that atypical E2Fs might be able to destabilize the cohesin complex. In support of this idea, we found that ectopic E2F7 competes for binding between SMC1 and the other core cohesin ring component RAD21. We transfected Flag-tagged SMC1 into HEK 293T cells with or without the ad-

dition of HA-tagged E2F7. Chromatin fractions were isolated and subjected to Flag immuno-precipitation. This experiment showed that less RAD21, and potentially also somewhat less SMC3 were pulled down by Flag-tagged SMC1 in cells co-transfected with E2F7. This indicates that E2F7 addition impairs the interaction between cohesin subunits (Fig. 4B).
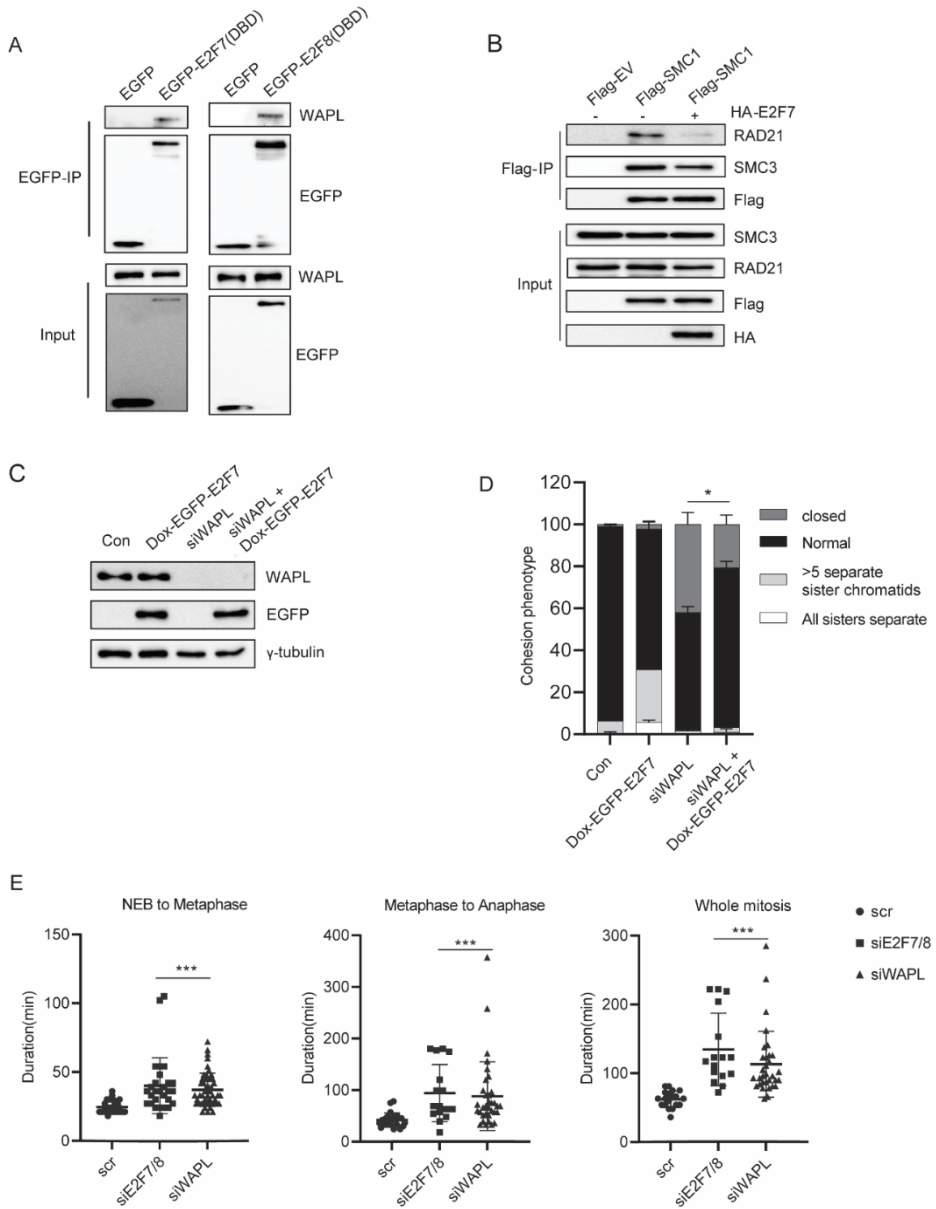

Figure 4. Atypical E2Fs destabilize cohesin integrity and promote mitosis progression.

Figure 4. Atypical E2Fs destabilize cohesin integrity and promote mitosis progression. A. Interaction between EGFP-tagged E2F7 or E2F8 DNA-binding mutant and endogenous WAPL. **B.** Flag immunoprecipitation to check the interaction between SMC1 and other two cohesin subunits, SMC3 and RAD21, in the presence of E2F7. HEK cells were transfected with Flag empty vector or Flag-tagged SMC1 and equal amount of HA empty vector or HA-tagged E2F7 as indicated. MG132 (1 µg/ml) was added 5 hours prior to harvesting cells. **C.** Immunoblots confirming the knockdown of *WAPL* and induction of EGFP-tagged E2F7 after doxycycline addition in Hela/TO E2F7-EGFP cells. **D.** Quantification of chromosome spreads from Hela/TO EGFP-E2F7 inducible cells. Cells were first transfected with siRNA against *WAPL* for 36 hours and then treated with doxycycline (200 ng/ml) for 12 hours. Nocodazole (200 ng/ml) was added 3 hours before collection of mitotic cells. **E.** Quantification of the time cells spend during NEB-to-Metaphase and Metaphase-to-Anaphase. Hela cells were transfected with indicated siRNAs. Hydroxyurea (2 mM) was added 36 hours after siRNA transfection. Sixteen hours later, cells were released from HU and subjected to live imaging.

Next, we tested whether E2F7/8 can facilitate cohesin removal independent from WAPL. To this end, we analyzed if doxycycline-inducible EGFP-E2F7 overexpression could still cause enhanced sister chromatid separation when WAPL was knocked down with siRNA. We first evaluated the impact of induced overexpression of E2F7 alone. We found that the number of cells with separated sister chromatids during prometaphase increased compared to control supporting our previous findings that E2F7 promotes cohesin release (Fig. 4C, D). Then we tested the effect of WAPL knockdown alone, and detected that the number of cells with closed chromosomes increased, consistent with previous studies demonstrating that WAPL is critical for cohesin release as well[25,26]. When E2F7 expression was induced in cells with WAPL knockdown the number of closed chromosomes decreased and shifted towards more normal chromosomes, demonstrating that E2F7 can promote cohesin release in the absence of WAPL. Taken together, these data suggest that atypical E2Fs can facilitate WAPL-independent cohesin release, likely through interfering with the integrity of the cohesin complex.

Given that cohesion has to be dissolved by WAPL to allow for timely mitotic progression and accurate sister chromatid segregation[10,27], we evaluated if E2F7/8 loss would result in mitotic defects. We monitored the mitotic progression of Hela cells transfected with siRNAs against either *E2F7/8* or *WAPL* by live cell imaging. We measured the duration from nuclear envelop breakdown (NEB) to the formation of metaphase plates, and then from metaphase to the onset of anaphase. Consistent with previous work, we found that *WAPL*-knockdown cells needed twice as much time to progress from prometaphase until the onset of anaphase relative to control cells (Fig. 4E). Remarkably, *E2F7/8* knockdown caused a very similar mitotic delay as *WAPL* knockdown. We then investigated if the observed mitotic defects are accompanied by chromosome segregation errors during anaphase, such as formation of chromosome bridges and lagging chromosomes. *WAPL*-knockdown cells released from a CDK1-inhibitor block displayed increased segregation errors, while knockdown of *E2F7/8* hardly affected segregation fidelity (Fig. S4C, D). This indicates that arm resolution defects need not neces-

sarily lead to segregation errors. Taken together our findings demonstrate that atypical E2Fs promote cohesin release and regulate timely progression through mitosis.

DISCUSSION

In vertebrate cells, most cohesin on chromosomes is released in the early stages of mitosis by WAPL, which is important for faithful chromosome segregation[9]. However, the loading and release of cohesin rings is a highly complex process involving multiple proteins, and a complete picture of how cohesin is removed from chromosomes is still lacking. We add another layer of complexity to this picture by showing that in mammalian cells, atypical E2Fs can interact with cohesin via SMC1, and destabilize the interaction between SMC1 and RAD21. Thus, we propose a model where binding of E2F7/8 to SMC1 can promote cohesin release in prophase. We envision a mechanism of action where E2F7/8 could open the SMC1/RAD21 interface, allowing the release of cohesin. Interestingly it was previously shown that WAPL promotes opening of the SMC3/RAD21 interface[28]. Our further observation that atypical E2Fs can induce cohesion loss also in the absence of WAPL would support the model that atypical E2Fs and WAPL might act at opposite ends of the RAD21 protein to open up cohesin rings.

Moreover, our results showed that atypical E2Fs did not affect cohesin levels on chromatin during S- or G2-phase, although this is when their expression levels peak. During S phase, cohesin is stabilized by acetylation and protected by Sororin, forming sister chromatid cohesion[16]. This could also explain why atypical E2Fs would not be able to facilitate cohesin release before the start of mitosis.

Our finding that two E2F transcription repressors have a non-canonical effect on cohesin release is unexpected, and raises the question why mammalian cells would combine these two different functions in one protein. Given that E2F7/8 bind to hundreds of cell cycle genes, which are highly expressed during S and G2-phase, it would place them physically close to sites of sister chromatid cohesion, where E2F7/8 can facilitate release during prophase. We propose that E2F7/8 by this proximity exerts its non-canonical activity, which in turn enables the formation of the archetypal X-shape of mitotic chromosomes.

3

MATERIALS AND METHODS

Cell culture, transfection and cell line generation

Hela, RPE1-hTERT, and HEK293T cell lines were purchased from ATCC and cultured in DMEM (41966052; Thermo Fisher Scientific) containing 10% fetal bovine serum (11550356; Fisher Scientific).

Tet repressor-expression Hela inducible cell lines (Hela/TO) were generated as previously described in [3] 0.2 µg/ml doxycycline (D9891, Sigma-Aldrich) was added to induce protein overexpression. The generation of *E2F7/8* double knockout RPE cell lines and confirmation of successful depletion were described in[29]. Histone H2B-iRFP expressing Hela cell line was produced by infecting Hela cells with H2B-iRFP containing lentiviral particles made with the third generation packaging plasmids in HEK cells. PLentiPGK DEST H2B-iRFP670 plasmid was purchased from Addgene (#90237). Equal expression of H2B-iRFP cells were sorted with flow cytometry for live cell imaging.

Transfection in HEK cells was performed by mixing 130 µg/ml PEI (polyethylenimine, 23966, Polysciences) with plasmids (15 µg) at a ratio of 1:1 in serum free DMEM medium. After 15 minutes incubation at room temperature, mixture was added to cells and wait 6 hours prior to refreshing with fresh medium. siRNA was transfected at a final concentration of 10 nM with RNAiMAX (13778075; Thermo Fisher Scientific) in cell culture well with ~50% confluency of cells.

Mass spectrometry

To prepare samples for SILAC, Hela/TO cell lines were pre-cultured with Heavy/Light medium for two weeks to incorporate isotopically labelled lysine (K8, 282986440, Silantes) and arginine (R10, 282986404, Silantes). EGFP-tagged E2F7 and -8 were induced to express with doxycycline for 16 hours. Then cells were lysed with RIPA buffer (50 mM Tris-HCl, 150 mM NaCl, 1 mM EDTA, 0.25% deoxycholic acid, 1% Nonidet-P40, 1 mM NaF and NaV_3O_4, and protease inhibitor cocktail (11873580001, Sigma Aldrich)), and subjected to EGFP immunoprecipitation. Detailed treatment of precipitated proteins prior to mass spectrometry and analysis of the raw data were described in our previous study[17].

Protein purification and *in vitro* interaction assay

GST tagged human E2F7b and E2F8 were expressed and induced in BL21 competent E. coli cells. 6x His tagged cohesin proteins were expressed and induced in BL21 (DE3) competent E. coli cells. 0.5 mM IPTG was used to induce protein expression.

For protein interaction *in vitro* assay, GST and GST tagged E2F7 and -8 were purified with Glutathione sepharose (GE17-0756) from 10 ml cell suspension. Then GST tagged proteins were incubated with ~10 µg 6x His tagged cohesin proteins purified with a Ni-NTA spin kit (31314, QIAGEN) overnight. Next day, Glutathione Sepharose was washed three times with washing buffer (50 mM Tris pH7.7, 150 mM KCl, 0.1% Triton X-100, 1 mM DTT) prior to being

suspended in 1x SDS loading buffer.

Generation of chromosome spreads

Hela cells were treated with nocodazole (200 ng/ml) for 3 hours to capture them in pro-metaphase. Cells were washed, trypsinised, and spun down. Supernatant was discarded, and pellets were resuspended. 1 ml 0,075 M KCl (37°C) was added while shaking constantly, and then kept at 37°C for 15 minutes. 500 µl methanol: acetic acid (3:1) fixative was added, and samples were centrifuged (5 minutes, 2000 rpm). Supernatant was removed, and fixative was carefully added to the pellets, followed by 20 minutes incubation at room temperature. Sample was spun down (5 minutes, 2000 rpm), and fixation procedure was repeated twice. After the last centrifuge step, pellets were resuspended in a 200 µl volume of fixative. Drop three drops (15-20 µl) from ±30 cm height on clean microscope slides and let dry. Coverslips were mounted on slides using Fluoroshield mounting medium containing DAPI (Sigma, F6057). Images were taken using a Leica TCS SPE-II confocal microscope and analyzed using Fiji software.

Fluorescence *in situ* hybridization (FISH)

FISH was performed as previously described[22]. In short, chromosome spreads were hybridized with probes for α-satellite regions on Chr16p13 (green) and Chr16p22 (red). Measurements of inter-chromosomal distances were done with Slidebook software.

Immunoprecipitation and immunoblotting

Cells were washed with 1X PBS twice and collected by scraping. Cell pellets were lysed with RIPA buffer for 30 minutes and supernatant was collected for a standard SDS-PAGE or immunoprecipitation. Antibodies used and dilution are listed in table S2.

For immunoprecipitation, cell lysate supernatants were cleared up with 20 ul Protein G Plus/Protein A agarose suspension (IP05-1.5, Calbiochem) firstly. For EGFP and GST immunoprecipitation, 20 ul GFP-Trap resin (gta-20, Chromotec) or Glutathione sepharose (GE17-0756) were added into cleared supernatant and incubated for 1 hour. For Flag and HA, 2 µg antibody was added to cleared supernatant and incubated overnight. Then, 20 ul Protein G Plus/Protein A agarose were added and incubated for 1 hour. After the pull-down, the above beads were washed three times with RIPA buffer and PBS before proceeding to SDS-PAGE immunoblot.

Chromatin fractionation

Three million cells were collected and lysed with 200 ul buffer A (10 mM HEPES, 10 mM KCl, 1.5 mM $MgCl_2$, 0.34 mM Sucrose, 10% glycerol, 1 mM DTT, 1x protease inhibitor cocktail) plus extra 0.1% Triton X-100 for 5 minutes on ice. Centrifuge at 1500 g for 4 min. The supernatant containing cytoplasmic proteins and the pellet containing the nuclei were then processed separately for protein isolation. The nuclei were washed with buffer A once and lysed with 200 ul buffer B (the elements of buffer A plus 3 mM EDTA and 0.2 mM EGTA) on ice for

10 min. The supernatant contained free nuclear proteins and the pellet contained chromatin-bound proteins. The chromatin fraction was washed twice with buffer B and suspended in 1 x SDS loading buffer for SDS-PAGE.

Immunofluorescence and live imaging

Cells were plated over cover slips (5 mm) and treated under desired conditions as indicated. By collecting, cells were washed with 1x PBS once and then fixed with 4% PFA at room temperature for 20 minutes. The PFA was discarded and the cells were washed with PBS twice. PBS containing 0.1% Triton X-100 was added and incubated for 20 minutes to permeabilize the cells. The coverslips were washed with PBS twice, dried and mounted on glass slides using Fluoroshield mounting medium containing DAPI (Sigma, F6057).

For live cell imaging, 25 thousand Hela cells containing RFP-H2B were plated in 4-well CELLview culture dishes (627975, Greiner) one day ahead prior to siRNAs transfection. Twenty-four hours after siRNA transfection, cells were treated with 0.2 mM thymidine for 16 hours. Cells were subjected to imaging after 8 hours of thymidine release. Images were acquired every 3 minutes for 6 hours on a Nikon A1R-STORM microscope using a 10x objective in a humidified chamber at 37°C, 5% CO_2. Cell tracking was performed manually with NIS Elements software.

Quantification and statistical analysis

Immunoblots, immunoprecipitation, chromosome spreads, immunofluorescence and FISH were repeated three times unless otherwise stated in the figure legends.

Statistical analyses were done by Kruskal-Wallis One Way Analysis of Variance on Ranks and Dunnett's Method for multiple comparisons for Fig 3B and 4E. Student's t tests were done for Fig S3E and S3C. * $P < 0.05$, ** $P < 0.01$, *** $P < 0.001$. Sample sizes and other experiment-specific statistical details are described in the figure legends.

ACKNOWLEDGEMENTS

AUTHOR CONTRIBUTIONS

QL, IT and EvL performed experiments, AM performed FISH assay and analyzed the data. JH helped with setting up and analyzing chromosome spreads assay. BR provided reagents, advice and co-wrote the manuscript. QL, BW and AdB conceived the study design and experimental approaches, analyzed data, and wrote the manuscript.

3

DECLARATION OF INTERESTS

The authors declare no competing interests.

SUPPLEMENTARY MATERIAL

Table 1: Antibodies for immunoblotting

Name	Company	Cat#	Dilution
GFP	Abcam	AB6673	1:1000
Flag	Sigma-Aldrich	F3165	1:3000
HA	Biolegend	16B12	1:3000
E2F7	Santa Cruz	SC-66870	1:1000
E2F8	Abcam	109596	1:1000
γ-tubulin	Sigma-Aldrich	T6557	1:1000
SMC1A	Bethyl	A300-055A	1:1000
SMC3	Bethyl	A300-060A	1:1000
RAD21	Sigma-Aldrich	05-908	1:1000
GST	Santa Cruz	sc-138	1:3000
WAPL	Santa Cruz	sc-365189	1:1000
H2B	Cell signaling	8135	1:1000
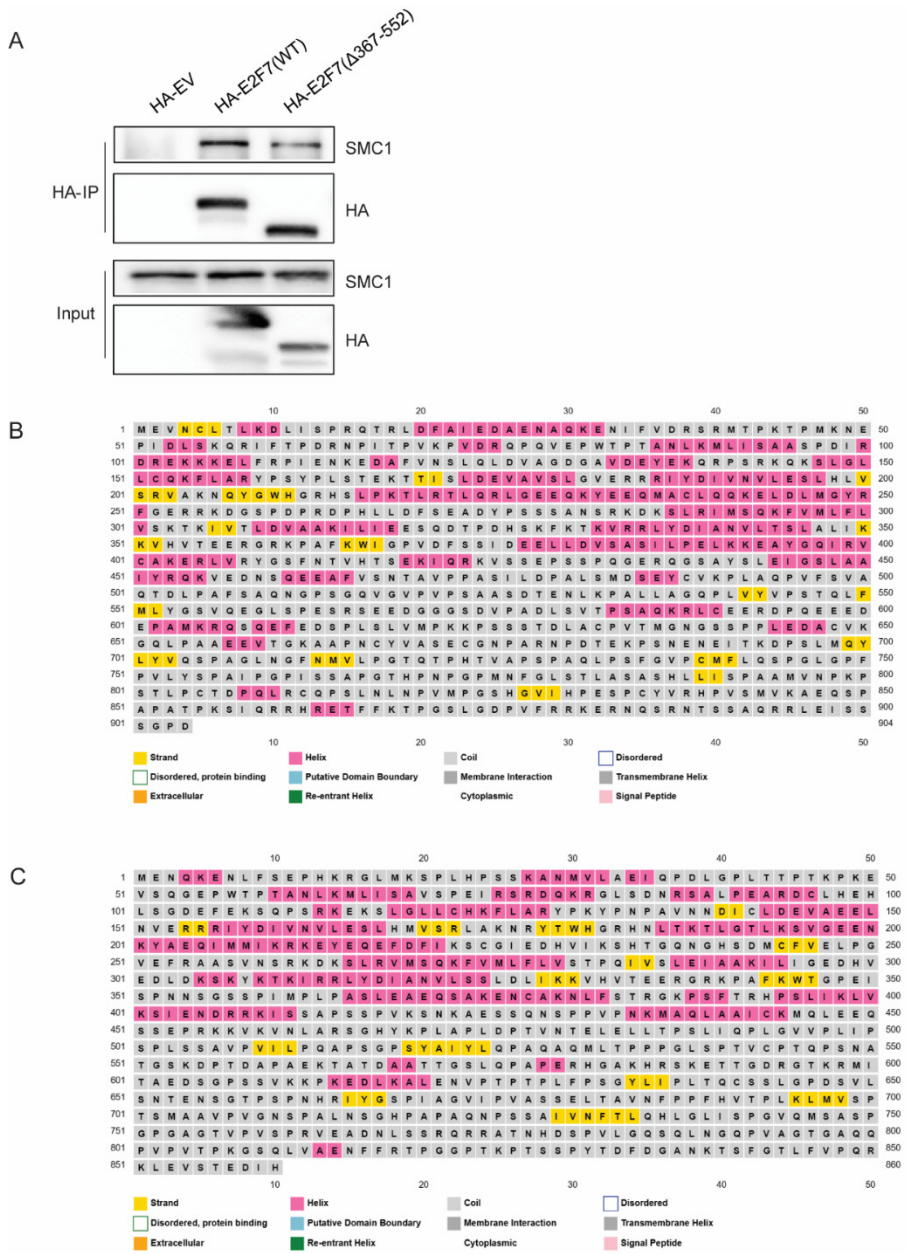
Figure S1. SMC1 binds atypical E2Fs via helix-rich domains. A. HA immunoprecipitation showing the interaction between the indicated E2F7 fragments and endogenous SMC1. **B.** Predicted secondary structure of murine E2F7 via an online platform developed by UCL Department of Computer Science. **C.** Predicted secondary structure of murine E2F8.
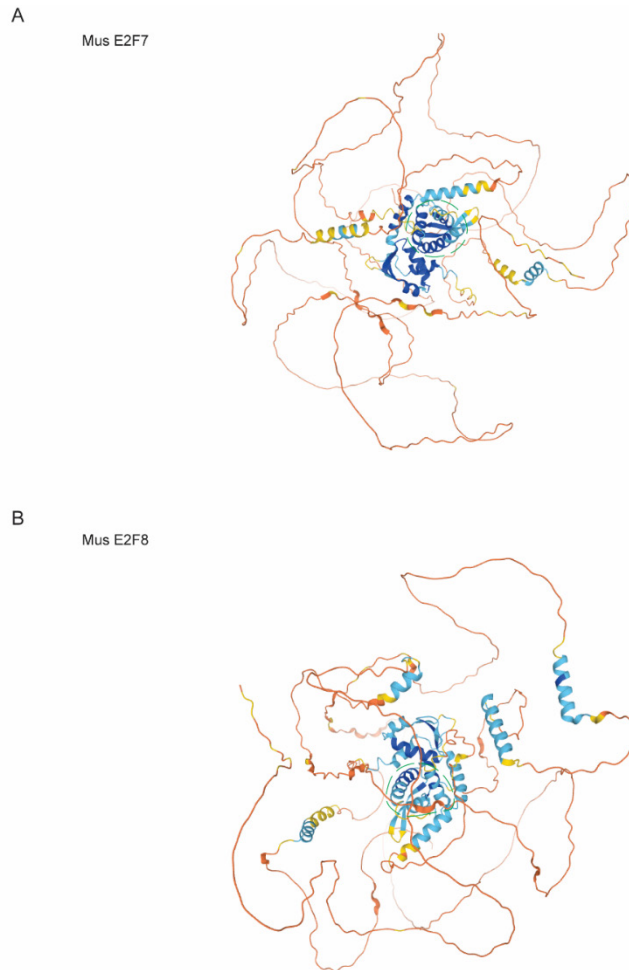
Figure S2. AlphaFold structure prediction of E2F7 and E2F8 protein. A. Overview of full murine E2F7 protein structure predicted in AlphaFold Protein Structure Database developed by Deepmind and EMBL-EBI. Predicted winged-helix formed between aa264-552 is marked with the green dashed circle. pLDDT corresponds to the model's prediction of its score on the local Distance Difference Test (IDDT-Cα). **B.** Overview of full murine E2F8 protein structure predicted in AlphaFold Protein Structure Database. Predicted winged-helix formed between aa243-541 is marked with the green dashed circle.
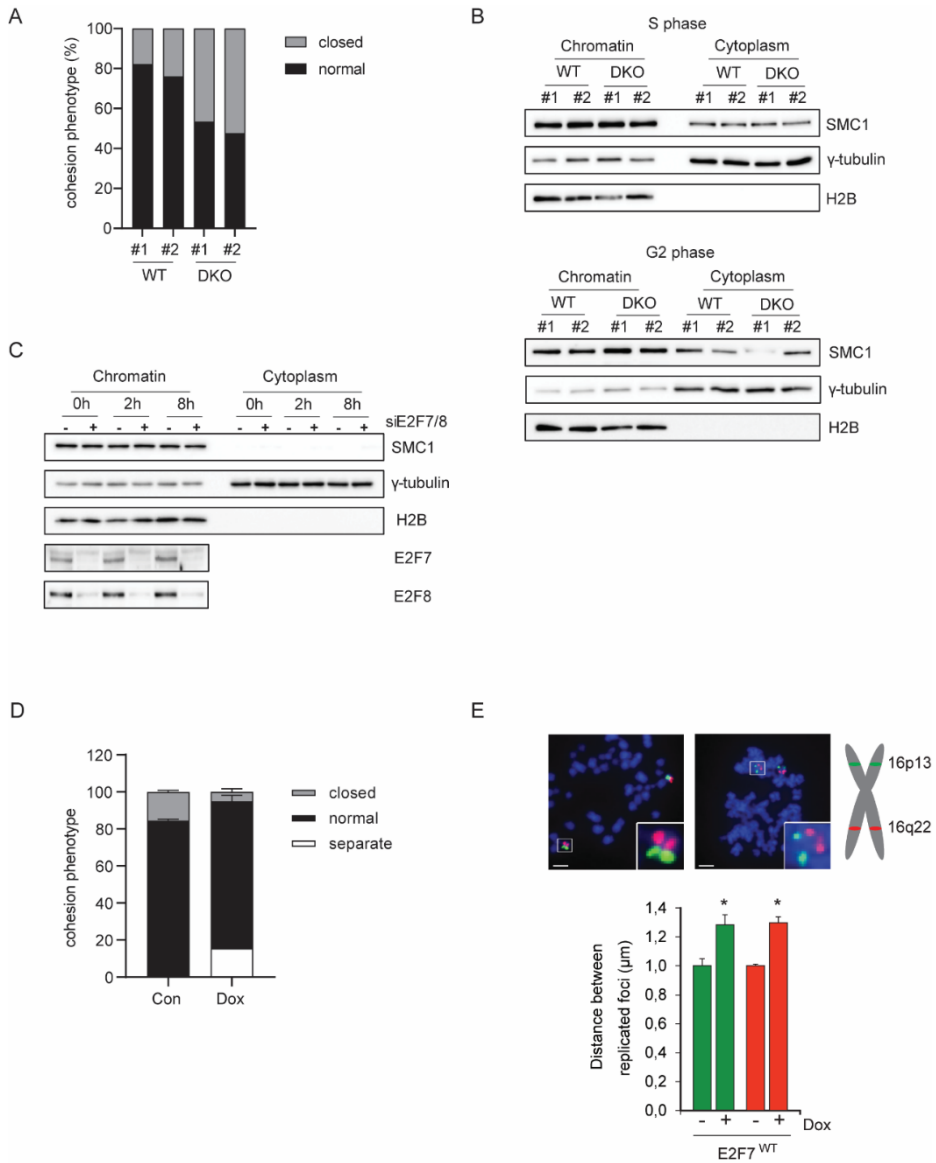
Figure S3. Loss of atypical E2Fs loss has no apparent effect on cohesin levels on chromatin in interphase.

Figure S3. Loss of atypical E2Fs loss has no apparent effect on cohesin levels on chromatin in interphase. A. Quantification of chromosome spreads from RPE *E2F7/8^{DKO}* and *wild type* (*WT*) cells (two clones showed for each genotype). **B.** Protein levels of SMC1 on chromatin in RPE *E2F7/8^{KO}* cells (clone #1 and #2) at S and G2 phases respectively. Cells were first synchronized in early S phase with Hydroxyurea (2 mM) overnight and then released for 3 hours to collect S phase cells and for 9 hours to collect G2 phase cells. H2B works as loading control of chromatin fraction and γ-tubulin for cytoplasm fraction. **C.** Detection of chromatin-bound SMC1 in Hela cells at S and G2 phases respectively. Cells were transfected with siRNAs against E2F7 and E2F8. After 36 hours, Hydroxyurea (2 mM) was added. 16 hours later, cells were released and collected at indicated time. **D.** Quantification of chromosome spreads after induction of E2F7 overexpression. E2F7-EGFP was induced for 12 hours with doxycycline (200 μg/ml). Nocodazole (200 ng/ml) was added 3 hours prior to harvesting mitotic cells. **E.** FISH staining of chromosome 16 with specific probes for 16p13 (green) and 16q22 (red) in Hela cells with wild type E2F7 induction, and quantification of distances between sister chromatids. Measures of inter-chromosomal distances were performed with Slidebook analysis software. Three independent replicates, with at least 50 measurements per condition, were performed.
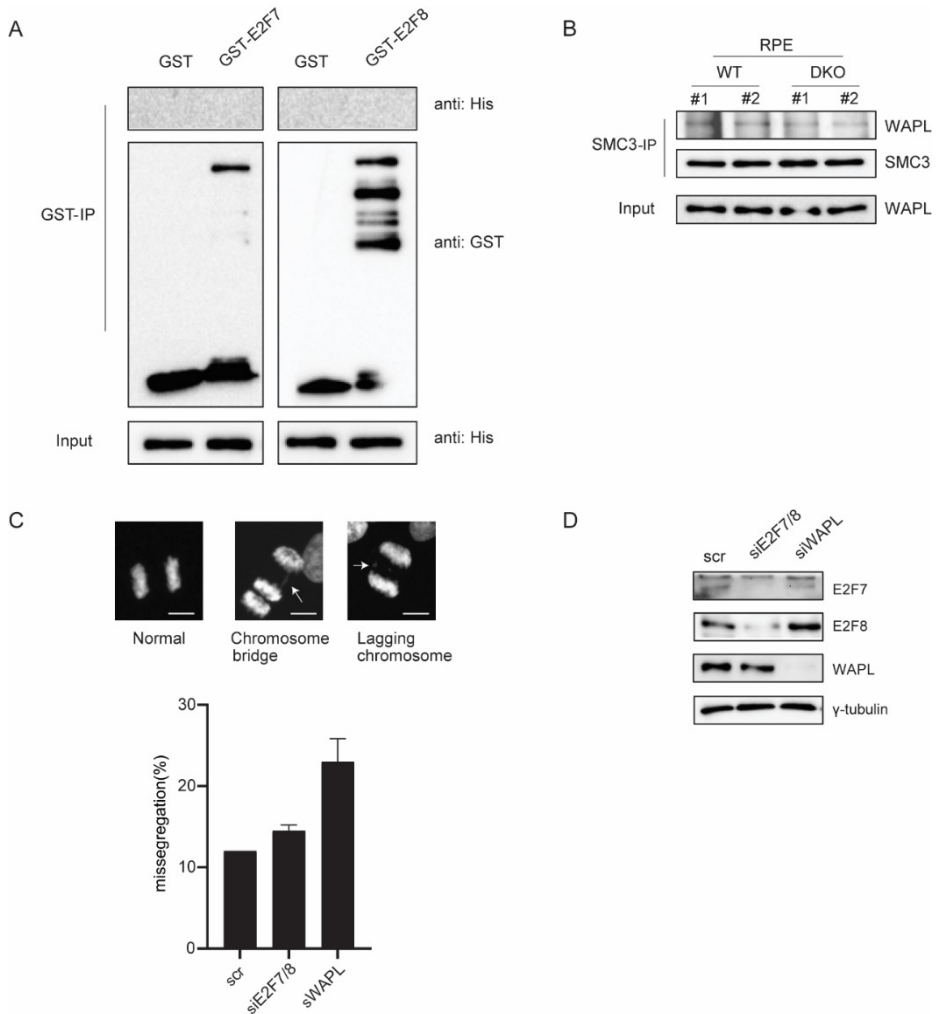
Figure S4. Atypical E2Fs deficiency has no notable effect on chromosome segregation. A. Interaction between atypical E2Fs and WAPL *in vitro*. GST and GST-tagged E2F7 and E2F8 were pulled down with GST resin from E.coli cell lysates, and incubated with ~10 μg 6His-tagged WAPL overnight. Immunoblotting was then performed. **B.** Test the interaction between SMC3 and WAPL in RPE *E2F7/8DKO* cells. *Wildtype* and *E2F7/8* knockout cells were lysed with RIPA buffer and incubated with 1 μg SMC3 primary antibody overnight. Next day, Protein A/G agaroses beads were added and incubated for 1 hour prior to immunoblotting. **C.** Quantification of chromosome mis-segregation in Hela cells transfected with indicated siRNAs. Thirty-six hours after siRNA transfection, CDK1 inhibitor (RO-3306) (7.5 μM) was added to synchronize cells in G2 phase. After another 16 hours, cells were released for 1 hour to collect anaphase cells. **D.** Immunoblots showing the knockdown of *E2F7*, *E2F8* and *WAPL* in C).

REFERENCES

1. Ren B, Cam H, Takahashi Y, et al. E2F integrates cell cycle progression with DNA repair, replication, and G(2)/M checkpoints. *Genes Dev.* 2002;16(2):245-256.

2. Kent LN, Leone G. The broken cycle: E2F dysfunction in cancer. *Nature Reviews Cancer.* 2019;19(6):326-338.

3. Westendorp B, Mokry M, Groot Koerkamp MJ, Holstege FC, Cuppen E, de Bruin A. E2F7 represses a network of oscillating cell cycle genes to control S-phase progression. *Nucleic acids research.* 2012;40(8):3511-3523.

4. Weijts BG, Bakker WJ, Cornelissen PW, et al. E2F7 and E2F8 promote angiogenesis through transcriptional activation of VEGFA in cooperation with HIF1. *EMBO J.* 2012;31(19):3871-3884.

5. Peters JM, Nishiyama T. Sister chromatid cohesion. *Cold Spring Harb Perspect Biol.* 2012;4(11):10.1101/cshperspect.a011130.

6. Yatskevich S, Rhodes J, Nasmyth K. Organization of Chromosomal DNA by SMC Complexes. *Annu Rev Genet.* 2019;53:445-482.

7. Waizenegger IC, Hauf S, Meinke A, Peters JM. Two distinct pathways remove mammalian cohesin from chromosome arms in prophase and from centromeres in anaphase. *Cell.* 2000;103(3):399-410.

8. Losada A, Hirano M, Hirano T. Identification of Xenopus SMC protein complexes required for sister chromatid cohesion. *Genes Dev.* 1998;12(13):1986-1997.

9. Haarhuis JHI, Elbatsh AMO, Van Den Broek B, et al. WAPL-mediated removal of cohesin protects against segregation errors and aneuploidy. *Current Biology.* 2013;23(20):2071-2077.

10. Tedeschi A, Wutz G, Huet S, et al. Wapl is an essential regulator of chromatin structure and chromosome segregation. *Nature.* 2013;501(7468):564-568.

11. Beckouet F, Srinivasan M, Roig MB, et al. Releasing Activity Disengages Cohesin's Smc3/Scc1 Interface in a Process Blocked by Acetylation. *Mol Cell.* 2016;61(4):563-574.

12. Murayama Y, Uhlmann F. DNA Entry into and Exit out of the Cohesin Ring by an Interlocking Gate Mechanism. *Cell (Cambridge).* 2015;163(7):1628-1640.

13. Buheitel J, Stemmann O. Prophase pathway-dependent removal of cohesin from human chromosomes requires opening of the Smc3-Scc1 gate. *EMBO J.* 2013;32(5):666-676.

14. Hauf S, Roitinger E, Koch B, Dittrich CM, Mechtler K, Peters JM. Dissociation of cohesin from chromosome arms and loss of arm cohesion during early mitosis depends on phosphorylation of SA2. *PLoS Biology.* 2005.

15. Nishiyama T, Sykora MM, Huis PJ, Mechtler K, Peters JM. Aurora B and Cdk1 mediate Wapl activation and release of acetylated cohesin from chromosomes by phosphorylating Sororin. *Proceedings of the National Academy of Sciences of the United States of America.* 2013.

16. Nishiyama T, Ladurner R, Schmitz J, et al. Sororin mediates sister chromatid cohesion by antagonizing Wapl. *Cell.* 2010;143(5):737-749.

17. Yuan R, Vos HR, Es RM, et al. Chk1 and 14-3-3 proteins inhibit atypical E2Fs to prevent a permanent cell cycle arrest. *The EMBO Journal.* 2018;37(5):1-17.

18. Lai JS, Herr W. Ethidium bromide provides a simple tool for identifying genuine DNA-independent protein associations. *Proc Natl Acad Sci U S A.* 1992;89(15):6958-6962.

19. Jones DT. Protein secondary structure prediction based on position-specific scoring matrices. *J Mol Biol.* 1999;292(2):195-202.

20. Jumper J, Evans R, Pritzel A, et al. Highly accurate protein structure prediction with AlphaFold. *Nature.* 2021;596(7873):583-589.

21. Morgunova E, Yin Y, Jolma A, et al. Structural insights into the DNA-binding specificity of E2F family transcription factors. *Nature communications.* 2015;6(1):10050.

22. Manning AL, Yazinski SA, Nicolay B, Bryll A, Zou L, Dyson NJ. Suppression of genome instability in prb-deficient cells by enhancement of chromosome cohesion. *Molecular Cell.* 2014;53(6):993-1004.

23. Li J, Ran C, Li E, et al. Synergistic Function of E2F7 and E2F8 Is Essential for Cell Survival and Embryonic Development. *Developmental cell.* 2008;14(1):62-75.

24. Thurlings I, Martínez-López LM, Westendorp B, et al. Synergistic functions of E2F7 and E2F8 are critical to suppress stress-induced skin cancer. *Oncogene.* 2017;36:829.

25. Kueng S, Hegemann B, Peters BH, et al. Wapl Controls the Dynamic Association of Cohesin with Chromatin. *Cell.* 2006;127(5):955-967.

3

26. Gandhi R, Gillespie PJ, Hirano T. Human Wapl is a cohesin-binding protein that promotes sister-chromatid resolution in mitotic prophase. *Curr Biol.* 2006;16(24):2406-2417.

27. Haarhuis JHI, Elbatsh AMO, Van Den Broek B, et al. WAPL-mediated removal of cohesin protects against segregation errors and aneuploidy. *Current Biology.* 2013;23(20):2071-2077.

28. Chan K, Roig M, Hu B, Beckouët F, Metson J, Nasmyth K. Cohesin's DNA Exit Gate Is Distinct from Its Entrance Gate and Is Regulated by Acetylation. *Cell (Cambridge).* 2012;150(5):961-974.

29. Yuan R, Liu Q, Segeren HA, et al. Cyclin F-dependent degradation of E2F7 is critical for DNA repair and G2-phase progression. *The EMBO Journal.* 2019;38(20):e101430.

3
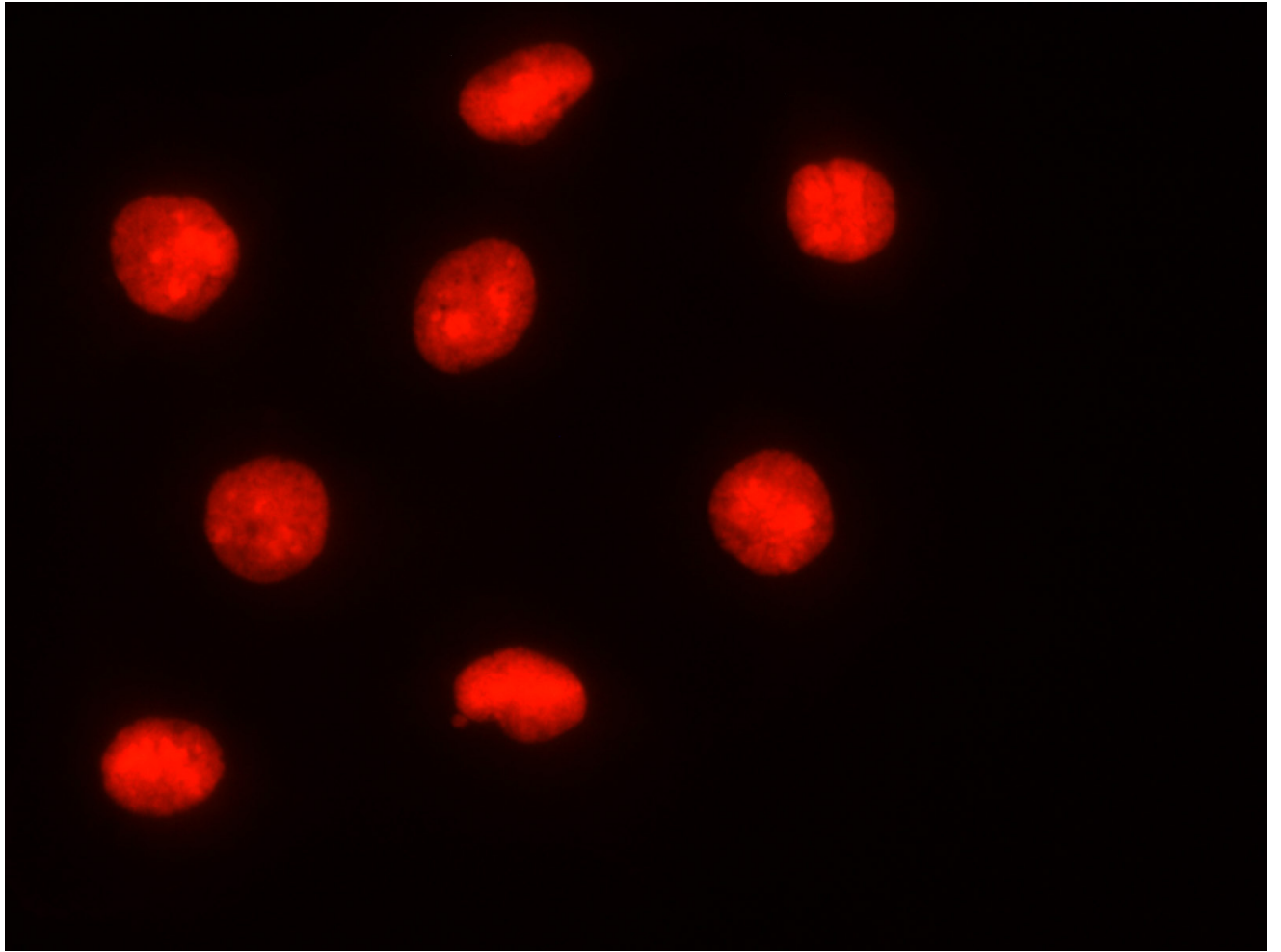
Chapter 4

E2F3 amplification causes replication stress in bladder cancer

Qingwu Liu[1], Esther A. Zaal[1], Jung-Chin Chang[1], Alain de Bruin[1,2], Bart Westendorp[1]

1 Department of Biomolecular Health Sciences, Faculty of Veterinary Medicine, Utrecht University, Utrecht, the Netherlands

2 Department of Pediatrics, University of Groningen, University Medical Center Groningen, Groningen, the Netherlands

ABSTRACT

Amplification of the *E2F3* locus is one of the most common somatic gene alterations in bladder cancer . *E2F3* amplification was also reported to positively associate with the advanced progression of bladder cancer, though the underlying mechanism is still not clear. Here, we show that patients and bladder cancer cell lines with *E2F3* amplification display elevated expression of a replication stress gene signature compared to tumor biopsies and cell lines with normal copy numbers. Furthermore, we found that inducible overexpression of E2F3 in bladder cancer cell lines caused replication stress, DNA damage, and even increased genome instability as measured by micronuclei formation. We show that E2F3 overexpression caused an imbalance in nucleoside metabolism, most likely due to excessive dNTP synthesis, and that suppletion with exogenous nucleosides could rescue this replication stress phenotype. Moreover, we show that E2F3 overexpression sensitizes bladder cancer cells to drugs that target the intra-S-phase checkpoint, such as ATR and WEE1 inhibitors. This indicates that *E2F3* amplification could serve as a biomarker to stratify patients with muscle-invasive bladder cancer who might benefit from the combinational treatment of first-line chemotherapeutic drugs and intra-S-phase checkpoint inhibitors.

INTRODUCTION

In mammalian cells, the CDK-RB-E2F signaling pathway is the main driver of cell cycle entry and DNA replication. In G1 phase, phosphorylation of the retinoblastoma protein (RB) by CDK4/6-cyclin D complexes releases E2F activators, E2F1-3, allowing them to bind to the promoter of target genes and upregulate their expression[1]. Among the E2F target genes, *CCNE1* and *CCNE2* (which encode two isoforms of cyclin E) and *FBXO5* (which encodes Emi1) are well-known to facilitate the G1/S transition[2], while *MCM2-7*, *CDC6*, *CDT1* and *ORC* are necessary for DNA synthesis[3]. Hence, the CDK-RB-E2F axis is highly regulated in normal cells to avoid unscheduled cell cycle entry and the formation of cancers. Indeed, *RB1* and *CDKN2A* (which encodes the CDK inhibitor P16[INK4A]) are tumor suppressor genes that are commonly mutated or lost in cancer. Furthermore genes encoding cyclin D or cyclin E proteins are amplified in many cancers, and act as oncogenes. The amplification of genes encoding activating E2Fs is less common, but intriguing, *E2F3* locus amplification was observed in up to 21% of patients with muscle-invasive urothelial carcinoma[4,5]. Amplification of *E2F3* is also relatively frequent in retinoblastoma and melanoma[6,7]. Previous studies showed that depletion of *E2F3* in bladder cancer cells harboring *E2F3* amplification impaired DNA replication and proliferation, indicating that ectopic E2F3 protein levels provided a growth advantage to tumor cells and thereby contributed the development of bladder cancer[8]. Because E2F3 is of great importance for normal cellular proliferation as well[9] it is difficult to elucidate the role of *E2F3* amplification on bladder tumorigenesis only by knockdown or knockout of *E2F3*. Previous work showed that E2F3 amplification typically co-occurs with loss of RB function[10], suggesting that these two oncogenic alterations synergize to override the G1/S checkpoint. However, we recently showed that inducible overexpression of E2F3 in non-transformed epithelial cells caused defect in cell cycle exit during G2 after the induction of DNA damage[11]. This indicates that the consequences of E2F3 amplification on proliferating cancer cells could extend beyond a G1/S checkpoint defect.

DNA replication stress (RS) can be defined as events that cause stalling and/or collapse of DNA replication forks[12]. Accumulating evidence shows that overexpression of oncogenes such as *RAS*, *MOS*, *MYC*, CCNE and *CDC25A* is sufficient to induce RS in cultured cells, and various underlying mechanisms have been described[13]. For example, increased global transcriptional activity, and conflicts between progressing replication forks and transcription machinery can be observed in HRAS[V12] -induced RS[11][14]. Similar phenotypes were also observed in cancer cells with cyclin E overexpression, where increased replication initiation and transcription led to RS[15]. Furthermore, cyclin E overexpression causes a decrease in dNTP pool, which is another source of RS[16]. Following oncogene-induced RS, the ATR/CHK1 pathway becomes active and suspends DNA synthesis, which can result in cell cycle arrest or senescence if the damaged replication forks cannot be recovered in a timely manner[12]. However, RS is not only detrimental to tumor proliferation, as it can lead to genetic variation that could

4

drive tumor evolution[17]. RS can cause DNA damage, which leads to genomic instability if not repaired properly.

Here, we reveal that E2F3 overexpression causes premature S-phase entry in bladder cancer cells, leading to replication stress, ATR/CHK1 activation and DNA damage. As a consequence, we observed that E2F3 overexpression caused micronuclei formation, suggesting genomic instability. We provide evidence that this increased RS is triggered by deprivation of the nucleoside pools and reduced rates of gene transcription during S-phase. Lastly, we discover that E2F3 overexpression can sensitize bladder cancer cells to three different intra-S-phase checkpoint inhibitors, which are currently being tested in clinical trials. Therefore, we propose that E2F3 amplification could serve as a potential biomarker for future clinical treatment of patients who could benefit from these checkpoint inhibitors.

RESULTS

E2F3 amplification causes overexpression of E2F target genes and cell cycle defects.
The chromosome 6p22 locus, which encodes the *E2F3* gene, is frequently amplified in human bladder cancer. To investigate the potential consequences of this amplification, we sought to analyze the transcriptomic differences between patients with intact *E2F3* and patients with *E2F3* amplification. To this end, we analyzed the RNA-sequencing data from the muscle-invasive bladder cancer (BLCA) patients of The Cancer Genome Atlas (TCGA) and examined the differentially expressed genes (DEGs) between patients with and without *E2F3* amplification. The tumors with amplified *E2F3* showed over 2200 significantly upregulated genes (Supplementary Table 1). *E2F3* was among the most strongly upregulated genes, confirming that *E2F3* copy number gains in bladder cancer biopsies are accompanied with enhanced expression of *E2F3* (Fig S1A).

Importantly, these gene expression differences are not biased by clinical variables such as the distribution of cancer types and tumor stages (Fig S1B and C). Then, we analyzed the key biological processes represented by the DEGs using gene set enrichment analysis (GSEA). Genes upregulated in *E2F3*-amplified bladder tumors displayed marked enrichment for multiple pathways associated with the cell cycle, such as "G2/M checkpoint" and "E2F targets" (Fig 1A). Downregulated transcripts (in total 2044) were mainly involved in processes related to innate immune responses and inflammation, but also P53 (Fig 1B). Hence, E2F3 amplification affects different cellular processes during bladder cancer development, but the most prominent effect is induction of E2F targets and other cell cycle genes.

To study in a more controlled setting the physiological consequences of *E2F3* amplification, we introduced a lentiviral doxycycline-inducible *E2F3A* overexpression system into two E2F3-intact bladder cancer cell lines, T24 and UMUC3. The *E2F3A* construct was fused to an mTurquoise2 fluorescent tag (Fig S1D)[11]. Given the effects of *E2F3* amplification on ex-

pression of cell cycle genes, we investigated the effect of E2F3 ectopic expression on cell proliferation in our E2F3 inducible cell lines. Because E2F3 is a key activating factor during G1/S transition, we first investigated if inducible overexpression of E2F3 accelerated S-phase entry. To this end, we arrested T24 cells in G1 phase with the CDK4/6 inhibitor Palbociclib and then released them from this block after 4 hours of E2F3 induction. We verified that 4 hours of doxycycline was sufficient to cause a robust induction of the E2F3 overexpression construct (Fig S1E). Cells were incubated with the thymidine analog 5-ethynyl-2'-deoxyuridine (EdU) and collected at different time points after Palbociclib release to track S-phase entry and cell cycle progression (Fig 1C). Consistent with its role as transcriptional activator of S-phase genes, E2F3 induction accelerated the entry of S phase (Fig 1C). In line with this, qPCR on synchronized G1 cells (6 hours after a nocodazole release) showed that E2F3 overexpression significantly promoted the expression of genes involved in replication origin licensing and firing in G1 cells (Fig S1F and G). When we performed DNA content analysis after the Palbociclib release, we noticed that after 24 hours an increased fraction of E2F3-overexpressing cells was still stranded in G2/M phase compared to control cells (Fig 1D and E). This suggests a delay in G2/M progression after E2F3 overexpression. Accordingly, we also observed that cell proliferation was significantly impaired after 3 days of continuous E2F3 induction by doxycycline (Fig S1H). Collectively, these data show that E2F3 overexpression in bladder cancer cells causes an acceleration in S-phase entry, which is offset by longer G2 duration.

Figure 1. E2F3 amplification causes overexpression of E2F target gens and cell cycle defects. A. Bar graph showing the pathways that upregulated genes from E2F3-amplified patients involve in. Black dotted lines indicates *p*-value of 0.05. **B.** Bar graph showing the pathways that downregulated genes from E2F3-amplified patients involve in. Black dotted lines indicates *p*-value of 0.05. **C.** Experimental work scheme and representative flow cytometry plots showing EdU incorporation in T24 cells released from Palbociclib (1 µM). Quadrangle inset indicates the Annexin V positive cells. Doxycycline was added 4 h prior to Palbociclib release. Cells were collected at indicated time points. Plot on the right shows the quantification of EdU positive cells from two separate experiments. *P<0.05 (unpaired two-tailed t-test). **D.** Representative cell cycle profile at indicated time points in T24 cells released from Palbociclib (1 µM) with or without E2F3 induction. **E.** Quantification of G2/M phase cells after 24 h release from Palbociclib with E2F3 induction in T24 cells. *P<0.05 (unpaired two-tailed t-test).
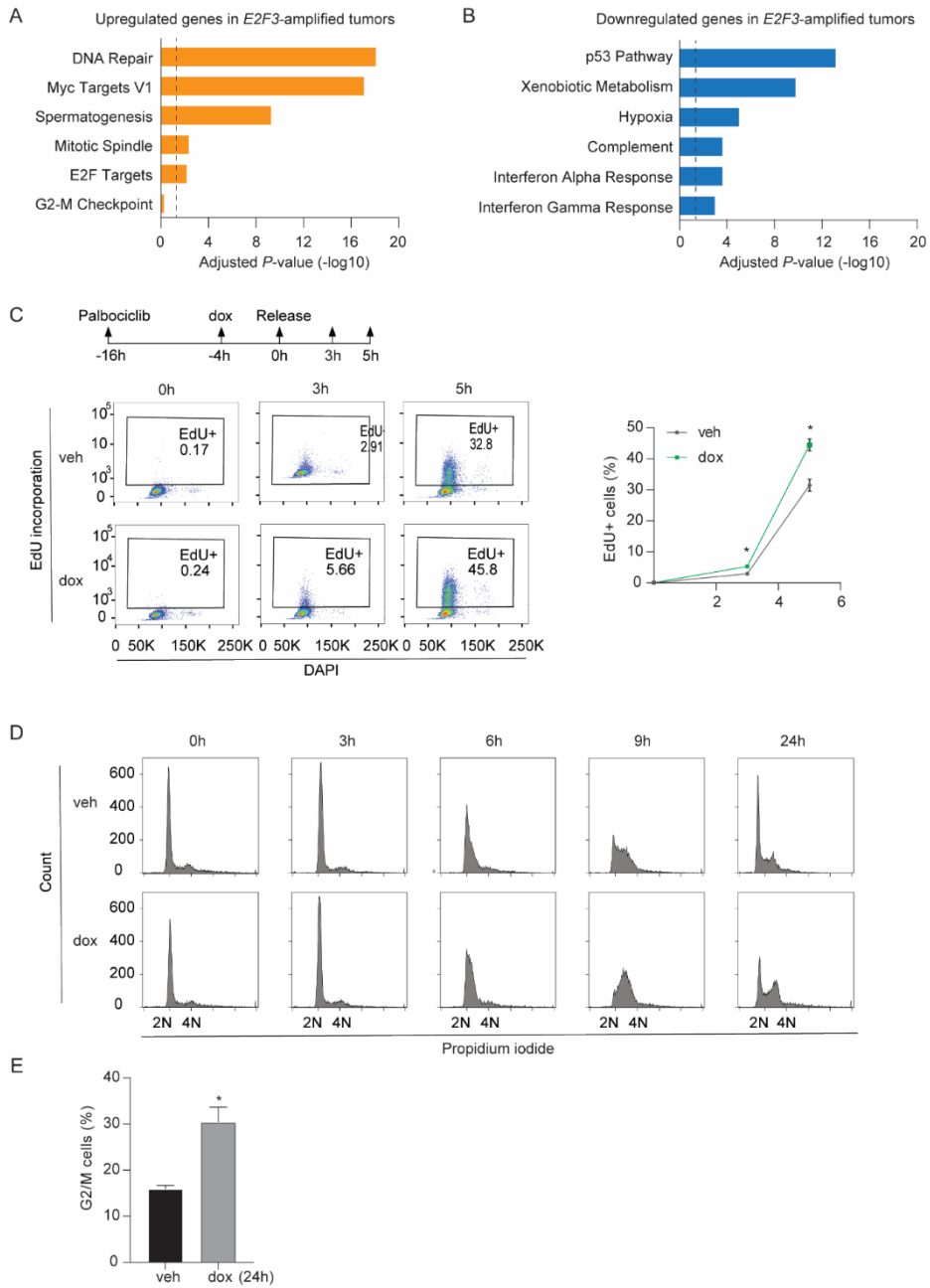
Figure 1. *E2F3* amplification causes overexpression of E2F target genes and cell cycle defects.

E2F3 overexpression causes replication stress.

Previously, it was revealed that aberrant activation of RB-E2F pathway by HPV-16 E6/E7 or cyclin E oncogenes caused replication stress and led to genome instability[16]. Given the delayed G2-M transition in E2F3-overexpressing bladder cancer cells, we wondered if E2F3 amplification might also be able to override the G1/S checkpoint and induce RS, thereby slowing cell proliferation. For this reason, we performed DNA fiber assays, in which cells were sequentially pulse-labeled with the thymidine analogs chlorodeoxyuridine (CIdU) and iododeoxyuridine (IdU) for 20 min each, followed by DNA fiber spreading. CIdU and IdU were detected by immunostaining using specific antibodies. After 2 days of E2F3 induction, a clear reduction in replication fork speed was observed in both T24 and UMUC3 cells by measuring the IdU fiber tract lengths (Fig 2A and B). In response to RS, cells activate ATR, which subsequently phosphorylates Chk1 at serine 345, to stabilize replication fork and delay cell cycle progression[18]. Indeed, western blotting for phosphorylated Chk1 (S345) in T24 and UMUC3 cells showed that the ATR/Chk1 pathway became active after 1 day of E2F3 overexpression and remained active for the duration of the 3 days exposure to doxycycline (Fig 2C and D). In line with E2F3-induced replication stress and Chk1 activation, the DNA damage marker γH2AX increased over time. Oncogene-induced replication stress and DNA damage can lead to genomic instability[19]. A widely used marker of genome instability is micronuclei, which contain the acentric DNA fragments due to mis-repaired DNA damage or chromosome mis-segregation during anaphase[20]. Likewise, we found that E2F3 induction caused a three-fold increase in cells containing micronuclei (Fig 2E). Overall, the data above suggest that E2F3 overexpression impairs DNA replication and induces genome instability.
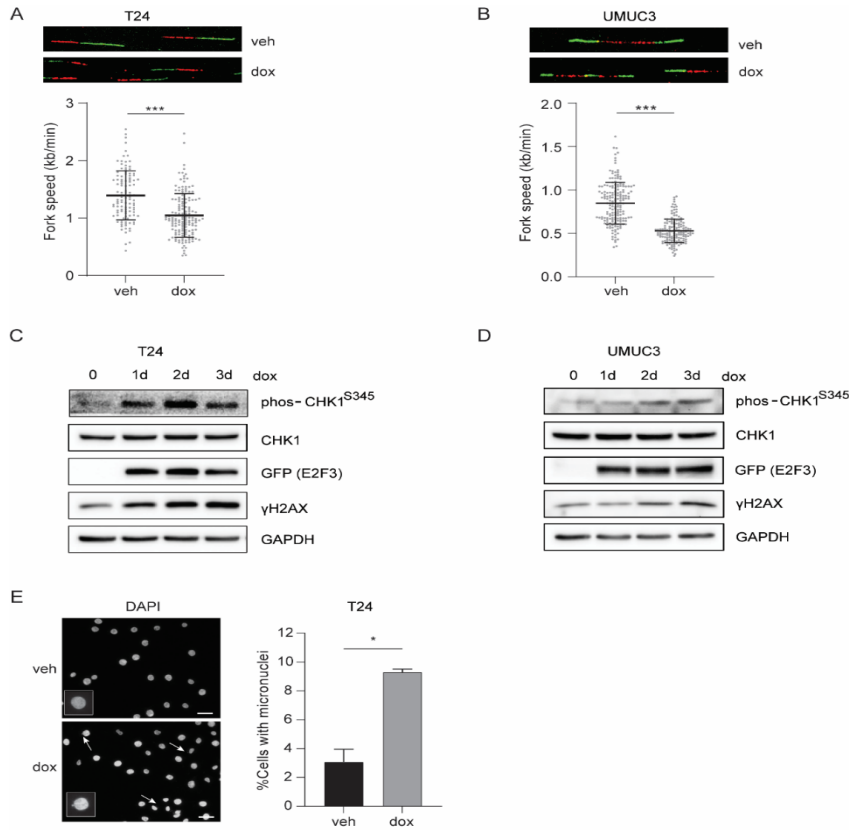
Figure 2. E2F3 overexpression causes replication stress. A. Representative DNA fibers counted and quantification of replication fork speed in T24 cells with or without 48h E2F3 induction. Quantification here shows one of two separate experiments. Crossbars represent median values per condition. **B.** Representative DNA fibers counted and quantification of replication fork speed in UMUC3 cells with or without 48h E2F3 induction. Crossbars represent average values per condition. **C.** Blotting showing the levels of indicated proteins after 1 day, 2 days and 3 days of E2F3 induction in T24 cells. **D.** Blotting showing the levels of indicated proteins after 1 day, 2 days and 3 days of E2F3 induction in UMUC3 cells. **E.** Representative nuclear with or without micronuclei and quantification of micronuclei in T24 cells with 48 h E2F3 induction. 150 cells were counted for each condition and repeated twice. Inset shows an enlarged nuclear. Scale bar, 20 μm. *$P<0.05$ (unpaired two-tailed t-test).

Ectopic E2F3 induces the expression of replication stress signature genes

We then asked if *E2F3* amplification and overexpression causes DNA replication stress *in vivo*. To answer this question, we studied if *E2F3* amplification affected expression of a recently published RS gene signature consisting of *C8ORF33*, *DDX27*, *MOCS3*, *NAT10*, *MPP6*, and *ZNF48*[21]. First, we determined the mRNA levels of the six RS signature genes after inducible E2F3 overexpression in T24 bladder cancer cells. Consistent with the RS phenotype we observed before, E2F3 induction led to the increase in expression of RS signature genes (Fig 3A). Then, we calculated the RS signature scores for *E2F3*-ampified versus non-amplified (intact) bladder cancer biopsies in the TCGA dataset. Interestingly, despite substantial inter-patient heterogeneity in this dataset, the *E2F3*-amplified group showed significantly higher RS signature scores (Fig 3B and S2A). To further verify that RS signature gene expression correlates with *E2F3* amplification, we also tested the mRNA levels of these RS signature genes in a panel of bladder cancer cell lines, three of which harbor *E2F3* amplifications. When comparing the average z-scores of the combined six RS signature genes, *E2F3*-amplified cell lines showed a significant increase (Fig 3C). When comparing the individual RS signature genes only *MPP6* increased significantly in *E2F3*-amplified cells (Fig S2B). This may be ascribed to the fact that only two of the three cell lines with *E2F3* amplification (5637 and HT-1376) showed consistently increased expression of the signature genes, while the third cell line (TCC-SUP) showed an intermediate phenotype, with upregulation of two of the six genes in the RS signature (Fig S2C). This variation appeared to be caused by differences in E2F3 protein expression levels, because immunoblotting showed that the protein levels of E2F3 were markedly higher in 5637 and HT-1376 cells than the TCC-SUP cells (Fig S2D).

As replication stress compromises the integrity of DNA replication and impacts on chromosome segregation at mitosis, we analyzed the effect of *E2F3* amplification on genomic stability in bladder cancer patients from the TCGA dataset. Expectedly, patients with amplified *E2F3* present higher levels of mutation counts and aneuploidy (Fig 3D and E). Collectively, our data demonstrate that *E2F3* overexpression due to gene amplification causes replication stress in bladder cancer patients and bladder cancer cell lines.

E2F3-induced replication stress can be relieved by nucleoside suppletion.

Next, we asked how E2F3 overexpression induced RS. Previous work showed that increased replication initiation and global transcriptional activity mediated cyclin E-induced RS[15]. E2F3 activation is downstream from RB hyperphosphorylation by cyclin/CDK complexes during late G1-phase and in turn E2F3 upregulates the level of cyclin E transcriptionally. Hence, we reasoned that E2F3 overexpression could induce RS in a similar fashion as cyclin E overexpression.
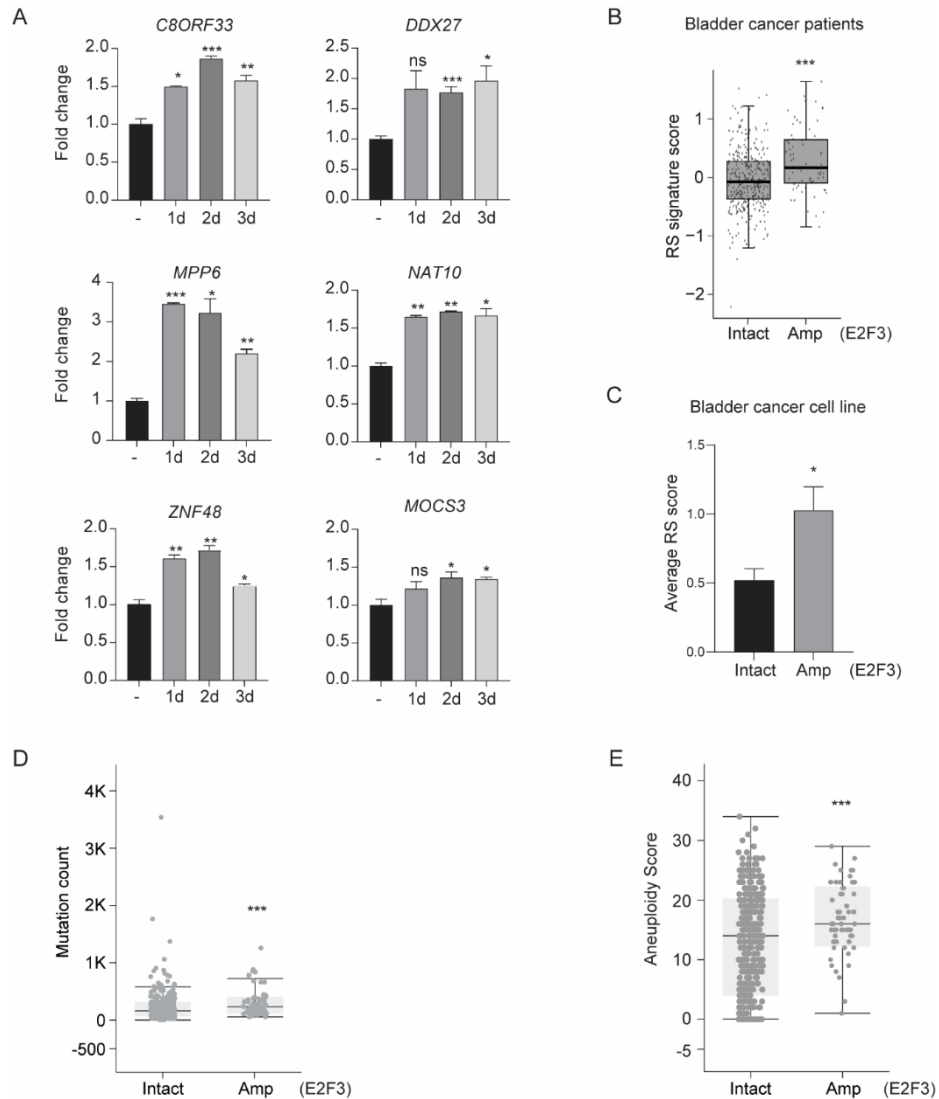
Figure 3. Ectopic E2F3 induces the expression of replication stress signature genes. A. The expression of RS signature genes in T24 cells after 1, 2 and 3 days of induction. *$P<0.05$, **$P<0.01$, ***$P<0.001$ (unpaired two-tailed t-test). **B.** Dot plot showing the replications stress (RS) scores in sub-groups of bladder cancer patients as indicated. The RNA-seq expression data of patients is retrieved from TCGA. RS scores represent the average value of the six RS signatures gene expression. **C.** RS scores of eight bladder cancer cell lines divided into *E2F3* intact and amplified groups. *$P<0.05$ (unpaired two-tailed t-test). **D.** Dot plot showing the mutation counts in sub-groups of bladder cancer patients as indicated. This data of patients is retrieved from TCGA. ***$P<0.001$ (Wilcoxon test). **E.** Dot plot showing the aneuploidy score in sub-groups of bladder cancer patients as indicated. This data is retrieved from TCGA. The aneuploidy score reflects the total number of chromosome arms with arm-level copy-number alterations in a sample. ***$P<0.001$ (Wilcoxon test).

We therefore analyzed replication origin firing rates by counting the incidence of newly fired DNA tracts. Three types of DNA tracks were considered: termination, on-going and origin firing (Fig 4A, inset). This analysis showed a substantial increase in the percentage of newly fired origins (Fig 4A) and decrease in on-going tracks (S3A) in the E2F3-overexpressing cells. Deprivation of deoxynucleotide (dNTP) pool was proposed to underlie the RS following ectopic origin firing, which could be rescued by exogenous supply of nucleosides[16]. To verify if this is also the case in bladder cancer cells with E2F3 overexpression, we supplied T24 cells with additional nucleosides (adenosine, guanosine, cytidine, and thymidine) and measured replication fork speed. This experiment showed that nucleoside supply indeed rescued the defects in replication fork speed and origin firing rates caused by E2F3 overexpression (Fig 4B and C). Moreover, nucleoside suppletion reduced DNA damage, as seen with γH2AX immunoblotting. (Fig 4D).

To verify that nucleotide pools are indeed depleted in E2F3-overexpressing cells, we measured nucleosides, nucleotides, and their precursors in T24 cells with or without 48 hours of E2F3 overexpression. Surprisingly, we did not observe a decrease but instead a consistent increase of all dNTPs in E2F3-overexpressing cells (Fig S3B). This strongly argues against a dNTP shortage being the prime cause of replication stress. However, the concentrations of the nucleosides adenosine, guanosine, cytidine, and thymidine were non-significantly but consistently reduced after E2F3 overexpression (Fig. S3C). As nucleosides are not only used for dNTP synthesis, but also as building blocks for mRNA synthesis, we wondered if E2F3 overexpression caused a change in global transcription. Therefore, we first measured the global transcription by quantifying nascent RNA synthesis after pulsing cells with the RNA-specific labeled nucleoside 5-ethynylurideine (EU) for 1 hour. As expected, the global RNA synthesis increased after 24 hours of E2F3 induction (Fig. 4E). However, transcription is elevated in cycling versus non-cycling cells, and the percentage of cycling cells was increased after E2F3-induction (Fig. 1C and D). Therefore, when we specifically quantified the nascent RNA synthesis in S phase cells (IdU positive), and observed a significant decrease of EU intensity after E2F3 induction (Fig. 4F). We postulate that E2F3 overexpression causes a shift in nucleoside metabolism that promotes the formation of deoxyribonucleotide (dNTP) but reduces ribonucleotide (NTP), thereby lowering transcription rates to favor DNA replication. This would in turn result in transcription-replication conflicts and replication stress.

Overall, the data above show that oncogenic E2F3 causes an imbalance in nucleoside and nucleotide metabolism, leading to reduced transcription during S-phase and excessive replication origin firing. Exogenous nucleoside suppletion can rescue E2F3-induced replication stress.
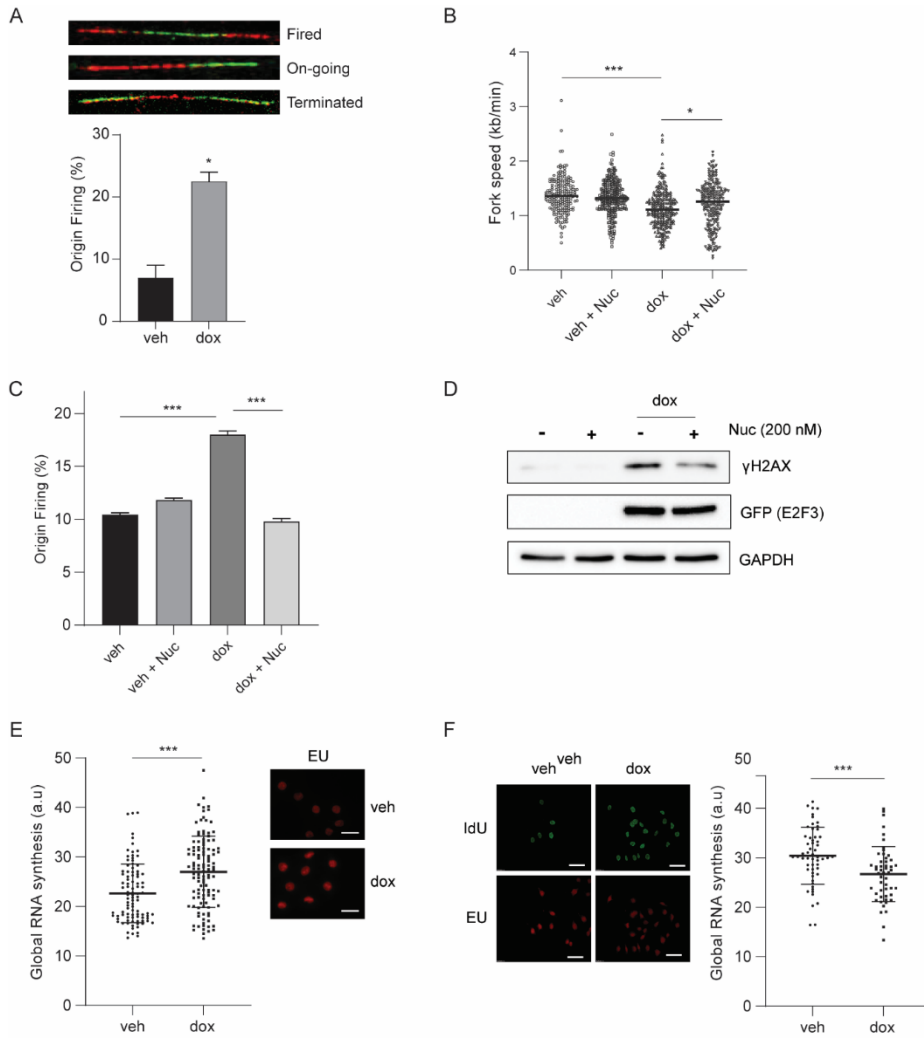
Figure 4. E2F3-induced replication stress can be relieved by nucleoside suppletion.

Figure 4. E2F3-induced replication stress can be relieved by nucleoside suppletion. A. Quantification of fired origins in T24 cells with 2 days of E2F3 induction. Three kinds of fibers were included in the quantification and presented here. Data from two separated experiments are pooled. *P<0.05 (Mann-Whitney Rank Sum test). **B.** Quantification of replication speed in T24 E2F3 inducible cells. Cells were treated with doxycycline for 2 days, and simultaneously exogenous nucleosides (200 nM) were supplied or not. Nucleosides were refreshed daily. *P<0.05, ***P<0.001 (Mann-Whitney Rank Sum test). **C.** Quantification of fired origins in T24 cells treated as B). Three kinds of fibers were included in the quantification and presented here as in A). Data from two separated experiments are pooled. *P<0.05 (Mann-Whitney Rank Sum test). **D.** Blotting showing the expression of indicated proteins in T24 E2F3 inducible cells treated as B). **E.** Quantification of EU incorporation in T24 cells. Cells were induced with doxycycline for 24 h and EU (1 mM) was added 1 h prior to collection. The intensity of EU staining was measured with Image J. Pictures on the right present the EU staining in cells with or without doxycycline addition. ***P<0.001 (Mann-Whitney Rank Sum test). **F.** Representative co-staining of EU and IdU in T24 cells. Cells were induced with doxycycline for 24 h. EU (1 mM) and IdU (250 µM) were added 1 h and 20 min prior to collection, respectively. Plot on the right shows the intensity of EU staining. ***P<0.001 (Mann-Whitney Rank Sum test). Scale bar, 20 µm.

E2F3 overexpression induces G2/M arrest and sensitizes cells to checkpoint inhibitors

Oncogene-induced replication stress causes cancer cells to rely heavily on the intra-S-phase checkpoint[22]. Thus, we hypothesized that E2F3-overexpression could sensitize bladder cancer cells to inhibitors of this checkpoint (ATR/CHK1/WEE1 inhibitors). To this end, we induced E2F3 expression in both T24 and UMUC3 cells and concurrently treated them with individual checkpoint inhibitors (ATR, CHK1, or WEE1) for 48 hours. E2F3 overexpression increased the sensitivity to all of these checkpoint inhibitors (Fig. 5A and S4A). To exclude the possible confounding effect of E2F3 overexpression slowing down cell proliferation, we calculated the IC50s of the checkpoint inhibitors. Indeed, E2F3 overexpression consistently decreased the IC50s of all three checkpoint inhibitors (Fig. 5B and S4B). Additionally, more apoptotic cells were detected with E2F3 induction and CHK1 inhibition compared to treating cells with CHK1 inhibitor alone (Fig. 5C). We also tested if E2F3 overexpression sensitizes bladder cancer cells to the first-line chemotherapeutic drugs cisplatin and gemcitabine[23]. However cell viability assays did not show a synergistic effect of the combination of E2F3 activation and the two chemo drugs (Fig. S4C). Together these data suggest that E2F3 overactivation sensitizes bladder cancer cells to intra-S-phase checkpoint inhibition, implying a potential role for E2F3 amplification in better stratification of patients in future clinical trials to test these inhibitors.
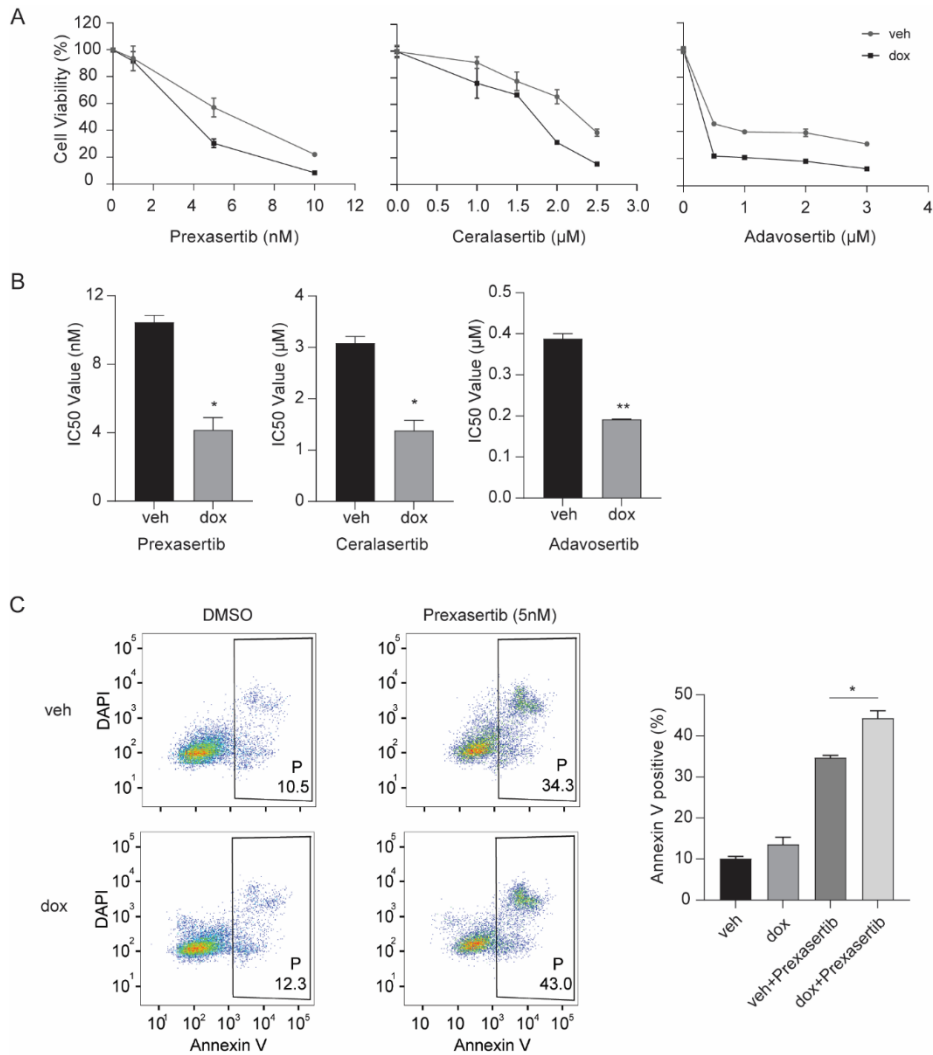
Figure 5. E2F3 overexpression sensitizes bladder cancer cells to checkpoint inhibitors. A. Representative plots showing the viability of T24 cells after 48 h checkpoint inhibitors treatment with or without E2F3 induction. MTT assay was performed to measure cell viability. **B.** IC50 detection for Prexasertib, Ceralasertib and Adavosertib in T24 cells. Cells were treated with indicated drug for 48 h and simultaneously doxycycline was added. MTT assay was performed to measure cell viability. *P<0.05, **P<0.01 (unpaired two-tailed t-test). **C.** Representative flow cytometry plots showing the detection of Annexin V positive cells. T24 cells were exposed to Prexasertib (5 nM) with or without doxycycline for 48 h. Annexin V staining was performed. Graph on the right shows the quantification of Annexin V positive cells from two separate experiments. *P<0.05 (unpaired two-tailed t-test).

DISCUSSION

In this study, we established E2F3 inducible cell lines to mimic *E2F3* amplification often seen in bladder cancer patients and investigated the effect of ectopic E2F3 expression on DNA replication dynamic and cell cycle progression. The data suggest that E2F3 overexpression disturbs nucleoside and nucleotide metabolism, and causes replication stress and impairs G2/M phase progression, while S phase entry is accelerated by E2F3 induction. Moreover, E2F3 overexpression was able to sensitize cancer cells to checkpoint inhibitors, indicative of a role of *E2F3* amplification as a potential biomarker to stratify patients for checkpoint inhibitor treatment.

E2F3 locus amplification has been thought to promote the malignancy of bladder cancer through enhancing cell proliferation[4,4,24]. In line with this, depletion of E2F3 in *E2F3*-amplified cell lines indeed reduces cell proliferation[8]. However, considering that E2F3 deficiency also impairs normal cell cycle progression, it is impossible to simply assert that *E2F3* amplification contributes to cell proliferation. Here, using doxycycline-inducible E2F3 expression in bladder cancer cell lines with normal copy numbers of the *E2F3* locus, we notice that overexpressing E2F3 impedes DNA replication fork progression and activates intra-S checkpoint. This is in line with the findings observed in cells with aberrant activation of CDK-RB axis. For example, a reduction in replication fork speed was detected in primary keratinocytes expressing the human papillomavirus oncogene E7, which targets RB protein. In addition, overexpressing cyclin E in human fibroblasts also gave rise to slower replication and induction of DNA damages[16]. A similar phenotype was detected in U2OS osteosarcoma cells with cyclin E overexpression[15]. Moreover, it was reported that stabilized E2F3 in S/G2 phase led to ectopic expression of E2F target genes in M phase, causing early S phase entry and subsequent replication stress[25]. Similarly, following E2F3 upregulation in G1 phase, we found that S-phase entry is accelerated, while more cells are arrested in G2- or /M-phase later, resulting from replication stress and accumulation of DNA damage.

Then how could *E2F3* act as an oncogene in muscle-invasive bladder cancer? Oncogene-induced replication stress is like a two-edged sword. Although it hampers DNA replication progression, it is also a major source of genome instability[19], which is a hallmark of cancer. The accumulation of genome instability is considered to drive cancer development and observed already in precancerous lesions[26]. Increasing evidences show that dysregulation of CDK-RB pathway can undermine genome integrity via interfering with DNA replication, such as RB loss[27] and cyclin D/E upregulation[28,29]. And additional gain in copy number of *E2F1* and *E2F3* was demonstrated to cause hepatocellular carcinoma in mice[30]. Hence, we reason that *E2F3* amplification promotes the progression of bladder cancer in patients through impairing genomic integrity, allowing for the subsequent selection of genomic alterations favoring in tumor malignancy. For instance, *E2F3* amplification was found to couple with RB loss in a subset of bladder tumor-derived cell lines[10]. Considering that *E2F3* amplification is more frequently seen than RB deletion in bladder cancer patients[5], it is likely that *E2F3* amplification

4

leads to RB loss via increased genome instability.

Replication stress has been seen as a vulnerable target for cancer treatment. But proper markers to indicate the levels of replication stress are missing. And recently the outcome of clinical trial where combination of ATR inhibitor and standard chemo drugs were tested in bladder cancer patients, falls short[31]. Hence, it might help to improve the efficacy of check-point inhibitors by stratifying patients with biomarkers of replication stress. Indeed, a previous study has showed that overexpression of cyclin E or Cdc25A was able to enhance the toxicity of ATR and WEE1 inhibitors *in vitro*[32]. With our finding that E2F3 overexpression also sensitizes cells to inhibition of ATR, CHK1 and WEE1, the mounting data supports the notion that ectopic expression of replication stress-inducing oncogenes could be used as criteria to select patients for treatments with checkpoint kinase inhibitors, including ATR, CHK1 and WEE1.

Taken together, this study reports that E2F3 overexpression is able to induce replication stress, and cell lines and patients harboring *E2F3* amplification share the same replication stress gene signatures with those containing other oncogenes, *CCNE1, MYC* and *CDC25A*. Furthermore, we find that aberrant E2F3 expression can enhance the sensitivity of cancer cells to checkpoint inhibitors, which sheds light on the necessity of stratifying patients with above oncogenes amplification to improve the efficacy of checkpoint inhibitors.

MATERIALS AND METHODS

Cell culture, cell line generation and reagent

HEK293T, TCC-SUP, HT1376, 5637, HT1197, T24, UMUC3, SW780 and RT4 cell lines were purchased from ATCC. HEK293T cells were cultured in DMEM (41966052, Thermo Fisher Scientific). TSS-SUP, HT1376, HT1197 and UMUC3 cells were cultured in EMEM (30-2003, ATCC). 5637 cells were cultured in RPMI-1640 (30-2001, ATCC). SW780 cells were cultured in Leibovitz's L-15 medium (30-2008, ATCC). RT4 and T24 cells were cultured in McCoy's 5a medium (30-2007, ATCC). All the forementioned media contain 10% fetal bovine serum (10500064, Life Technologies). And cells were cultures at 37°, 5% CO_2.

T24 and UMUC3 cell lines containing Tet Repressor and E2F3 were created using lentiviral transduction with the third-generation lentiviral packaging system as previously described (Moreno et al., 2020). Briefly, HEK293T cells in 100 cm dish were transfected with 9 µg lentiviral packaging plasmids and 9 µg constructs of interest using 90 µg PEI (Polyethylenimine, 23966). E2F3 overexpression was induced by adding 200 ng/ml doxycycline (D9891, Sigma Aldrich).

Gemcitabine (S1714), Cisplatin (S1166), Prexasertib (S7178), Ceralasertib (S7693), Adavosertib (S1525) and Palbociclib (S1116) were purchased from Selleck chemicals. Nocodazole (M1404) was from Sigma Aldrich. Nucleosides (adenosine (A4036), thymidine (T1895), cytidine (C4654) and guanosine (G6264)) and hydroxyurea (H8627) were all purchased from Sigma Aldrich.

Immunoblotting

Cells were washed twice with ice cold 1x PBS and collected by scraping and spinning. Cell pellet was lysed with RIPA buffer (50 mM Tris-HCl, 1 mM EDTA, 150 mM NaCl, 0.25% deoxycholic acid, 1% NP-40, 1mM NaF, 1mM Na_3VO_4 and protease inhibitor cocktail (11873580001, Sigma Aldrich)) for 30 minutes on ice. Then supernatant was collected for a standard SDS-PAGE or immunoprecipitation. Antibodies used in this study are listed in Table 1.

Immunofluorescence

Cells were plated over cover slips (5 mm) and treated under desired conditions as indicated. By collecting, cells were washed once with 1x PBS and then fixed with 4% PFA at room temperature for 20 minutes. The PFA was discarded and cells were washed with 1x PBS twice. PBS containing 0.1% Triton X-100 was added and incubated for 20 minutes to permeabilize the cells. The coverslips were washed with 1x PBS twice and blocked with 5% BSA for 30 minutes. Next, cells were stained with primary and secondary antibodies respectively, 2 hours at room temperature. Lastly, cover slips were dried and mounted on glass slides using Fluoroshield mounting medium containing DAPI (Sigma, F6057).

DNA fiber analysis

Cells were pulse-labeled with 25 µM CldU and followed by 250 µM for 20 minitues respectively. DNA fibers were prepared as previously described (Benedict B, et al., 2018). Pictures were taken with a Olympus BX51 fluorescence microscope under the 40x objective. The length and quantification of number of different types of DNA tracks were manually analyzed with ImageJ software. The track length was calculated using the conversion factor 1 µm = 2.59 kb.

Quantitative PCR

RNA isolation, cDNA synthesis and quantitative PCR were performed as previously described (Westendorp B, et al., 2012). Gene mRNA levels were determined using $\Delta\Delta C_t$ method for multiple-reference gene correction (GAPDH, ACTIN, RPS18 were used). Primer sequences are provided in Table 1.

EU incorporation assay

Cells were plated over cover slips and pulsed with 1 mM EU for 1 hour prior to collection. The rest assay was performed according to the manufacturer's instructions in the Click-iT RNA Alexa Fluor 594 Imaging Kit (C10330, Invitrogen). Pictures were taken with a Olympus BX51 fluorescence microscope under the 40x objective. ImageJ was used to measure the mean Alexa Fluor 594 fluorescence intensities.

Flow cytometry

For cell cycle analysis, cells were trypsinized and fixed with 1x PBS containing 70% Ethanol in 4° overnight. Cells were washed twice with ice cold 1x TBS and resuspend with propidium iodide (PI, P4170, Sigma Aldrich) staining buffer (20 µg/ml PI, 250 µg/ml RNase A and 0.1% BSA). Samples were run on a BD LSRFORTESSA X-20 cell analyzer. For Annexin-V staining, cells were trypsinized and stained according to the manufacturer's instructions (A35110, Thermo Fisher). For EdU incorporation assay, cells were pulse-labeled with 10 µM EdU for 1 hour prior to collection. EdU staining was carried out according to the manufacturer's instructions in the Click-iT Plus EdU Alexa Fluor 647 assay kit(C10634, Thermo Fisher).

MTT assay

Cells were plated in 96-well plate and treated as desired. Cells were washed with 1x PBS once and treated with full medium containing 5 mg/ml MTT (3-(4,5-Dimethylthiazol-2-yl, M6494, Invitrogen) for 4 hours at 37°, 5% CO_2. Medium containing MTT was discarded and 150 µl DMSO was added. Samples were measured at the wavelength of 490 µm with a Clariostar Plus Microplate Reader. MTT conversion was plotted relative to the untreated cells in each condition. Per experiment, five replicates per condition were included. Averages and stan-

dard deviation of the five replicates were plotted.

Mass spectrometry

Cell pellets were extracted in 100 µL lysis buffer containing methanol/acetonitrile/dH2O (2:2:1). Samples were centrifuged at 16000g for 15 minutes at 4 °C to remove cell debris and proteins and supernatants were collected for LC-MS analysis.

LC-MS analysis was performed on a Q-Exactive HF mass spectrometer (Thermo Scientific) coupled to a Vanquish autosampler and pump (Thermo Scientific). The MS operated in polarity-switching mode with spray voltages of 4.5 kV and -3.5 kV. Metabolites were separated using a Sequant ZIC-pHILIC column (2.1 x 150 mm, 5 µm, guard column 2.1 x 20 mm, 5 µm; Merck) with elution buffers acetonitrile (A) and eluent B (20 mM $(NH4)2CO3$, 0.1% NH4OH in ULC/MS grade water (Biosolve)). Gradient ran from 20% eluent B to 60% eluent B in 20 minutes, followed by a wash step at 80% and equilibration at 20%. Flow rate was set at 100 µl/min. Analysis was performed using LCquan software (Thermo Scientific). Metabolites were identified and quantified on the basis of exact mass within 5 ppm and further validated by concordance with retention times of standards. Peak intensities were normalized based on total ion count.

Statistical analysis

Immunoblots, immunofluorescence, MTT assay, DNA fiber assay, flow cytometry and qPCR were repeated three times unless otherwise stated in the figure legends.

Statistical analyses were done by Pearson's Chi-squared tests for Fig 2G and S1A. * P < 0.05, ** P < 0.01, *** P < 0.001. Sample sizes and other experiment-specific statistical details are described in the figure legends.

ACKNOWLEDGEMENTS

AUTHOR CONTRIBUTIONS

QL performed experiments, EA and JC performed mass spectrometry analysis, BW analyzed the data from TCGA. QL, BW and AdB conceived the study design and experimental approaches, analyzed data, and wrote the manuscript.

COMPETING INTERESTS

The authors declare no competing interests.

SUPPLEMENTARY MATERIAL

Table 1: Antibodies used for immunoblotting

Name	Company	Catalog	Dilution
GFP	Abcam	AB6673	1:3000
p-CHK1 (S345)	Cell signaling	2348	1:1000
CHK1	Cell signaling	2360	1:1000
γH2AX	Cell signaling	9718	1:1000
GAPDH	Cell signaling	2118	1:1000
BrdU	Abcam	Ab6326	1:100
BrdU	BD Biosciences	347580	1:300
E2F3	Santa Cruz	sc-56665	1:1000

Table 2: qPCR primers

Gene	Forward primer (5'-3')	Reverse primer (5'-3')
CDC6	AAACCCGATCCCAGGCACAG	AGGCAGGGCTTTTACACGAGGAG
CDC45	CTTGAAGTTCCCGCCTATGAAG	GCATGGTTTGCTCCACTATCTC
CDT1	CGTCCAGGACATGATGCGTAGG	TTGAAGGTGGGGACACTGCG
DBF4	GGGCAAAAGAGTTGGTAGTGG	ACTTATCGCCATCTGTTTGGATT
MCM5	ACACGGATGTAGGAGCTTCG	ACACGGATGTAGGAGCTTCG
CCNE2	TTGGCTATGCGTGAGGAAGT	TGCTCTTCGGTGGTGTCATA
C8ORF33	CAGAAGAAGTTCCCCTAAGCG	TGCTCCAATAGCCTGCTCTTT
DDX27	AGGAGGCTGCGAAAAGTTAAG	GGTTCCGATTAAGCCGAGGT
MOCS3	TGCCCGGATCAAACACCAG	GGGACCGAGGAATCTTTGGG
MPP6	AGACTGGGACAATTCAGGACC	GCATTTTGGCTACCTCCTCAT
NAT10	GCCTCTTGTAAGAAGTGTCTCG	TCTTTTCAGAGATGCCCTCGAT
ZNF48	GATTGGACAAGAGGCCGACT	TCACTCCCTAGACCTGTGCG
GAPDH	CTCTGCTCCTCCTGTTCG	GCCCAATACGACCAAATCC
ACTIN	GATCGGCGGCTCCATCCTG	GACTCGTCATACTCCTGCTTGC
RPS18	AGTTCCAGCATATTTTGCGAG	CTCTTGGTGAGGTCAATGTC
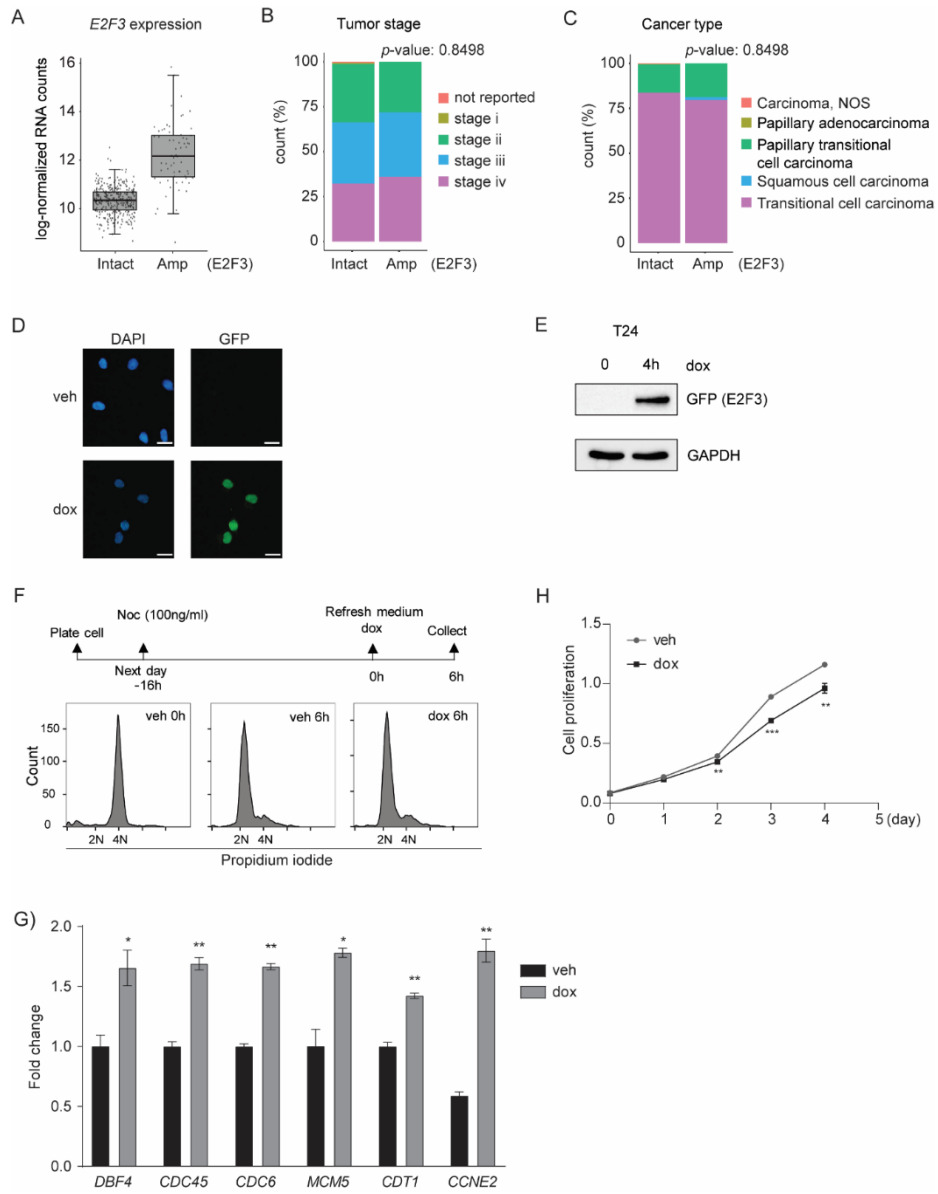
Figure S1. *E2F3* amplification increases E2F3 protein levels and E2F-dependent transcription in G1 phase.

Figure S1. *E2F3* **amplification increases E2F3 protein levels and E2F-dependent transcription in G1 phase. A.** Graph showing the *E2F3* gene expression in bladder cancer patients with intact or amplified *E2F3* loci. **B.** Graph showing the distribution of tumor stages in bladder cancer patients. **C.** Graph showing the distribution of cancer types in bladder cancer patients. **D.** Nuclear and GFP staining in UMUC3 cells after 24 h E2F3 induction. Scale bar, 20 μm. **E.** Blotting showing the induction of E2F3-EGFP after 4 h doxycycline treatment in T24 cells. **F.** Experimental work scheme and cell cycle profile at 0 and 6 h after nocodazole (100 ng/ml) release in T24 cells with or without E2F3 induction. **G.** The transcriptional expression of E2F targets in T24 cells treated as D). *P<0.05, **P<0.01 (unpaired two-tailed t-test). **H.** Plot showing the proliferation of T24 cells overtime with E2F3 induction. MTT assay was performed to measure the viable cells. Doxycycline (200 ng/ml) was refreshed daily. **P<0.01, ***P<0.001 (unpaired two-tailed t-test).

4
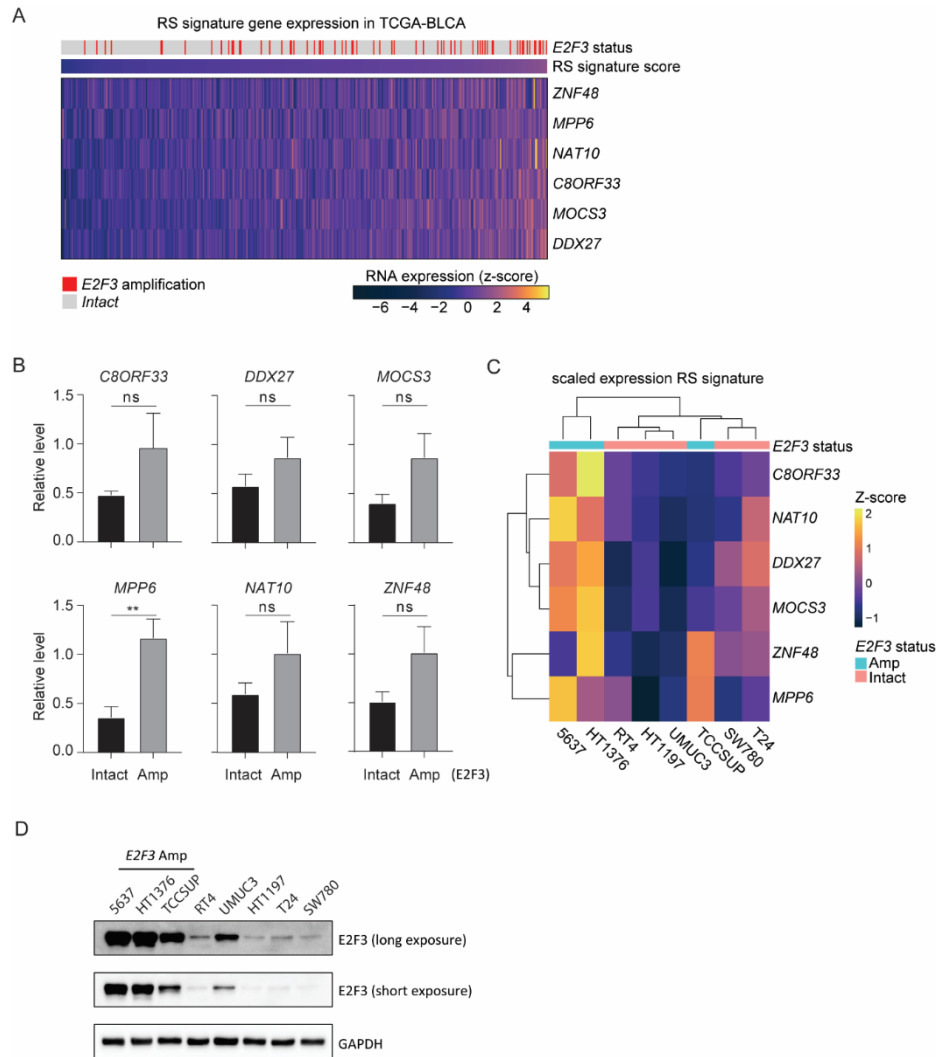
Figure S2. E2F3 amplification correlates with the expression of replication stress signature genes positively.
A. Heatmap showing the expression of individual RS signature genes in bladder cancer patients with intact or amplified *E2F3* loci. **B.** Heatmap showing the transcriptional expression of six RS signature genes in eight bladder cancer cell lines. **C.** Dot plots showing the transcriptional expression of six RS signature genes in eight bladder cancer cell lines. ns: no significance, **$P<0.01$ (unpaired two-tailed t-test). **D.** Blotting showing the protein expression of E2F3 in eight bladder cancer cell lines. Cells were treated with Hydroxyurea (2 mM) for 16 h prior to collection.
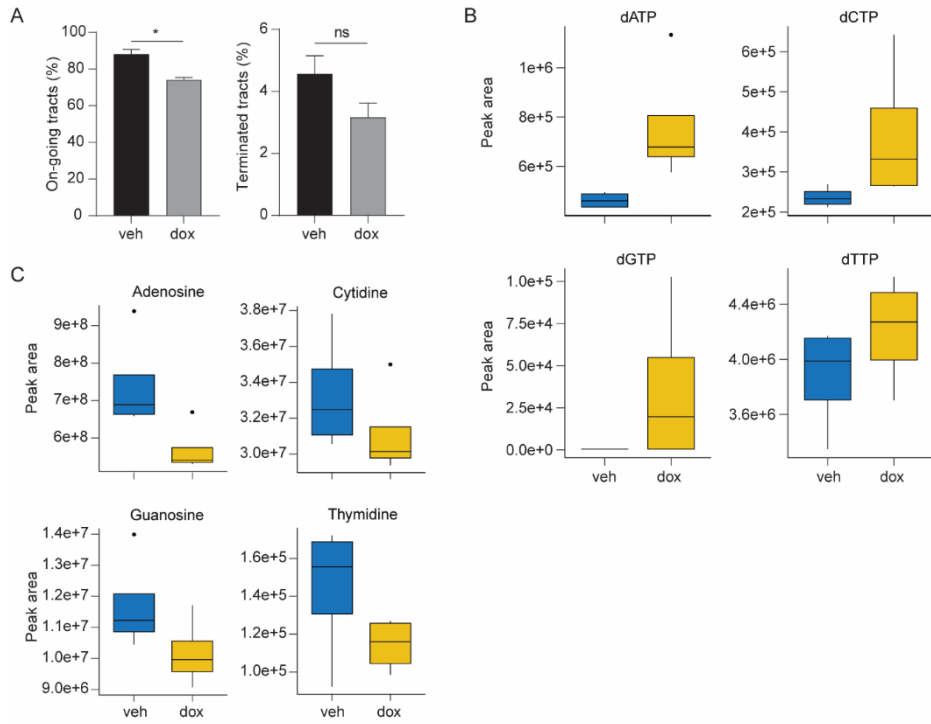
Figure S3. E2F3 overexpression increases the levels of nucleotides. A. Quantification of on-going and terminated fiber tracts in T24 cells with 2 days of E2F3 induction. Data from two separated experiments are pooled. *P<0.05 (Mann-Whitney Rank Sum test). **B.** Plots showing the levels of individual nucleotides in T24 cells with 2 days of E2F3 induction. 4 replicates were included. **C.** Plots showing the levels of individual nucleosides in T24 cells with 2 days of E2F3 induction. 4 replicates were included.
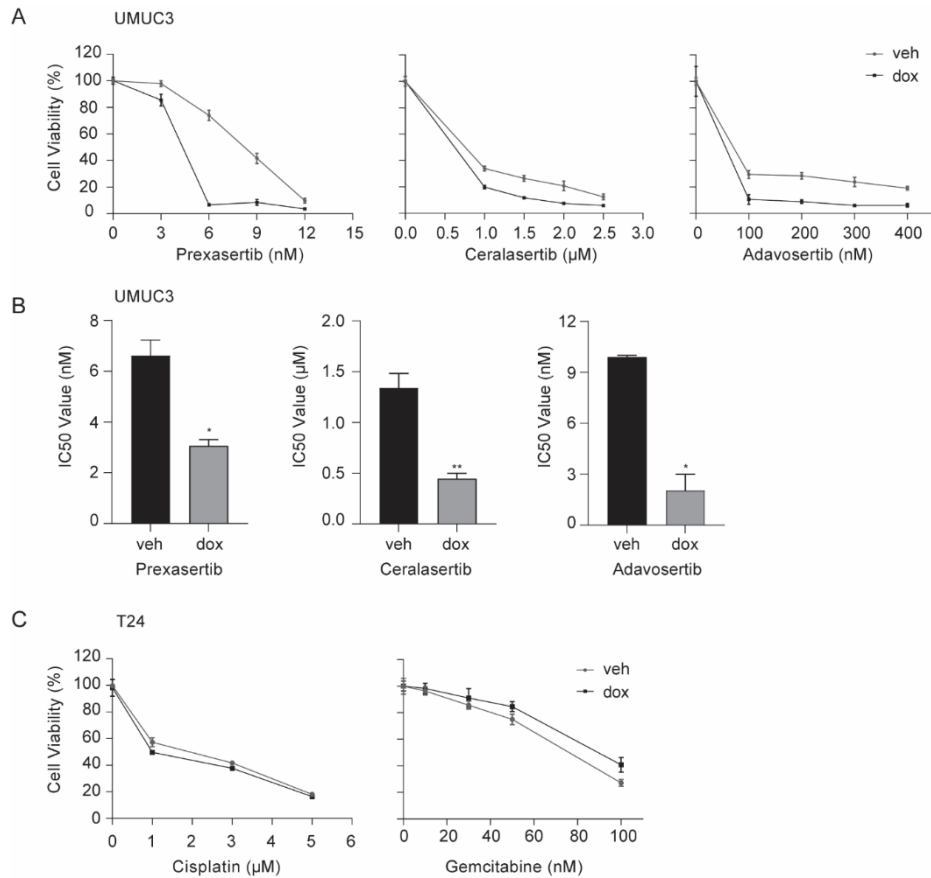
Figure S4. E2F3 overexpression sensitizes UMUC3 cells to checkpoint inhibitors. A. Plots showing the viability of UMUC3 cells after 48 h checkpoint inhibitors treatment with or without E2F3 induction. MTT assay was performed to measure cell viability. **B.** IC50 detection for Prexasertib, Ceralasertib and Adavosertib in UMUC3 cells. Cells were treated with indicated drug for 48 h and simultaneously doxycycline was added. MTT assay was performed to measure cell viability. *$P<0.05$, **$P<0.01$ (unpaired two-tailed t-test). **C.** Plots showing the viability of T24 cells after 48 h chemo drugs treatment with or without E2F3 induction. MTT assay was performed to measure cell viability.

REFERENCES

1. Bertoli C, Skotheim JM, de Bruin RA. Control of cell cycle transcription during G1 and S phases. *Nat Rev Mol Cell Biol.* 2013;14(8):518-528.

2. Hwang HC, Clurman BE. Cyclin E in normal and neoplastic cell cycles. *Oncogene.* 2005;24(17):2776-2786.

3. Limas JC, Cook JG. Preparation for DNA replication: the key to a successful S phase. *FEBS Lett.* 2019;593(20):2853-2867.

4. Oeggerli M, Tomovska S, Schraml P, et al. E2F3 amplification and overexpression is associated with invasive tumor growth and rapid tumor cell proliferation in urinary bladder cancer. *Oncogene.* 2004;23(33):5616-5623.

5. Robertson AG, Kim J, Al-Ahmadie H, et al. Comprehensive Molecular Characterization of Muscle-Invasive Bladder Cancer. *Cell.* 2017;171(3):540-556.e25.

6. Feng Z, Peng C, Li D, et al. E2F3 promotes cancer growth and is overexpressed through copy number variation in human melanoma. *Onco Targets Ther.* 2018;11:5303-5313.

7. Cooper CS, Nicholson AG, Foster C, et al. Nuclear overexpression of the E2F3 transcription factor in human lung cancer. *Lung Cancer.* 2006;54(2):155-162.

8. Oeggerli M, Schraml P, Ruiz C, et al. E2F3 is the main target gene of the 6p22 amplicon with high specificity for human bladder cancer. *Oncogene.* 2006;25(49):6538-6543.

9. Humbert PO, Verona R, Trimarchi JM, Rogers C, Dandapani S, Lees JA. E2f3 is critical for normal cellular proliferation. *Genes Dev.* 2000;14(6):690-703.

10. Hurst CD, Tomlinson DC, Williams SV, Platt FM, Knowles MA. Inactivation of the Rb pathway and overexpression of both isoforms of E2F3 are obligate events in bladder tumours with 6p22 amplification. *Oncogene.* 2008;27(19):2716-2727.

11. Segeren HA, van Rijnberk LM, Moreno E, et al. Excessive E2F Transcription in Single Cancer Cells Precludes Transient Cell-Cycle Exit after DNA Damage. *Cell Rep.* 2020;33(9):108449.

12. Zeman MK, Cimprich KA. Causes and consequences of replication stress. *Nat Cell Biol.* 2014;16(1):2-9.

13. Macheret M, Halazonetis TD. DNA replication stress as a hallmark of cancer. *Annu Rev Pathol.* 2015;10:425-448.

14. Helmrich A, Ballarino M, Tora L. Collisions between replication and transcription complexes cause common fragile site instability at the longest human genes. *Mol Cell.* 2011;44(6):966-977.

15. Jones RM, Mortusewicz O, Afzal I, et al. Increased replication initiation and conflicts with transcription underlie Cyclin E-induced replication stress. *Oncogene.* 2013;32(32):3744-3753.

16. Bester AC, Roniger M, Oren YS, et al. Nucleotide deficiency promotes genomic instability in early stages of cancer development. *Cell.* 2011;145(3):435-446.

17. Zeman MK, Cimprich KA. Causes and consequences of replication stress. *Nat Cell Biol.* 2014;16(1):2-9.

18. Grallert B, Boye E. The multiple facets of the intra-S checkpoint. *Cell Cycle.* 2008;7(15):2315-2320.

19. Sarni D, Kerem B. Oncogene-Induced Replication Stress Drives Genome Instability and Tumorigenesis. *Int J Mol Sci.* 2017;18(7).

20. Zhang CZ, Spektor A, Cornils H, et al. Chromothripsis from DNA damage in micronuclei. *Nature.* 2015;522(7555):179-184.

21. Guerrero Llobet S, Bhattacharya A, Everts M, et al. An mRNA expression-based signature for oncogene-induced replication-stress. *Oncogene.* 2022.

22. Bartek J, Lukas C, Lukas J. Checking on DNA damage in S phase. *Nat Rev Mol Cell Biol.* 2004;5(10):792-804.

23. Grossman HB, Natale RB, Tangen CM, et al. Neoadjuvant chemotherapy plus cystectomy compared with cystectomy alone for locally advanced bladder cancer. *N Engl J Med.* 2003;349(9):859-866.

24. Shen H, Morrison CD, Zhang J, et al. 6p22.3 Amplification as a Biomarker and Potential Therapeutic Target of Advanced Stage Bladder Cancer. *Oncotarget.* 2013;4(11):2124-2134.

25. Clijsters L, Hoencamp C, Calis JJA, et al. Cyclin F Controls Cell-Cycle Transcriptional Outputs by Directing the Degradation of the Three Activator E2Fs. *Mol Cell.* 2019;74(6):1264-1277.e7.

26. Gorgoulis VG, Vassiliou LV, Karakaidos P, et al. Activation of the DNA damage checkpoint and genomic instability in human precancerous lesions. *Nature.* 2005;434(7035):907-913.

27. Mayhew CN, Carter SL, Fox SR, et al. RB loss abrogates cell cycle control and genome integrity to promote liver tumorigenesis. *Gastroenterology.* 2007;133(3):976-984.

28. Maiani E, Milletti G, Nazio F, et al. AMBRA1 regulates cyclin D to guard S-phase entry and genomic integrity. *Nature.* 2021;592(7856):799-803.

29. Akli S, Zheng P, Multani AS, et al. Tumor-specific low molecular weight forms of cyclin E induce genomic instability and resistance to p21, p27, and antiestrogens in breast cancer. *Cancer Res.* 2004;64(9):3198-3208.

30. Kent LN, Bae S, Tsai SY, et al. Dosage-dependent copy number gains in E2f1 and E2f3 drive hepatocellular carcinoma. *J Clin Invest.* 2017;127(3):830-842.

31. Pal SK, Frankel PH, Mortazavi A, et al. Effect of Cisplatin and Gemcitabine With or Without Berzosertib in Patients With Advanced Urothelial Carcinoma: A Phase 2 Randomized Clinical Trial. *JAMA Oncol.* 2021;7(10):1536-1543.

32. Kok YP, Guerrero Llobet S, Schoonen PM, et al. Overexpression of Cyclin E1 or Cdc25A leads to replication stress, mitotic aberrancies, and increased sensitivity to replication checkpoint inhibitors. *Oncogenesis.* 2020;9(10):88.

4

Chapter 5

General Discussion

In this thesis, we explored the significance of properly regulating E2F transcription factors in the normal cell cycle. We found that atypical E2Fs, E2F7 and E2F8, are important for DNA damage repair and chromosome segregation during G2-M phase in a transcription-dependent and -independent manner, respectively (**chapter 2 & 3**). Additionally, ectopic expression of E2F3 protein, originating from *E2F3* loci amplification, was found to be capable to cause DNA replication stress and subsequently challenge the integrity of the genome (**chapter 4**). Collectively, these three studies reveal the importance of proper controlling of E2F activity for maintaining stability of the genome. In this last chapter of my thesis, firstly I will discuss the importance of fine regulating the protein levels of E2F factors during cell cycle progression. Secondly, I will discuss functions of E2Fs beyond controlling gene transcription. Finally I will zoom into the interplay between atypical E2Fs and sister chromatid cohesion, and outline how cohesin preserves genome stability through the dynamic association with DNA.

Fine tuning the levels of E2F transcription factors is critical for proper cell cycle progression and tissue homeostasis.

A cell cycle could not proceed properly without the precise control of E2F transcription factors. The main reason is that a large set of genes regulated by E2Fs is involved in cell cycle phase transition, DNA replication and repair[1,2]. To manage the timely expression of E2F target genes, cells have evolved multiple ways to finely regulate the levels of E2F activators and repressors during different cell cycle phases.

In early G1-phase, E2F activators (E2F1-3) are lowly expressed and they are functionally repressed by RB1 in mammalian cells to avoid premature G1/S transition[1]. When RB1 is phosphorylated and E2F activators are released. Subsequently E2F activators transcriptionally upregulate their own mRNA levels and corresponding protein levels, which triggers the rapid increase of E2F target gene expression and promotes S phase entry and DNA replication[2]. Overriding the G1/S checkpoint is one key aspect of tumorigenesis and *RB1* is often lost or mutated in cancer patients. Importantly, abnormally high expression of activator E2Fs in *RB1*-proficient cells can also cause tumorigenesis. For example, copy number gains in *E2f1* or *E2f3* in mice are sufficient to cause spontaneous hepatocellular carcinomas[3]. In line with this, we showed in **chapter 4** that ectopic E2F3 expression was able to override the repression by RB1 and induced premature entry of S phase. This phenotype is consistent with that observed in cells with overexpressed cyclin E or RB1 depletion[4,5], indicating that transcriptional repression of activator E2Fs is important to prevent untimely S-phase initiation in cells with intact RB1. This G1/S checkpoint-overriding effect can thus explain why *E2F3* gene amplification is often seen in cancer patients. Nevertheless, early S phase entry comes with a cost. E2F3 overexpression led to slower DNA replication, intra-S checkpoint activation and DNA damage, which was followed by delayed S/G2/M progression (Figure 1). Given these drawbacks imposed by E2F3 overexpression, it is intriguing to investigate why a subset of bladder

cancer patients still harbor *E2F3* amplification. One possible explanation is that bladder cancer cells containing *E2F3* loci amplification have already developed tactics, like boosting the nucleotide pool and protecting stalled replication forks[6], to tolerate E2F3-induced replication stress. In support of this, we did observe less DNA damage by supplying bladder cancer cells with nucleosides. Additionally, Ribonucleotide reductase, RRM2 and RAD51 are both E2F targets[7], which are important for *de novo* nucleotide (dNTP) production and replication fork protection[8,9]. Thus, one can conceive that *E2F3* amplification, on one hand, accelerates S phase entry and causes replication stress. On the other hand, it favors cells to tolerate replication stress by upregulating genes such as *RRM2* and *RAD51*. Nevertheless, increasing the expression of those RS tolerance genes is not enough to mitigate all the replication stress induced by E2F3 overexpression (***chapter 4***). So could cancer cells in fact benefit from a limited amount of RS caused by *E2F3* amplification? There is mounting evidence that oncogene-induced replication stress impairs genome integrity, driving the development of early-stage cancer[10]. Indeed, using a transgenic mouse model, cyclin E overexpression was found able to induce mammary carcinoma and hepatocellular carcinoma[11,12]. Moreover, we found that bladder cancer patients with *E2F3* amplification had higher number of mutation counts and levels of aneuploidy (***Chapter 4***). Hence, *E2F3* amplification might contribute to tumor progression via increasing the tumor mutational burden. In any case, restricted gene expression of E2F transcription activators is of critical importance to preserve proper G1-S transition and genome stability.
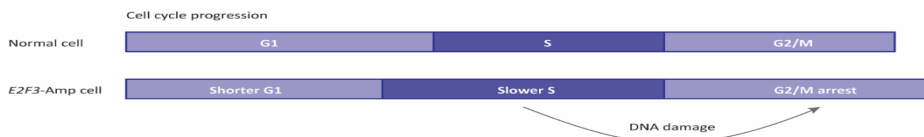
Figure 1. Effect of *E2F3* amplification on cell cycle progression. *E2F3* amplification leads to ectopic expression of E2F3 protein in G1 phase, which results in early S phase entry and DNA replication stress. DNA damage raising from impaired DNA replication delays G2/M phase progression.

As cells progress through S phase, phosphorylation by cyclin A-CDK2 complexes was reported to inhibit the DNA binding activity of E2F1[13]. Furthermore, the levels of the repressor proteins E2F7 and -8 peak by mid-S phase to mediate a downswing of E2F-dependent gene transcription[14]. Together, these oscillations and alterations of activating and repressing E2F factors bring down the levels of E2F targets towards the end of S-phase. To achieve the downswing of E2F activators, apart from the transcriptional suppression by E2F repressors, a recent study showed that SCF^cyclin F complex is responsible for the degradation of E2F1-3 in S and G2 phase[15]. Mutations in E2F1-3 that prevent cyclin F binding led to persistent expression

of these proteins and correspondingly higher levels of E2F targets in S-G2 phase, which was found to shorten the next G1 phase progression and induce DNA damage. On the other hand, the transcriptional downregulation of E2F-dependent transcription via repressor E2Fs is also important for appropriate S phase progression and genomic integrity. Sustained E2F-dependent transcription in S phase through E2F6 depletion was able to speed up S phase progression and cause cell cycle arrest over time[16]. Our previous studies showed that combined deletion of the E2F7 and -8 repressor proteins could override cell cycle exit after DNA damage and proceed to mitosis at the price of promoting genome instability[17]. Therefore, downregulation of E2F activators in both transcriptional and post-translational levels is required for proper DNA replication and genome stability in S phase.
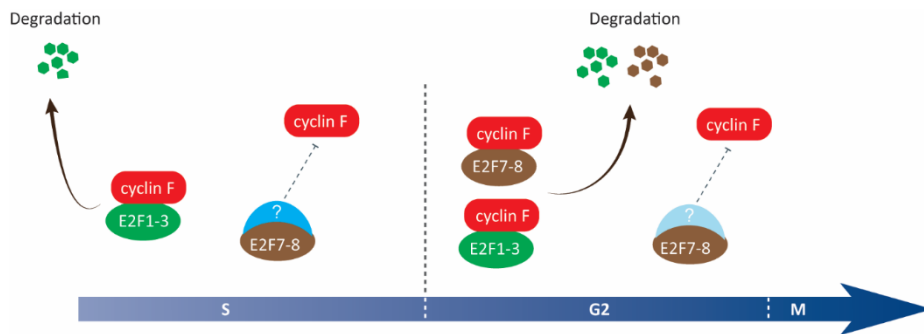
Figure 2. Fine regulation of E2F factors in cell cycle progression. E2F activators (E2F1-3) are targeted by cyclin F for degradation from the mid-S to G2 phase. Meanwhile, E2F7/8 might be protected by an unknown factor or post-translational modification (like phosphorylation) from cyclin F-mediated degradation until the onset of G2 phase, while a portion of E2F7/8 is still preserved and retained until anaphase (symbolized by the light-blue shading of the protective factor).

While it is important for cells to downregulate the expression of E2F target genes in S-G2 phase through E2F repressors, we observed that the protein levels of E2F7/8 already decreased in G2 phase when the first E2F7/8 degron we found previously, APC/C^{Cdh1}, is still inactive[14]. In **chapter 2**, we proved that the degradation of E2F7/8 was mediated by SCF$^{cyclin\ F}$ as well. This partial degradation of E2F7/8 in G2 phase allows for the expression of some key E2F targets, such as RAD51, BRCA1/2 and CHK1, enabling cells to dissolve the potential endogenous DNA lesions deriving from DNA replication. Additionally, downregulation of E2F7/8 allows retention of E2F targets involved in DNA replication. For example, the DNA licensing factors (CDC6 and CDT1) were shown to expressed in G2 and early mitosis in preparation for the later DNA origin assembly in next cell cycle[18]. However, it is counterintuitive that cyclin F targets both activator and repressor E2Fs. An explanation could be that there is a timely order, such that activators are targeted for degradation in S phase[15], while E2F7/8 are protected from degradation until G2 phase (Figure 2). E2F7/8 could for example be protected

from cyclin F via temporary binding to a protective factor or a post-translational modification.

Taken together, mammalian cells must maintain an exquisite balance of activator and repressor E2Fs by both transcriptional and post-translational control mechanisms to ensure proper transitions of cell cycle phases and maintain genome stability.

Non-canonical roles of E2F factors independent of their transcriptional activity.

As mentioned before, E2F proteins mostly function downstream of CDK-RB axis as transcription factors to either activate or inhibit expression of a largely overlapping set of target genes. This raises the question why mammals would need as many as 8 different family members. One plausible reason is that E2Fs are versatile proteins that can have functions beyond direct transcription control. Multiple studies have presented roles of E2F factors independent of their transcriptional activity in chromatin regulation, DNA damage repair and multiciliogenesis, adding the complexity to the functions of E2F family. The best studied example is E2F1. Both in mammals and plants, E2F1 was found to localize at DNA double strand breaks (DSBs) together with RB[19-21]. The localization of E2F1 to DSBs is associated with homologous recombination by promoting RAD51 binding[21]. Furthermore, RB-E2F1 complexes can also mediate the binding of chromatin modifying enzymes, which enhance access to the repair machinery and facilitate DNA end processing[20,22]. Apart from the role of E2F factors in DNA damage repair, E2F4 also functions to promote multiciliogenesis through an interaction with the centriole replication machinery in cytoplasm[23,24]. And recently another E2F3 isoform, E2F3d was reported to physically interact with microtubule-associated protein 1A/1B-light chain 3 (LC3) on outer mitochondrial membranes to induce mitophagy[25]. All these findings indicate that E2F factors can function beyond genes transcriptional regulation. So far, there is only a very limited number of studies on non-transcriptional functions of atypical E2Fs. Zalmas and coworkers reported that E2F7 may localize at DSBs to recruit different chromatin remodelers (HDAC1/2) to contribute to the DNA repair process[26]. We could not detect E2F7 recruitment to DSBs in our lab[27], but during the work leading to this thesis we discovered another transcription-independent role of atypical E2Fs. We observed that E2F7/8 interact with the cohesin subunit SMC1 to facilitate cohesin release during prophase of mitosis, most likely by interfering with the Rad21-SMC1 interface (Figure 3). For E2F7, we showed that this interaction did not rely on the presence of chromatin, but on a helix-rich segment of E2F7 spanning amino acids 263-553. Depletion of E2F7 and E2F8 impaired cohesin removal from the chromosome arms during mitosis, resulting in delayed mitosis.
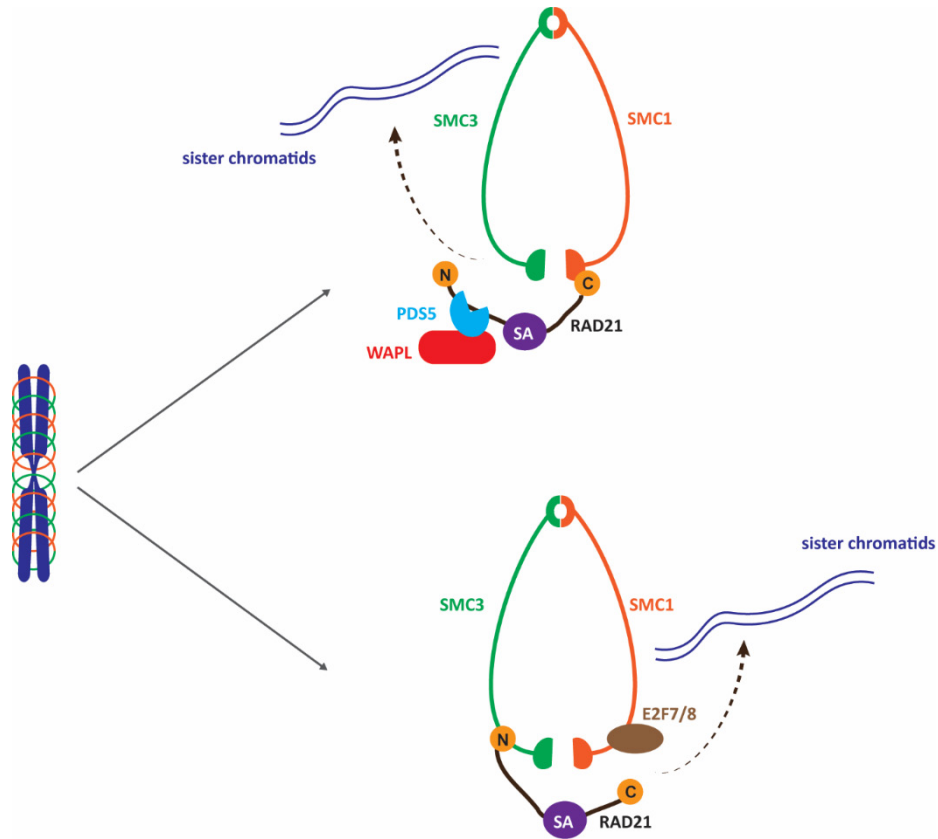
Figure 3. A speculative model of cohesin release during prophase. While WAPL removes cohesin on arms of sister chromatids by promoting the "DNA exit" formed by SMC3 and RAD21 N-terminus (upper model), E2F7/8 might be able to remove a portion of cohesin from chromosome by disengaging the interaction of SMC1 and RAD21 C-terminus (lower model).

Of note, although the protein levels of E2F7/8 peak in S/G2 phase, we observed that the effect of these two E2Fs on cohesin occurred only during M- and had no impact during S- or G2- phase. Possibly, DNA-binding cohesin complexes are stabilized and protected from E2F7/8-mediated release through post-translational modifications, similar to how cells prevent cohesin removal from WAPL during S-G2 phase. Specifically, cohesin loading on DNA is coupled with acetylation modification and subsequent Sororin binding, which can then compete with the binding between RAD21 and WAPL, thus promoting the formation of cohesion[28,29]. Since we found E2F7/8 particularly bound to SMC1, Sororin might not be able to resist E2F7/8 binding to cohesin. Thereby we speculate that E2F7/8 binding to SMC1 binding can be prevented by unknown factors and cannot dissociate cohesin from chromatin until the onset of mitosis.

Another intriguing question is how cells precisely control the protein levels of E2F7/8 in G2 phase. On one hand, E2F7/8 are targeted for degradation during G2 to prevent excessive repression of target genes that are critical for DNA repair and timely G2 phase progression (**chapter 2**). On the other hand, a certain portion of E2F7/8 should be preserved for cohesin release during prophase. Most likely a portion of E2F7/8 is protected against degradation via post-translational modifications. There are multiple putative CDK and PLK1 phosphorylation sites in E2F7/8 predicted by an online tool ELM (http://elm.eu.org/) (Table 1 and 2). Thereby, we speculate that these mitotic kinases might be able to phosphorylate a subset of E2F7/8 and stabilize them. Future studies using site-directed mutagenesis are required to test this hypothesis.

Position	Human E2F7	Description	Probability
S13	DLI S PR	Short version of the CDK phosphorylation sites	1.929E-03
S638	DLA S PK		
S861	VPV T PK		
T45	APK T PIK	Canonical version of the CDK phosphorylation sites	1.929E-03
T61	KKF T PER		
T68	NPI T PVK		
S430	EPS S PYR		
S95	SAA S PDIR	Longer version of the CDK phosphorylation sites	1.929E-03
S39	VDR S RMA	PLK1 phosphorylation sites	7.674E-03
S525	VDV S LAS		
S784	VNF S LPG		

Table 1. Putative phosphorylation on human E2F7 protein by CDKs and PLK1. (Adopted from http://elm. eu.org/searchdb.html)

Complex networks regulate dynamic association of cohesin and DNA to preserve genome stability.

Cohesin is involved in coordination of many processes that affect genome integrity, such as gene transcription, DNA replication and repair, and mitotic chromosome segregation[30]. To coordinate these processes, cohesin associates with DNA during the cell cycle in a dynamic manner which is achieved through post-translational modifications of cohesin subunits and cohesin-binding factors. Below I will discuss the current state of knowledge and formulate outstanding research questions about dynamic regulation of cohesin during DNA replication,

5

repair and chromosome segregation.

Position	Human E2F8	Description	Probability
S762	VPV S PR	Short version of the CDK phosphoryla-tion sites	1.929E-03
T812	VPV T PK		
T20	LMK T PLK	Canonical version of the CDK phosphor-ylation sites	1.929E-03
T44	PLT T PTK		
S417	APS S PIK		
T696	FHV T PLK		
S71	SAV S PEIR	Longer version of the CDK phosphoryla-tion sites	1.929E-03
S664	SAL S PNHR		
T189	LNK T LGT	PLK1 phosphorylation sites	7.674E-03
S661	ENS S ALS		
T686	SEL T AVN		
T737	VNF T LQH		
T847	ANK T SLG		

Table 2. Putative phosphorylation on human E2F8 protein by CDKs and PLK1. (Adopted from http://elm.eu.org/searchdb.html)

Both in the Xenopus egg extract system and human cells, cohesin is recruited to the pre-replication complex (pre-RC) via the interaction between cohesin loaders NIPBL/MAU2 (SCC2/SCC4 in Xenopus) and DBF4-dependent kinase (DDK)[31-33] in human. DDK-mediated phosphorylation of MCM2-7, key components of pre-RC, triggers the binding of GINS and CDC45 to form the CDC45/MCM2-7/GINS (CMG) complex and initiates replication. Thus, it was proposed that the binding of NIPBL/MAU2 to pre-RC at the G1/S transition mediated the subsequent loading of cohesin during S phase, essential for the formation of sister chromatid cohesion (SCC)[31]. How this pool of pre-RC anchored cohesin is protected from WAPL-mediated removal is not known yet. However, it is clear that DNA replication is accompanied by SCC establishment and that a subset of replisome components, like Ctf4, Tof1, Csm3, and Chl1 in yeast and their corresponding orthologs WDHD1, TIMELESS, TIPIN, and DDX11 in metazoans, are required for SCC formation[34,35]. To date it is still elusive how the ring-shaped cohesin complexes entrap the duplicated DNA molecules. Due to size constraints, it is unlikely that the entire replisome can pass through the cohesin ring[36]. Therefore, it was proposed that as DNA replication initiates, replisome-binding cohesin rings might dissociate transiently from single strand DNA but still interact with some replisome components. After DNA replication is finished, replisome-binding cohesin rings deposit behind the replication fork to establish SCC[31]. This hypothesis is supported by the finding that in WAPL-deficient human cells, co-hesin loaded in G1 remains associated with chromatin through S phase[37]. And replication

fork progression is hampered by artificially tethering the SMC head domains, precluding ring opening. Although the cohesin pre-bound to pre-RC in G1 phase is used to establish cohesion, de novo cohesin loading in S phase may be still needed. Recent studies in yeast showed that SCC2/SCC4 was required in replicating cells for cohesion establishment[38,39]. It remains to be seen if this is also the case in human cells.

There is accumulating evidence that cohesion dynamics play an important role in the response to replication stress. Firstly, cohesin was found to accumulate at sites of stalled forks, depending on RPA-coated ssDNA and chromatin remodeling[40,41]. The loading of cohesin can recruit BRCA2 and RAD51 to protect stalled forks and repair DNA lesions via homologous recombination[42-44]. On the other hand, a portion of cohesin needs to dissociate from DNA by WAPL instead, because the inhibition of cohesin mobility by knocking down WAPL clearly impaired cell viability under replication stress conditions[45]. Thus, WAPL-mediated removal of cohesin may facilitate its accumulation at stalled forks to aid repair and restart. How cells control these complex cohesion dynamics in conditions of replication stress remains to be defined.

Figure 4. Chromosome spreads. The left picture shows representative chromosome spreads from normal cells (X-shaped sister chromatids), the right from *E2F7/8* or *WAPL* deficient cells (paralleled sister chromatid arms).

The dissociation of SCC starts when a cell enters mitosis. To date, WAPL is the only well-established factor responsible for the removal of cohesin from chromosome arms during prophase[46]. Hence, WAPL deficiency results in closed sister chromatids instead of normal X-shaped ones in prometaphase (Figure 4). In **chapter 3**, we provide evidence that E2F7/8 also participate in cohesin release in a WAPL-independent manner. Indeed, we found that E2F7 overexpression was able to reduce the percentage of cells with closed sister chromatids after *WAPL* knockdown. Our findings raise the question why mammalian cells need two different types of proteins, i.e. atypical E2Fs and WAPL, to release cohesin in prophase. To answer this question, it is important to first discuss the biological function of cohesin removal along the chromosome arms during prophase. Separase, which becomes active at the onset

of anaphase, removes centromeric cohesin. However, this protein can also remove cohesin along the chromosome arms, thus allowing for mitosis progression in WAPL-depleted cells. However, WAPL-deficient RPE (retinal pigment epithelium) cells show severe chromosome segregation errors and eventually undergo a P53-dependent cell cycle arrest[47]. Mechanistically, it was shown that timely cohesin removal during prophase is important to focus aurora kinase B to centrometric regions to ensure efficient correction of erroneous microtubule-kinetochore attachments. Aurora B is crucial to correct the erroneous kinetochore-microtubule attachment[48]. Given this importance of rapid removal of cohesin from chromosome arms, it seems logical that not only WAPL, but also other proteins such as atypical E2Fs, can mediate cohesin release during prophase. However it is important to note that E2F7/8 cannot fully compensate for the loss of WAPL (***Chapter 3***). Additionally, one recent study reported a new protein, called WIZ (Widely Interspaced Zinc fingers protein), which can interact with cohesin complex and change the levels and distribution of cohesin occupancy across the genome independently of WAPL[49,50]. The purpose of having the WIZ-mediated cohesin localization on chromatin was believed to properly control the dynamic of cohesin during DNA loops formation, hence regulating gene expression. Next, how WIZ and WAPL distinguish which portion of cohesin they should target would be interesting to explore. Likewise, it would be relevant to investigate if E2F7/8 can only target a specific portion of cohesin . However, it is important to note that overexpression of E2F7 increased the separation of sister chromatids during prophase (*Chapter 3*). This indicates that the cohesin-releasing activity of E2F7/8 is limited by the protein levels of E2F7/8 which are downregulated by cyclin F-mediated degradation. All in all, it is becoming increasingly clear that timely removal from chromosomes involves multiple different proteins to ensure timely and error-free mitosis progression in mammalian cells. Malfunctions in these proteins can be tolerated by cells to some extent, but may eventually lead to aneuploidy and even contribute to development of cancer.

Conclusion

In this thesis, we show that multiple E2F factors, namely E2F3, E2F7 and E2F8, play versatile and crucial roles in maintaining genome integrity throughout the mammalian cell cycle. We found out that fine regulation of E2F-dependent transcription by timely coordinating the levels of E2F factors is essential for proper cell cycle progression and maintenance of genomic stability. On top of this, one novel and noncanonical function of atypical E2Fs was discovered that they physically bind and release cohesin during prophase, promoting mitosis progression. Together, our findings contribute to an improved understanding of the highly complex cell cycle coordination by the E2F transcription factor family.

5

REFERENCES

1. Chen HZ, Tsai SY, Leone G. Emerging roles of E2Fs in cancer: an exit from cell cycle control. *Nat Rev Cancer.* 2009;9(11):785-797.

2. Ren B, Cam H, Takahashi Y, et al. E2F integrates cell cycle progression with DNA repair, replication, and G(2)/M checkpoints. *Genes Dev.* 2002;16(2):245-256.

3. Kent LN, Bae S, Tsai SY, et al. Dosage-dependent copy number gains in E2f1 and E2f3 drive hepatocellular carcinoma. *J Clin Invest.* 2017;127(3):830-842.

4. Macheret M, Halazonetis TD. Intragenic origins due to short G1 phases underlie onco-gene-induced DNA replication stress. *Nature.* 2018;555(7694):112-116.

5. Almasan A, Yin Y, Kelly RE, et al. Deficiency of retinoblastoma protein leads to inappropri-ate S-phase entry, activation of E2F-responsive genes, and apoptosis. *Proc Natl Acad Sci U S A.* 1995;92(12):5436-5440.

6. Dobbelstein M, Sørensen CS. Exploiting replicative stress to treat cancer. *Nat Rev Drug Discov.* 2015;14(6):405-423.

7. Westendorp B, Mokry M, Groot Koerkamp, Marian J. A., Holstege FCP, Cuppen E, de Bruin A. E2F7 represses a network of oscillating cell cycle genes to control S-phase progression. *Nucleic Acids Res.* 2012;40(8):3511-3523.

8. Rasmussen RD, Gajjar MK, Tuckova L, et al. BRCA1-regulated RRM2 expression protects glioblastoma cells from endogenous replication stress and promotes tumorigenicity. *Nat Commun.* 2016;7:13398.

9. Jensen RB, Carreira A, Kowalczykowski SC. Purified human BRCA2 stimulates RAD51-me-diated recombination. *Nature.* 2010;467(7316):678-683.

10. Donley N, Thayer MJ. DNA replication timing, genome stability and cancer: late and/or delayed DNA replication timing is associated with increased genomic instability. *Semin Can-cer Biol.* 2013;23(2):80-89.

11. Montazeri H, Bouzari S, Azadmanesh K, Ostad SN, Ghahremani MH. Overexpres-sion of Cyclin E and its Low Molecular Weight Isoforms Cooperate with Loss of p53 in Promoting Oncogenic Properties of MCF-7 Breast Cancer Cells. *Asian Pac J Cancer Prev.* 2015;16(17):7575-7582.

12. Aziz K, Limzerwala JF, Sturmlechner I, et al. Ccne1 Overexpression Causes Chromo-some Instability in Liver Cells and Liver Tumor Development in Mice. *Gastroenterology.*

2019;157(1):210-226.e12.

13. Xu M, Sheppard KA, Peng CY, Yee AS, Piwnica-Worms H. Cyclin A/CDK2 binds directly to E2F-1 and inhibits the DNA-binding activity of E2F-1/DP-1 by phosphorylation. *Mol Cell Biol.* 1994;14(12):8420-8431.

14. Boekhout M, Yuan R, Wondergem AP, et al. Feedback regulation between atypical E2Fs and APC/CCdh1 coordinates cell cycle progression. *EMBO Rep.* 2016;17(3):414-427.

15. Clijsters L, Hoencamp C, Calis JJA, et al. Cyclin F Controls Cell-Cycle Transcriptional Outputs by Directing the Degradation of the Three Activator E2Fs. *Mol Cell.* 2019;74(6):1264-1277.e7.

16. Pennycook BR, Vesela E, Peripolli S, et al. E2F-dependent transcription determines replication capacity and S phase length. *Nat Commun.* 2020;11(1):3503-z.

17. Segeren HA, van Rijnberk LM, Moreno E, et al. Excessive E2F Transcription in Single Cancer Cells Precludes Transient Cell-Cycle Exit after DNA Damage. *Cell Rep.* 2020;33(9):108449.

18. Clijsters L, Ogink J, Wolthuis R. The spindle checkpoint, APC/C(Cdc20), and APC/C(Cdh1) play distinct roles in connecting mitosis to S phase. *J Cell Biol.* 2013;201(7):1013-1026.

19. Chen J, Zhu F, Weaks RL, et al. E2F1 promotes the recruitment of DNA repair factors to sites of DNA double-strand breaks. *Cell Cycle.* 2011;10(8):1287-1294.

20. Velez-Cruz R, Manickavinayaham S, Biswas AK, et al. RB localizes to DNA double-strand breaks and promotes DNA end resection and homologous recombination through the recruitment of BRG1. *Genes Dev.* 2016;30(22):2500-2512.

21. Biedermann S, Harashima H, Chen P, et al. The retinoblastoma homolog RBR1 mediates localization of the repair protein RAD51 to DNA lesions in Arabidopsis. *EMBO J.* 2017;36(9):1279-1297.

22. Manickavinayaham S, Vélez-Cruz R, Biswas AK, et al. E2F1 acetylation directs p300/CBP-mediated histone acetylation at DNA double-strand breaks to facilitate repair. *Nat Commun.* 2019;10(1):4951.

23. Mori M, Hazan R, Danielian PS, et al. Cytoplasmic E2f4 forms organizing centres for initiation of centriole amplification during multiciliogenesis. *Nat Commun.* 2017;8:15857.

24. Hazan R, Mori M, Danielian PS, et al. E2F4's cytoplasmic role in multiciliogenesis is mediated via an N-terminal domain that binds two components of the centriole replication

5

machinery, Deup1 and SAS6. *Mol Biol Cell.* 2021;32(20):ar1.

25. Araki K, Kawauchi K, Sugimoto W, et al. Mitochondrial protein E2F3d, a distinctive E2F3 product, mediates hypoxia-induced mitophagy in cancer cells. *Commun Biol.* 2019;2:3.

26. Zalmas LP, Coutts AS, Helleday T, La Thangue NB. E2F-7 couples DNA damage-dependent transcription with the DNA repair process. *Cell Cycle.* 2013;12(18):3037-3051.

27. Yuan R, Vos HR, van Es RM, et al. Chk1 and 14-3-3 proteins inhibit atypical E2Fs to prevent a permanent cell cycle arrest. *EMBO J.* 2018;37(5):10.15252/embj.201797877. Epub 2018 Jan 23.

28. Nishiyama T, Ladurner R, Schmitz J, et al. Sororin mediates sister chromatid cohesion by antagonizing Wapl. *Cell.* 2010;143(5):737-749.

29. Rolef Ben-Shahar T, Heeger S, Lehane C, et al. Eco1-dependent cohesin acetylation during establishment of sister chromatid cohesion. *Science.* 2008;321(5888):563-566.

30. Mehta GD, Rizvi SMA, Ghosh SK. Cohesin: a guardian of genome integrity. *Biochim Biophys Acta.* 2012;1823(8):1324-1342.

31. Zheng G, Kanchwala M, Xing C, Yu H. MCM2-7-dependent cohesin loading during S phase promotes sister-chromatid cohesion. *Elife.* 2018;7:10.7554/eLife.33920.

32. Takahashi TS, Yiu P, Chou MF, Gygi S, Walter JC. Recruitment of Xenopus Scc2 and cohesin to chromatin requires the pre-replication complex. *Nat Cell Biol.* 2004;6(10):991-996.

33. Gillespie PJ, Hirano T. Scc2 couples replication licensing to sister chromatid cohesion in Xenopus egg extracts. *Curr Biol.* 2004;14(17):1598-1603.

34. Leman AR, Noguchi C, Lee CY, Noguchi E. Human Timeless and Tipin stabilize replication forks and facilitate sister-chromatid cohesion. *J Cell Sci.* 2010;123(Pt 5):660-670.

35. Chan RC, Chan A, Jeon M, et al. Chromosome cohesion is regulated by a clock gene paralogue TIM-1. *Nature.* 2003;423(6943):1002-1009.

36. Stigler J, Çamdere GÖ, Koshland DE, Greene EC. Single-Molecule Imaging Reveals a Collapsed Conformational State for DNA-Bound Cohesin. *Cell Rep.* 2016;15(5):988-998.

37. Rhodes JDP, Haarhuis JHI, Grimm JB, Rowland BD, Lavis LD, Nasmyth KA. Cohesin Can Remain Associated with Chromosomes during DNA Replication. *Cell Rep.* 2017;20(12):2749-2755.

38. Murayama Y, Samora CP, Kurokawa Y, Iwasaki H, Uhlmann F. Establishment of DNA-DNA Interactions by the Cohesin Ring. *Cell.* 2018;172(3):465-477.e15.

39. Srinivasan M, Petela NJ, Scheinost JC, et al. Scc2 counteracts a Wapl-independent mechanism that releases cohesin from chromosomes during G1. *Elife.* 2019;8.

40. Tittel-Elmer M, Lengronne A, Davidson MB, et al. Cohesin association to replication sites depends on rad50 and promotes fork restart. *Mol Cell.* 2012;48(1):98-108.

41. Delamarre A, Barthe A, de la Roche Saint-André, Christophe, et al. MRX Increases Chromatin Accessibility at Stalled Replication Forks to Promote Nascent DNA Resection and Cohesin Loading. *Mol Cell.* 2020;77(2):395-410.e3.

42. Morales C, Ruiz-Torres M, Rodríguez-Acebes S, et al. PDS5 proteins are required for proper cohesin dynamics and participate in replication fork protection. *J Biol Chem.* 2020;295(1):146-157.

43. Brough R, Bajrami I, Vatcheva R, et al. APRIN is a cell cycle specific BRCA2-interacting protein required for genome integrity and a predictor of outcome after chemotherapy in breast cancer. *EMBO J.* 2012;31(5):1160-1176.

44. Couturier AM, Fleury H, Patenaude A, et al. Roles for APRIN (PDS5B) in homologous recombination and in ovarian cancer prediction. *Nucleic Acids Res.* 2016;44(22):10879-10897.

45. Benedict B, van Schie, Janne J. M., Oostra AB, et al. WAPL-Dependent Repair of Damaged DNA Replication Forks Underlies Oncogene-Induced Loss of Sister Chromatid Cohesion. *Dev Cell.* 2020;52(6):683-698.e7.

46. Kueng S, Hegemann B, Peters BH, et al. Wapl Controls the Dynamic Association of Cohesin with Chromatin. *Cell.* 2006;127(5):955-967.

47. Haarhuis JHI, Elbatsh AMO, van den Broek B, et al. WAPL-mediated removal of cohesin protects against segregation errors and aneuploidy. *Curr Biol.* 2013;23(20):2071-2077.

48. Gregan J, Polakova S, Zhang L, Tolić-Nørrelykke IM, Cimini D. Merotelic kinetochore attachment: causes and effects. *Trends Cell Biol.* 2011;21(6):374-381.

49. Justice M, Carico ZM, Stefan HC, Dowen JM. A WIZ/Cohesin/CTCF Complex Anchors DNA Loops to Define Gene Expression and Cell Identity. *Cell Rep.* 2020;31(2):107503.

50. Justice M, Bryan AF, Limas JC, Cook JG, Dowen JM. Chromosomal localization of cohesin is differentially regulated by WIZ, WAPL, and G9a. *BMC Genomics.* 2022;23(1):337.

5

Chapter 6

Addendum

Nederlandse samenvatting

Layman summary

Curriculum Vitae

List of publications

Acknowledgements

NEDERLANDSE SAMENVATTING

In ons lichaam vinden iedere dag miljarden celdelingen (mitoses) plaats. Iedere mitose moet leiden tot twee genetisch identieke cellen en daarom wordt dit proces op allerlei manieren gecontroleerd. Bij kanker zijn de regulatiemechanismen op de celdeling weggevallen, waardoor er invasief groeiende tumoren onstaan. Kanker is wereldwijd de belangrijkste doodsoorzaak, en vormt daarom nog steeds een enorm maatschappelijk probleem. Om betere kankerbehandelingen te ontwikkelen is het heel belangrijk dat we beter gaan begrijpen hoe de verschillende moleculaire controlemechanismen van de celdeling in elkaar grijpen en hoe deze verstoord zijn bij kanker.

Het proces van vorming van twee dochtercellen uit één moedercel wordt de celcyclus genoemd. Deze cyclus is verdeeld in 4 fasen (G1, S, G2 en M). Tijdens G1 groeit de cel, en produceert zij moleculen die essentieel zijn voor het starten van de S fase. Tijdens S fase wordt het DNA gerepliceerd. Tijdens G2 wordt het zojuist gekopieerde DNA gecontroleerd op fouten en indien nodig gerepareerd, en wordt de M (mitose) fase voorbereid. Tijdens M fase vindt dan de daadwerkelijke deling plaats. M fase wordt verder onderverdeeld in vier fasen (profase, metafase, anafase en telofase) waarin de gedupliceerde chromosomen (zuster chromatiden) gelijk worden verdeeld over de twee dochtercellen.

Wanneer een cel wordt gestimuleerd door groeisignalen, worden er meerdere signaleringsroutes aangeschakeld om de celcyclus te starten. Een centrale rol hierin is weggelegd voor de cycline/CDK-RB1-E2F route, die de DNA replicatie en dus S fase kan aanschakelen. E2Fs zijn een familie van transcriptiefactoren, die bestaat uit acht verschillende leden (E2F1-8) in zoogdiercellen. Samen reguleren deze acht E2Fs de transcriptie van een groot aantal genen. Gentranscriptie produceert boodschapper RNA (mRNA) moleculen, die worden vertaald naar eiwitten die allerlei verschillende functies kunnen uitvoeren. E2Fs kunnen ruwweg worden ingedeeld in activatoren (E2F1-3) en remmers (E2F4-8) van transcriptie. In rustende cellen bindt RB1 aan de activerende E2Fs en onderdrukt daarmee hun functie. Echter, in ongecontroleerd groeiende kankercellen is de transcriptie van E2F-afhankelijke genen meestal hyperactief, bijvoorbeeld door mutatie van het *RB1* gen of amplificatie van genen die coderen voor cycline eiwitten die ervoor zorgen dat RB1 niet aan E2Fs kan binden. *In vivo* studies lieten in genetisch gemanipuleerde muizen lieten zien dat uitschakeling van RB1 of overexpressie van cyclines de kans op het ontstaan van kwaadaardige tumoren sterk vergroten. Dit laat zien hoe belangrijk de juiste controle van E2F-afhankelijke transcriptie is voor het in stand houden van homeostase in weefsels.

E2Fs beïnvloeden meer aspecten van de celcyclus dan alleen de transitie van G1 naar S fase, maar het complexe samenspel van al deze acht E2F familieleden is nog slechts ten dele opgehelderd. Daarom hebben we in dit proefschrift verdere studie gedaan naar de regulatie en functie van drie E2F factoren, namelijk E2F3, E2F7 en E2F8, tijdens de celcyclus.

In **hoofdstuk 1** introduceren we wat er tot dusver bekend was over de functies van E2Fs in regulatie van de verschillende fases van de celcyclus. Verder introduceren we een ringvormig eiwitcomplex genaamd cohesin en zijn functie in het behouden van genetische integriteit. Verderop in het proefschrift zou blijken dat E2Fs cohesin beïnvloeden.

In **hoofdstuk 2** laten we zien dat E2F7 en -8 worden afgebroken door een eiwitcomplex genaamd SCF^cyclin F tijdens de G2 fase van de celcyclus. Hoewel E2F7 en -8 nodig zijn tijdens late S en G2 fase om de E2F-afhankelijke transcriptie moeten remmen zodra de DNA-replicatie voltooid wordt, moet hun activiteit in toom worden gehouden. We vonden dat dit waarschijnlijk nodig is om de expressie van E2F-afhankelijke genen die betrokken zijn bij DNA reparatie tijdens G2 hoog genoeg te houden. We laten zien dat verhoging van E2F7/8 via depletie van cyclin F DNA schade veroorzaakt, en dat co-depletie van E2F7/8 deze schade voorkomt. Gedeeltelijk afremmen van E2F7/8 activiteit is dus essentieel voor G2 progressie en behoud van genetische stabiliteit.

Echter, gedeeltelijke expressie van E2F7 tijdens G2 en M fase is wel belangrijk. In **hoofdstuk 3** beschrijven een onverwachte functie van E2F7 en -8. We vonden namelijk dat ze niet alleen aan DNA binden, maar ook aan cohesin. Cohesin omsluit gekopieerde chromosomen tijdens S fase om de zuster chromatiden bij elkaar te houden tot de start van mitose. Dan wordt cohesin verwijderd en kan de celdeling plaatsvinden. Wij laten zien dat E2F7 en -8 nodig zijn voor het efficiënt verwijderen van cohesin van de chromatiden tijdens profase van de mitose. Depletie van E2F7/8 resulteerde in abnormaal hoge hoeveelheden cohesin op de chromosomen in profase, en dit had tot gevolg dat cellen er veel langer dan normaal over deden om mitose te voltooien. Hoofdstukken 2 en 3 laten samen zien dat de hoeveelheid E2F7 en E2F8 in cellen nauwkeurig afgesteld moet zijn om de G2 en M fase van de celcyclus probleemloos te laten verlopen.

In het werk beschreven in **hoofdstuk 4** verlegden wij onze aandacht naar de activerende tak van de E2F familie. We beschrijven in dit hoodstuk de effecten van *E2F3* amplificatie. Deze genamplificatie, die resulteert in sterk verhoogde expressie van E2F3 eiwit, wordt vaak gezien bij blaaskankerpatiënten. We vonden dat geïnduceerde overexpressie van E2F3 in blaaskanker cellijnen voldoende was om suppressie door RB1 te omzeilen en cellen versneld S fase in te laten gaan. Deze versnelde start van S fase ging echter wel ten koste van replicatiestress, die zich uitte als vertraagde DNA synthese en een verhoogde hoeveelheid DNA schade. We hebben vervolgens genexpressiedata van blaaskankerpatienten geanalyseerd en vonden hierin ook aanwijzingen voor replicatiestress als gevolg van *E2F3* amplificatie. In cellijnen laten we tenslotte zien dat deze E2F3-afhankelijke replicatiestress kankercellen extra gevoelig lijkt te maken voor een groep medicijnen genaamd intra-S-phase checkpoint remmers.

In **hoofdstuk 5** brengen we al deze bevindingen samen en beschrijven de laatste

inzichten in de coordinatie van E2F factoren tijdens de celcyclus, en het belang daarvan in het beschermen van de genetische stabiliteit van cellen. Ook bediscussiëren we de huidige stand van kennis over de dynamiek waarmee cohesin chromosomen bindt en weer loslaat. We gaan in op de vraag via welk moleculair mechanisme E2F7 en -8 kunnen bijdragen aan het loskoppelen van cohesin van chromosomen tijdens mitose. Tezamen geeft het werk beschreven in dit proefschrift nieuwe inzichten in de manieren waarop E2F eiwitten betrokken zijn bij het intact houden van de genetische informatie tijdens de celcyclus.

LAYMAN SUMMARY

In our body, hundreds of billions of cell divisions (mitoses) occur every day, and each mitosis must produce two daughter cells with identical genomic information. This is a highly controlled process to maintain tissue homeostasis. However, in cancers cell proliferation takes place in an uncontrolled manner, leading to malignant tumor formation. Cancer is the main cause of death worldwide, and an enormous burden on society. To discover better ways to treat cancer, it is of critical importance to understand the molecular mechanisms underlying cell division.

The production of to two daughter cells from one single mother cell is called the cell cycle, which is divided into four phases (G1, S, G2 and M). In G1 phase, the cell grows in size and synthesizes components essential for S phase when DNA is replicated. During G2 phase the newly copied DNA is checked and repaired and the cell is prepared for M phase, in which the actual cell division process takes place. M phase is further subdivided into four phases (prophase, metaphase, anaphase and telophase), during which duplicated chromosomes (sister chromatids) are evenly separated into the daughter cells.

As a cell is stimulated by growth signals, multiple signaling pathways become active to initiate the cell cycle. Among the pathways, cyclin/CDK-RB1-E2F pathway is an important axis, driving the G1-S phase transition and promoting DNA replication. E2Fs are a family of transcription factors, which consists of eight different members (E2F1-8) in mammalian cells. Together, these eight different E2Fs can regulate the transcription of a large number of target genes. Gene transcription produces messenger RNA (mRNA), which can be translated to corresponding proteins that execute all sorts of functions. According to their transcriptional function, E2Fs are classified into activators (E2F1-3) and repressors (E2F4-8). Normally in quiescent cells, RB1 binds to E2F activators and suppresses their transcriptional activity. However, in uncontrolled proliferating cancer cells, E2F-dependent transcriptional activity is usually hyperactive, due to RB1 loss and/or amplification of cyclin proteins which can phosphorylate RB1 to release E2Fs. *In vivo* studies showed that mice with *RB1* loss or cyclin protein overexpression are clearly predisposed to develop tumors. Hence, proper control of E2F-dependent transcription is crucial for normal tissue homeostasis. E2F transcription factors control more aspects of the cell cycle than only the G1/S transition, but the complex regulation and interplay of all these eight different E2F family members is still incompletely understood.

In this dissertation, we studied the regulation and function of three E2F factors, that is E2F3, E2F7 and E2F8, during cell cycle. Particularly, in ***chapter 1***, we introduce the roles of E2Fs people have found in regulation of cell cycle progression. in addition, a ring-shaped protein complex, called cohesin, and its function in maintaining genome stability is depicted as well. In ***chapter 2***, we reveal that E2F7 and -8 are subjected to SCF$^{cyclin F}$-mediated degrada-

tion in G2 phase. Although high expression of E2F7 and -8 in S and G2 phase is necessary for downregulation of E2F-dependent transcription once DNA replication gets completed, this expression must be limited to allow the expression of E2F target genes involved in DNA repair to resolve potential DNA damage in G2 phase. We demonstrate that elevation of E2F7/8 via cyclin F depletion remarkably increases the levels of DNA damage and slows down G2 phase progression, while co-depletion of E2F7/8 can rescue this effect. Therefore, partial downregulation of E2F7 and -8 by SCF$^{cyclin F}$ is essential for G2 phase progression and genome integrity.

In **chapter 3**, we then describe a noncanonical function of E2F7 and -8. Specifically, we found that E2F7 and -8 are able to physically interact with cohesin. Cohesin is able to entrap duplicated DNA in S phase to link sister chromatids until the onset of mitosis when cohesin is removed to allow for separation of chromatids. We could show that E2F7 and -8 are required for this cohesin removal during prophase. E2F7/8-deficient cells showed abnormally high amounts of chromosome-bound cohesin prophase, but this also had functional consequences, as these cells spent more time to finish mitosis. Thus, E2F7 and -8 are involved in G2-M phase progression in both transcriptional and non-transcriptional manners, to facilitate genome stability.

In **chapter 4** we switched our focus to the activating arm of the E2F family, and studied the role of *E2F3* amplification, which is often seen in bladder cancer patients. *E2F3* amplification corresponds to strongly elevated levels of E2F3 protein. By ectopic induction of E2F3 in bladder cancer cell lines, we showed that E2F3 overexpression can overcome the suppression from RB1 and accelerate S phase entry. However, this accelerated cell cycle entry comes at the cost of replication stress. This replication stress was seen as slowing down of DNA synthesis and induction of DNA damage. Further analysis of gene expression data from bladder cancer patients revealed that patients with *E2F3* amplification display higher levels of replication stress. We show in our bladder cancer cell lines that this E2F3-induced replication stress may sensitize cells to a class of drugs called intra-S-phase checkpoint inhibitors.

Lastly, in **chapter 5**, we bring all these findings together and discuss the importance of coordinated regulation of E2F factors during cell cycle progression to preserve genome integrity. Additionally, we also depict the current state of knowledge on how cohesin dynamically associates with DNA, and speculate how possibly E2F7 and -8 contribute to cohesin release during mitosis. Overall, our findings provide new insights on how E2F factors engage in maintenance of genome stability.

CURRICULUM VITAE

Qingwu Liu was born on September 11th 1990 in Datong, Shanxi Province of China. After finishing his high school study in the county of Lingqiu in 2010, he majored in life science in Shanxi University out of the interest in artificial organs. During his bachelor, he developed a keen interest in molecular cell biology. Hence, he enrolled in the master program Biochemistry and Molecular biology at East China Normal University in 2014. He joined the lab of Prof. Xiaotao Li and studied the role of REGγ in the development of colitis under the supervision of Dr. Yongyan Dang. After receiving his master degree in 2017, Qingwu continued his study as a PhD candidate at the department of Biomolecular Health Sciences at the Faculty of Veterinary Medicine, Utrecht University under the supervision of Prof. Alain de Bruin (Promoter) and Dr. Bart Westendorp (co-promoter). The research conducted during his PhD aimed to uncover the roles of E2Fs in coordinating cell cycle progression and genomic integrity. the results of this PhD work are presented in this thesis.

6

LIST OF PUBLICATIONS

1. **Liu, Q**., Thurlings, I., van Liere, E.A., Manning, A., Haarhuis, J., Rowland, B.D., Westendorp, B., & de Bruin, A. (2022). Atypical E2Fs interact with SMC1 to promote cohesin release during mitosis. (under revision in Cell Reports).

2. Tan, X., Tong, L., Li, L., Xu, J., Xie, S., Ji, L., Fu, J., **Liu, Q**., Shen, S., Liu, Y., Xiao, Y., Gao, F., Moses, R. E., Bardeesy, N., Wang, Y., Zhang, J., Tang, L., Li, L., Wong, K. K., Song, D., … Li, X. (2021). Loss of Smad4 promotes aggressive lung cancer metastasis by de-repression of PAK3 via miRNA regulation. Nature communications, 12(1), 4853. https://doi.org/10.1038/s41467-021-24898-9

3. Tong, L., Shen, S., Huang, Q., Fu, J., Wang, T., Pan, L., Zhang, P., Chen, G., Huang, T., Li, K., **Liu, Q**., Xie, S., Yang, X., Moses, R. E., Li, X., & Li, L. (2020). Proteasome-dependent degradation of Smad7 is critical for lung cancer metastasis. Cell death and differentiation, 27(6), 1795–1806. https://doi.org/10.1038/s41418-019-0459-6

4. Yuan, R., **Liu, Q**., Segeren, H. A., Yuniati, L., Guardavaccaro, D., Lebbink, R. J., Westendorp, B., & de Bruin, A. (2019). Cyclin F-dependent degradation of E2F7 is critical for DNA repair and G2-phase progression. The EMBO journal, 38(20), e101430. https://doi.org/10.15252/embj.2018101430

ACKNOWLEDGEMENTS

Time really flies. It seems like only yesterday that an ignorant boy arrived in the science park of Utrecht. He was dressed in a thin denim jacket with two suitcases and a backpack, trembling in the cold wind and drizzle and waiting for **Yuan** to help him find the keys to the living building in the early morning of the autumn in 2017. It turned out that the keys were just in the small black box beside the door of the building. Apparently, he was not really ready for the kickoff of the life in the Netherlands. Likewise, in the past five years, I can't remember how many "keys" I was offered by you guys, my dear colleagues, friends, and my family. Without these "keys", it's impossible for me to reach here with this book.

Alain, thank you very much for giving me this great opportunity to study in your lab. After four-year of bachelor and three-year master study in China, I planned to have a period of study abroad. Luckily I found the interesting topics in our group online and got the position offered by you. Additionally, thanks to your patience, allowing me to explore the first project leisurely and guiding me through the major and minor problems I met during the Friday meetings in the first year of my PhD. But on science, you are very critical, from which I learnt and benefited a lot. Honestly, I have to say that I still feel a bit pressure before the monthly meeting now, had better check the presentation a couple of more times and think about the possible questions you might ask. Lastly, you are also warm. You paid for the courses to improve my crappy English and also the unusually expensive flight ticket to China after two and half years that I had not visited my family. Therefore, as my friends and parents always say, I am so fortunate to do PhD in our group.

Bart, thank you very much for your dedicated daily supervision. Thanks to those weekly meetings, so that I can get timely responses and helpful inputs on the new results and next steps, which I appreciate a lot. And the most important point I learnt from you I think is how to approach a new research question, which actually not only influences how I deal with research problems, but also the ones I meet in daily life. Moreover, I am impressed by the efficiency and quality you have to balance the work and family, considering you have regular meetings with PhD students and Postdocs every week, and review tons of paper works at the same time. Very grateful for the efforts and time you took to review and revise my thesis and manuscripts. I guess it was not easy to get what I wrote in the first version. Without you, I am not able to make them. Lastly, It is always quite relaxing to talk to you, no matter about research or daily life at Hubrecht. But also, I still remember the couple of talks we had on the way home. That's really a lot of fun.

Thanks to my PhD committee, **Benjamin Rowland** and **Susanne Lens**. Your advices in the yearly meeting were of great help. Also thanks to the reading committee, **Hein te Riele**, **Tom Stout**, **Jan Molenaar** and **Puck Knipscheer**, for taking time to assess this doctoral dissertation.

PhD fellows, **Yuan, Eva** and **Jet**, how lucky to have you guys around during my study here. You finished your PhD and left the lab one by one. But you are always there whenever I need help. **Yuan**, of course, thanks again for helping me find the first "keys" to the first day of life in Holland. There are too many thanks to you. You taught me the Western Blotting, which becomes a key assay I did almost "every day" in the past five years. And the tips you

shared with me on doing experiments still play a role currently. Besides, you helped me find the place where I still stay now and transport the second hand mattress and fridge with your car to my apartment. You have been a good example to learn from both in and out of the lab. **Eva**, I miss a lot the time when you were in the lab. What a warm girl you are! Always patient to listen to the issues I had from experiments and life, and gave me your advices. It's also you that encouraged me to experience different things, like Macumba, the last revelry before COVID. Thanks for all the fun moments you made. "Professor to be" **Jet**, my bench neighbor, I am impressed how efficient you are to handle everything, lab work, presentations, thesis, marathon, cycling ……and thanks for helping me with flow cytometry, PCR and live imaging setting, and also my first poster. So many bummers I met were solved with your great help. By the way, thanks as well for correcting my English many times, like "a cup of beer", haha….. wish you all the success with your Postdoc study and wait to congratulate your next nice findings.

"Doctors to be", **Anneloes, Thomas, Orsi** and **Alejandra,** so nice to have you all in the PhD team. **Anneloes**, even though you joined us lately, we knew from the first day I stepped in our old office room. Thank you for your kindness and patience, you always could get what I wanna express in my poor English, particularly in first couple of months. Good luck with your following research, I hundred-percent believe it will be another big success. **Thomas**, I am so honored to have you as my paranymph. Because I know there is a smart guy standing behind me. So please "rescue" me while I am stuck by the questions from the opponents (:P). Thanks for the house-warmings you held. That is when I could enjoy nice pasta without considering the cost, haha... Good luck with the paper writing, I am sure you will get nice publications with those fascinating data. **Orsi**, thanks for sharing with me the information about working in a company, and also the encouragements you gave during my thesis writing. I will always keep it in mind. **Alejandra**, we do not talk often, cause you work in another building. But your calmness and intellect impressed me much. Good luck with all the following PhD work.

Elsbeth, thanks a lot for the orderings and instructions in the lab throughout my whole PhD. I love to hear you talk about the fun stories about **Cayetano**. It must be quite fun to have **Cayetano** around in the life. **Saskia**, thank you for sharing with me all the information about your family and housing issues. Good luck with your fitness work, you will make it I believe. **Laura**, thanks for the cookies and chocolates you brought from Italy, it is dramatic you managed your PhD and family with two kids at the same time. Wish you a happy life with **Luca** and your two lovely boys. **Rachel**, thanks for the offers of help in my paper writing, so kind of you. **Jaime**, thanks for all the cakes and ice cream you made for us. I will definitely miss them. **Tara**, thanks for all the meetings you helped arrange.

Bram, thanks for all the advices you gave during the lab meeting, wish you all the best with the full job in NKI. **Kate**, I am so admirable of the enthusiasm you have in running, as well as in work. I hope I can still keep high motivation in tennis when I go home like you. Besides, thanks to talking to you and **John** in person, I learnt that American English is another level to practice, haha…. Hope I will still be used to talking to people when traveling in US someday. Good luck with the Postdoc work and continue enjoying the life in the Netherlands. **Jung-Chin**, so amazed by your quick thinking and extensive knowledge, and also the capability you have to do researches both in Utrecht and Amsterdam. Thanks for the helpful suggestions you gave in the lab meeting and performing the mass spectrometry experiment. **Anita**, it is really impressive that you do everything so dedicatedly and meticulously. This is also reflect-

ed by the nice questions and inputs you share in the meeting. Good luck with the Postdoc work, I am really looking forward to seeing the transmission of DNA fragment between cells. **Aaron**, it is really interesting to talk to you and learn about your work as a grant writer. Good luck with the rest grant writing this year. **Alice**, nice to meet you at the end of my PhD, and exciting to learn you got some promising results from canine patients recently. So keep going and you will get more fascinating data.

Enric, what an enthusiastic guy you are! It is always relaxing to talk to you in the lab. Thank you for all the suggestions on doing research, as well as the strategies of dating (:P). I will keep it in mind. **Frank**, so luck to have the birthday at the same day with you and celebrate the last two birthdays together. I will remember there is another guy celebrate his birthday when I am having my birthday in China. **Richard**, thanks a lot for your kind supports and help in setting up the live imaging experiments. **Hanneke,** thanks for your dedication in the E2F3 project. You "dig" out so much cool information from both wet lab work and silico analysis. Good luck with your master study. **Marianna**, it is nice you pick up tennis again. Good luck with your report writing and tennis training. **Anne**, thanks for all the fun moments you offered in the lab and good luck with your clinical study. **Vivian**, my private tennis coach, thanks so much for the tips on correcting my serve, forehand, backhand, volley, basically every technique of tennis. I will miss your tennis and of course you after back to China. Good luck with your PhD.

Hi tennis gang in Utrecht, 建程, 育贤, **Eduardo**, **Maarten**, **Casper**, **Tomas**, **Stefan** and **Tim**, so luck to meet up you guys on the courts in Olympos. Especially, 建程, 每次和你约球都很期待。 和你打球得时候，恍惚感觉自己都是另一个level了。不过确实，感觉和你打了一年多后，我更喜欢打快球了。 希望以后我们还能有机会打球，祝 实验顺利，明年按期毕业！ **Eduardo**, really nice to meet you, you are such a warm and smart guy. Thank you for the tips you gave on my tennis, and I will miss the time when we played tennis and watched the matches together. Good luck with your work and see you around!

呼，终于可以用中文了。五年过得好快，虽然没有很多科研产出，但很幸运收获了众多的友谊。正是因为有了大家的陪伴，才让这异国的五年时光变得更加值得回忆和珍惜。

首先，感谢 **中国留学基金委**（**CSC**）的支助，让我有机会在海外学习!

莉姐，川，潘牧师，非常怀念我们四个人团契的时光，一块儿做饭，一块儿查经，那段时间是我成长最快的阶段，后来大家逐渐离开乌特，加上疫情来袭，查经也就中断。谢谢你们在我第一年的鼓励，让我逐渐适应在这边的学习和生活。祝愿你们的工作和生活都继续蒙神祝福。

感谢从一到荷兰就认识的同学们，**书阳，当汉，万象，蕾姐，爽，东升，春燕，晓白，浦桥，燕燕，洪琳（好邻居），相洁，恺洋，培凯，龙哥**，怀念和大家聚餐，徒步，聊天的时光。夫妻组合的同学们，**浩瑞**和**陆琳玉**，**老邱**和**杨明曦**，感谢你们的慷慨，容我

多次去你们家蹭饭。我也不想的，无奈你们做饭太好吃了，哈哈。。。**之涵**，认识你不久，你就搬去Leiden了。但后来每次见你，都有你的百般问候，鼓励，你是我见过在科研上最努力的同学，相信会有更多的好的成果出来，等你回国建组，做更多有趣的东西！**健男**，这五年为数不多的几次喝断片儿的时候都是拜你所赐，不过也是确实喝得很开心，回国有机会再聚啊！**雪峰**，要说荷兰有好基友，那有且只能是你了（:P）。两次圣诞旅行，在学校时不时的出去喝一杯，烧烤，游泳，划船，一块儿逛阿姆。。。这五年几乎是一块儿来一块儿回国。感谢你当我paranymph，祝愿咱俩都答辩顺利，一块儿搭机回国大吃大喝啊！**君豪，老张，璐璐**（周末无聊活动小组）忘了从什么时候起，我们四个开始每个月一次聚餐，就算疫情最严重的时候还是会"顶风作案"。一块儿做饭，吐槽实验室，吐槽课题，那是每个月为数不多放松的时刻。祝愿**君豪**能早日成为历史系大牛，教授，**老张** 能找一份施展你才华的工作，**璐璐** 早日完成revision，毕业回国和男友团聚。

不觉中，在Hubrecht building 已经呆了四年。**桂卫**师兄，**林琳**师姐，**代松**师兄，**李洋**师兄，每次和你们聊天，都能受益良多，祝愿你们科研上产出越来越多，早日回国建组。**嘉怡**，谢谢你在走廊、上班下班路上聊天时给的鼓励和建议，祝福你Postdoc的工作顺风顺水，早日拿到GRANT。**家彬**，羡慕你很好得融入了这边的生活，继续加油，早日发paper。**杜杰**，RMCU颜值担当，家庭美满，PhD也马上结束。虽然在实验室聊天的时候，不时会听你吐槽课题，但不曾见你停止过实验，四楼总是能见到你穿着实验服跑来跑去的身影。Hang in there，等你回国拿教职的好消息。**小乐**，感谢你和**张楠**过去几年每逢端午中秋，都不忘你"孤苦伶仃"的师兄，带来好吃的粽子月饼。也特别开心见到你这几年的成长，已经是RMCU分子细胞方面的大牛。祝愿你和**张楠** 的课题接下来顺顺利利，早日毕业，一块儿回国。**陶禹**，谢谢你不时的鼓励，你的博士才刚开始，祝愿你接下来几年能收获high IF papers，争取超越你的叶师兄和老王师兄。**老王**，我到现在也想不通，你为啥要paper有paper，要对象有对象，你不是人生赢家谁是？！实验间隙，能和你侃侃大山是一天中最愉快的时光。祝福你和**王嫂**，早日答辩，建立你俩的小家！**叶博**，咱俩这七年的难兄难弟，怎么突然就剩我一个了（/(ㄒoㄒ)/~~）。不过看到你能一步步的实现自己的人生计划，我是非常开心得。如今有了**王梦**，**小哈哈**，肩上又多了一份责任，但肯定也是一份让你变得更优秀的动力。祝愿你接下来不论是找博后还是工作，都能水到渠成，小家庭幸福美满。

俊俊，万万没想到你居然弯道超车，提前毕业了。如今，老婆贤惠，品品可爱，你也成功入职上海细胞治疗领域的潜力公司，我还能祝福你什么呢，只能等你内推给你打下手了（:P）。很开心，疫情后你搬来我住的楼，一块儿聊学术，聊人生的时光总是过得很快。希望咱们还能上海见，继续把酒言欢。**彭总**，和你喝酒总是很放松，在乌特吞云吐雾的日子随着你回国一去不复返了。 等我回去，咱是不是有机会总要续上，难得浮生半日闲嘛！还有**晟哥**，感谢在Eindhoven的盛情款待，很愿意和你聊天，你在好多事儿上的见解都很独到，受益颇多。 **邵芳，施尧**，很高兴认识你俩，邵芳的whiskey，施尧的饺子面，给博士的最后一年增加不少乐趣。**佳伟，宏尚**，硕士毕业一别，就很难再见。很为你骄傲，**佳伟**，我们四个（还有叶博）一块儿从本科生宿舍搬出后，你第一个发paper，第一个博士毕业，第一个拿到职位建组，成为独立PI。继续加油啊，等你在学术上不断高升的

消息！**宏尚**，去年上海的短暂小聚，甚是怀念。听到你博士以后的计划，很是为你开心，接下来就是答辩，然后回去和**冬青**团聚，确定岗位，实现家庭工作双圆满了，祝一切顺利啊！

接下来要感谢球友们。很难想象，如果这五年来没有你们陪伴，周末会少了多少乐趣。**老吴**，很幸运来荷兰不久就认识了你。五年来，跟你打球应该是最多的，每次打，都会发现你又有进步，真的挺厉害。接下来恐怕就是回国继续约了，祝福你和Yuhui的幸福小生活，回国约了！**魏宇**，短暂的一年来荷交流，偏偏还赶上疫情，但我们还是打了很多次球，怀念有你，**思予**，**韶涵**，**王强**在这儿的那个夏天，打球，划船，吃饭。等我回去，给你当伴郎，见证你和**王强**的幸福！**佳伊，**恭喜你拿到UU的PhD position，可惜我也要回去了，不然还可以多打几次球。不过你肯定还能在Olympos找到球友的，祝福你接下来的博士求学阶段，发大文章，早日毕业!! **老高**，**曾老师**，**雨辰**，**强哥**，**金宇**，很可惜最后一年才开始熟络起来，刚立冬，已经开始怀念这个夏天我们约球的日子了。接下来就等你们回国，我们再约了！祝大家球技日趋精进，我们国内球场battle了！

最后，最应该感谢我的家人。**爸**，**妈**，感谢你们从小至今的谆谆教导、以身作则，才让我自从走出家门，在不同城市、国家求学的时候，有着你们身上的坚韧和谦逊。也要特别感谢爸妈一直以来的无条件支持和鼓励。你们何曾不想我回到你们身边，陪伴你们，但你们从来不说，只说"想考哪儿就考哪儿吧。" 每当面临抉择的时候，你们的一句 "顺其自然，尽力就好" 更是对我莫名的宽慰。感谢爸妈这些年的辛勤付出，为了抚养三个小孩儿，从务农，到小生意，跑出租，帮别人看小孩儿，你们从来没停下来休息过一下。天底下，好的父母大抵也就是你们的样子了吧。祝愿爸妈，接下来能少工作，多休息，身体健健康康，不要再太为子女的事操心，多关心自己，享受生活。两个弟弟，**刘青山**，**刘青虎**，还有弟妹们，**莎莎**，**田雪**，感谢你们这些年对爸妈的陪伴和照顾，也感谢你们的理解，作为大哥，没能回去参加你们的婚礼，帮些许的忙。现在想来，愈发后悔。因为有你们在爸妈身边，才让我少了些许对爸妈的挂念和亏欠，谢谢你们。祝愿你们两个小家庭，和谐美满，幸福安康。还有我可爱的大侄儿，**敬安**，小伙子要慢点长大，过一个happy的童年！

庆午
Utrecht, 11.2022